A Process Mineralogical Study on the effect of Alteration on the Flotation of Great Dyke Platinum Group Element (PGE) Ores

A dissertation submitted in fulfilment of the requirements for the degree of Master of Science in Chemical Engineering at the University of Cape Town

Theophilus C. Dzingai
(MSc (Eng) Chemical Engineering Student)

Supervised by:
Dr. Megan Becker
Dr. Margreth Tadie
Dr. Belinda McFadzean

20 December 2017

Plagiarism Declaration

I know the meaning of plagiarism and declare that all the work in the document, save for that which is properly acknowledged, is my own. This thesis/dissertation has been submitted to the Turnitin module (or equivalent similarity and originality checking software) and I confirm that my supervisor has seen my report and any concerns revealed by such have been resolved with my supervisor.

Date: 20 December 2017

Name	Student Number	Signature
Theophilus C. Dzingai	DZNTHE001	Signed by candidate

Abstract

Ores from the same deposit may exhibit extensive variability in their mineralogy and texture. The ability to quantify this variability linked to metallurgical performance is one of the primary goals of process mineralogy and geometallurgy. Ultimately this information can be used to inform decisions around all core activities of mining and processing. This study focusses on identifying the key mineralogical differences between three Great Dyke platinum group element (PGE) ores in Zimbabwe. These ores are known to be characterized by extensive oxidation and alteration resulting in numerous metallurgical challenges in recovering the PGE.

The behaviour of three different ores sampled along the strike of the Great Dyke is compared, focusing on mineralogical composition, rheological characteristics and batch flotation performance. The contribution of the differences in mineralogy (bulk mineralogy, base metal sulfide (BMS) liberation and association, and naturally floating gangue) to processing challenges and potential opportunities to manage these was considered. It was noted that slight differences in mineralogy, particularly BMS liberation and association, yielded notable differences in copper, nickel, platinum and palladium recoveries. The most oxidized ore was found to have lower recoveries due to the oxidation of the BMS, though a deeper understanding of the oxidation and flotation behaviour of PGEs (and platinum group minerals - PGMs) is still necessary. Through the mineralogical analysis of the batch flotation concentrates it was observed that more finely disseminated and yet locked (unliberated) talc resulted in higher amounts of naturally floating gangue (NFG).

The effect of 3 polymeric carboxymethyl cellulose (CMC) depressants, differing in degree of substitution, was also evaluated in terms of their ability to depress the naturally floating gangue and mitigate any rheological complexities that may be associated with these ores, through the electrostatic repulsion of the negatively charged carboxylate groups. There was no significant advantage of one depressant over the others in the batch flotation tests or in the rheology tests. The more oxidized ore was found to contain relatively low amounts of phyllosilicate minerals and, therefore, no rheological problem was present that would have required a chemical solution. There were no noticeable differences in the rheology of the slurries of the 3 ores. This was likely to be due to the dampening or buffering effect of the high proportion of minerals that do not contribute to rheological complexity. Changing of depressant type also had no effect in this case possibly due to the same reasons. In addition to this, the region after which the rheological complexity of all 3 ore types begins to increase exponentially is from 30-35 vol.% solids concentration (60-65 wt.% for an ore with a specific gravity of 3.3). It is therefore advisable for Great Dyke operations not to exceed these solids concentrations as this would exacerbate the processing challenges associated with rheological complexity. The use of such solids concentrations during flotation is however unlikely though this may be the case in other parts of the processing circuit, e.g. comminution, and should thus be noted.

The decoupling of the terms referring to alteration (that is oxidation and hydrolysis/hydration) is also presented in this study together with the effects of these different types of alteration on the processing of PGE ores. Oxidation affects the valuable minerals and thus flotation recoveries whilst hydrolysis/hydration acts on the gangue minerals and therefore mainly affects concentrate grade. The more oxidized ore sample in this study had undergone the oxidation type of alteration, rather than hydrolysis/hydration and the processing challenge associated with it lies not in the gangue but with the valuable minerals.

Finally, it was shown that investigating an ore's characteristics solely on mineralogy may not necessarily give a full prediction of the ore's response but the linking of the mineralogical characterization with metallurgical test work gives a more holistic view.

Acknowledgements

First and foremost, I would like to express my gratitude to my Lord, Jesus Christ, the creator of heaven and earth. Thank you Lord for your love for me, your ability at work in and through me, your favour upon my life, your guidance in all I do. All of this is because You first loved me!

My sincere gratitude goes to my supervisors, Dr Megan Becker, Dr Belinda McFadzean and Dr Margreth Tadie. Thank you for believing in me and putting in your all continually for the success of this project. Words cannot quantify the extent of my appreciation for the amount of time you put into always giving me timeous and effective feedback. I can truly say thank you for guiding me all through the way, I am forever indebted to you. Thank you for all you've taught me through this time. Thank you Dr Becker for seeing something in me right from the start, and thanks to the whole team for grooming, nurturing and bringing out the best in me.

Grateful thanks to the UCT Department of Chemical Engineering as well as CMR staff and students. They have made this project a delight! Thank you for the flotation and process mineralogy group meetings which helped a lot when things were not that clear, particularly at the start. Thanks to Gaynor Yorath for her enthusiasm and assistance with the QEMSCAN analyses, together with Mpho, Olga, Lucy and Warren. Thanks to Shireen, Monde and Francina for their help in the lab. Thanks to Lorraine for always being joyful and excited to work on preparing my samples. Thank you, A'isha, for your help with rheology tests. Thank you Gary for the analysis of the depressants. Thank you Dr Kirsten Corin for helping with the XRD analyses. Thank you Mrs Jenny Wiese for the help with certain literature I needed for this study. My thanks go to the team in Analytical Lab – Stephanie, Zulfa, Russel, Zandie, Ella. Thank you Andrea for helping me to get this final document. Thank you all, I am grateful to be associated with you.

My appreciation goes to Senmin (Pty) Ltd and the National Research Foundation (NRF) for their support and funding of this research. Thank you Mr Patrick Dicks for your valuable guidance right from the start. Thank you Mr Jules Aupiais. My thanks also go to Mimosa Mining Company (Pvt) Ltd and Zimplats Holdings Ltd for the ore samples and their assistance throughout the duration of the study. This work is based on the research supported in part by the National Research Foundation of South Africa (Grant Number 86054). Any opinions, findings and conclusions or recommendations expressed in any publication generated by the NRF supported research is that of the authors, and that the NRF accepts no liability whatsoever in this regard.

I would also like to thank my family - Daddy, Mummy, Tafadzwa, Ropafadzo, Takudzwa, Tawananyasha. Thank you for desiring the best for me always. We have come this far and we go on with and for our Lord! Thanks to my parents for selflessly encouraging me to go on! I am a product of all you have put in through the years and I will make certain that it is all worthwhile. Thanks to my Pastors (Pastor Percy, Pastor Karen, Pastor Chris) and family in Believers' LoveWorld and Christ Embassy Cape Town. Thank you for your words, thank you for the fellowship. Thanks to my friends who were there throughout this project, how could I ever describe the love you've shown me. Thanks to all who have played a role in my life to this moment. #ToEvenGreaterHeights

List of Publications and Presentations

Dzingai, T., Becker, M., Tadie, M. and McFadzean B., 2015. The Effect of Phyllosilicate Minerals on the Flotation of Great Dyke PGE ores. *SAIMM MinProc Conference 2015*, 7-8 August 2015, Cape Town.

Dzingai, T., McFadzean B., Gerdien, A., Yorath, G., Tadie, M. and. Becker, M., 2017. Considering Rheology as a Key Geometallurgical Tool. *35th International Geological Congress*, 27 August – 4 September 2016. Cape Town.

Dzingai, T., Becker, M., Tadie, M. and McFadzean B., 2017. The Effect of Oxidation on the Mineralogy and Flotation of Great Dyke PGE ores. *MEI Process Mineralogy 17*, 20-22 March 2017, Cape Town.

Dzingai, T., Becker, M., Tadie, M. and McFadzean B., 2017. The Effect of Oxidation on the Mineralogy and Flotation of Great Dyke PGE ores. *SAIMM Minerals Research Showcase 2017*, 3-4 August 2017, Cape Town.

Dzingai, T., Becker, M., Tadie, M. and McFadzean B., 2017. Mineralogical variations of Great Dyke PGE ores and their effect on Flotation Performance. *Minerals Engineering*, Under review.

Table of Contents

List of Figures

List of Tables

Nomenclature

Glossary

Area %	The portion of the 2-dimensional exposed surface that is of a certain characteristic on a QEMSCAN image
Association	The perimeter of the grain or particle under investigation in relation to the surrounding mineral/(s)
Cumulus	Igneous rocks formed by the accumulation of crystal grains from a magma by settling or floating
Degree of Substitution	The average number of carboxyl groups per monomer unit. It represents the extent of the negative charge on the CMCs
Grain	An element of a particle consisting a single mineral type
Incipient	At the initial stage, not yet pronounced
Intercumulus	Minerals filling in the interstitial spaces/interstices/gaps between the cumulus mineral in a rock
Liberated	Mineral grains possessing an Area % greater than 90% of the particle/(s) under analysis
Liberation	The area percent that is exposed
Locked	Mineral grains possessing an Area % less than 30% of the particle/(s) under analysis
Loss on ignition	LOI is the sum of the moisture content and bound water, where bound water is representative of the percentage of the sample that comprises of water molecules present in the structure of hydrous silicates
Middlings	Mineral grains possessing an Area % greater than to 30% but less than and equal to 90% of the particle/(s) under analysis (High Grade Middlings: $90 \geq$ Area % Mineral > 60, Low Grade Middlings: $60 \geq$ Area % Mineral > 30)
Particle	A fragment of a rock made up of several mineral grains
Pervasive	Wide spread
Relict mineral	A mineral which has remained unaltered after a geological process
Stratiform	Arranged/or occurring in layers

Acronyms

BM	Base Metal
BMS	Base Metal Sulfide
CMC	Carboxymethyl Cellulose
DS	Degree of Substitution
LOI	Loss on ignition
MIM-S	Mimosa Sulfide
PGE	Platinum Group Element
PGM	Platinum Group Mineral
PSD	Particle Size Distribution
QEMSCAN	Quantitative Evaluation of Minerals by SCANning electron microscopy
QXRD	Quantitative X-Ray Diffraction
QXRF	Quantitative X-Ray Fluorescence
TDS	Total Dissolved Solids
wt.%	Weight Percent
vol.%	Volume Percent
ZP-O	Zimplats Incipient Oxide
ZP-S	Zimplats Sulfide

Mineral Formulas

Amphibole(Hornblende)	$(Ca,Na)_2(Mg,Fe,Al)_5(Al,Si)_8O_{22}(OH)_2$
Bornite	Cu_5FeS_4
Calcite	$CaCO_3$
Chalcocite	Cu_2S
Chalcopyrite	$CuFeS_2$
Chlorite	$(Mg,Fe)_3(Si,Al)_4O_{10}(OH)_2.(Mg,Fe)_3(OH)_6$
Chrysocolla	$(Cu,Al)_2H_2Si_2O_5(OH)_4.n(H2O)$
Clinopyroxene	$Ca(Mg,Fe)Si_2O_6$
Cooperite/braggite	(Pt,Pd,Ni)S
Covellite	CuS
Cuprite	Cu_2O
Galena	PbS
Malachite	$Cu_2CO_3(OH)_2$
Mica (Biotite/Phlogopite)	$KMg_{2.5}Fe^{2+}_{0.5}AlSi_3O_{10}(OH)_{1.75}F_{0.25}$/ $KMg_3AlSi_3O_{10}F(OH)$
Millerite	NiS
Moncheite	$Pt_{0.75}Pd_{0.25}Te_{1.5}Bi_{0.5}$
Olivine	$Mg_{1.6}Fe^{2+}_{0.4}(SiO_4)$
Orthopyroxene	$(Mg,Fe)_2Si_2O_6$
Pentlandite	$(Fe,Ni)_9S_8$
Plagioclase	NaAlSi3O8 - CaAl2Si2O8
Pyrite	FeS_2
Pyrrhotite	$Fe_{1-x}S$ (x=0 to 0.2)
Quartz	SiO_2
Serpentine	$(Mg,Fe,Ni,Al,Zn,Mn)_{2-3}(Si,Al,Fe)_2O_5(OH)_4$
Sperrylite	$PtAs_2$
Talc	$Mg_3Si_4O_{10}(OH)_2$
Violarite	$Fe^{2+}Ni_2S_4$

Chapter 1- Introduction

This introductory chapter gives a brief overview of the motivation of this study. The background is presented in Section 1.1 and is followed by the Problem Statement (Section 1.2). The aims and objectives of this work are detailed in Section 1.3. The scope of the study follows in Section 1.4 and finally an outline of the dissertation (Section 1.5).

1.1 Background

The ability to cater for ore variability is a major challenge faced by the mining industry. Many existing plants cannot cater for this ore variability since their design specifications were focused on averaged ore characteristics (Powell, 2013). Figure 1.1 shows an example of such variability on recovery. As design flexibility is not always an option for existing plants, the need for optimization of these plants based on process mineralogy is increasing (Baum, 2014; Shaw *et al.*, 2013; Lotter *et al.*, 2011). One of the key contributors to ore variability is the role of oxidation and alteration on a 'pristine' ore deposit. Oxidation, especially of the sulfide minerals, has led to reduced valuable mineral recoveries (Eksteen *et al.*, 2016; Oberthür *et al.*, 2013; Evans, 2002). There is therefore a need for an understanding of the mineralogical aspects of ore variability and assessment of how this can be managed. Ways of managing ore variability include ore sorting, stockpiling and campaigning, blending or the use of certain reagent suites based on the mineralogy of the run-of-mine ore.

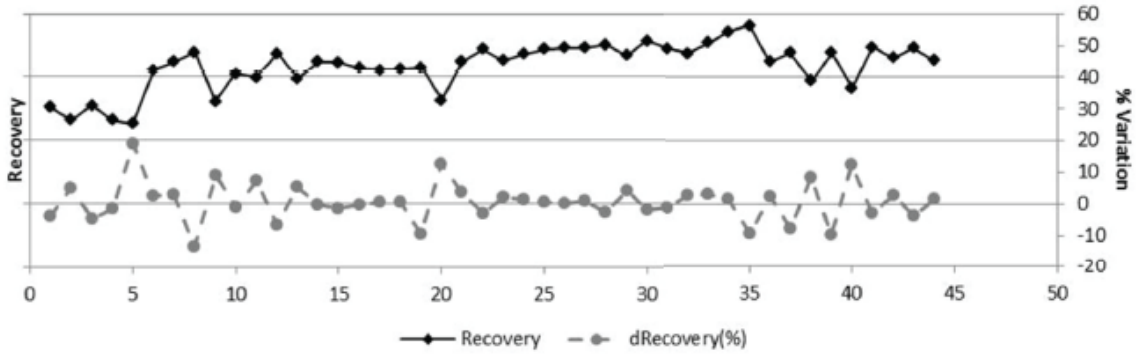

Figure 1.1: A geostatistical model of the impact on 1 week metal recovery from mining without blending (Shaw *et al.*, 2013)

The Great Dyke in Zimbabwe is the world's second largest platinum group element (PGE – Pt, Pd, Ir, Ru, Rh, Os) resource (8 680 t PGEs (4E – Pt, Pd, Rh and Au)) after the Bushveld complex (63 300 t PGE (4E)) in South Africa (Mudd, 2012; Oberthür *et al.*, 2013). It is a stratiform intrusion stretching ~560 km in the NNE direction across the country, with a width varying between 4 to 11 km. PGEs are critical to the future of global sustainability because of their applications in the arena of catalysis, electronics, hydrogen fuel cells, and medicinal purposes (cancer treatment and pacemakers) (World Platinum Investment Council, 2016; Johnson Matthey, 2016; Cawthorn, 2010).

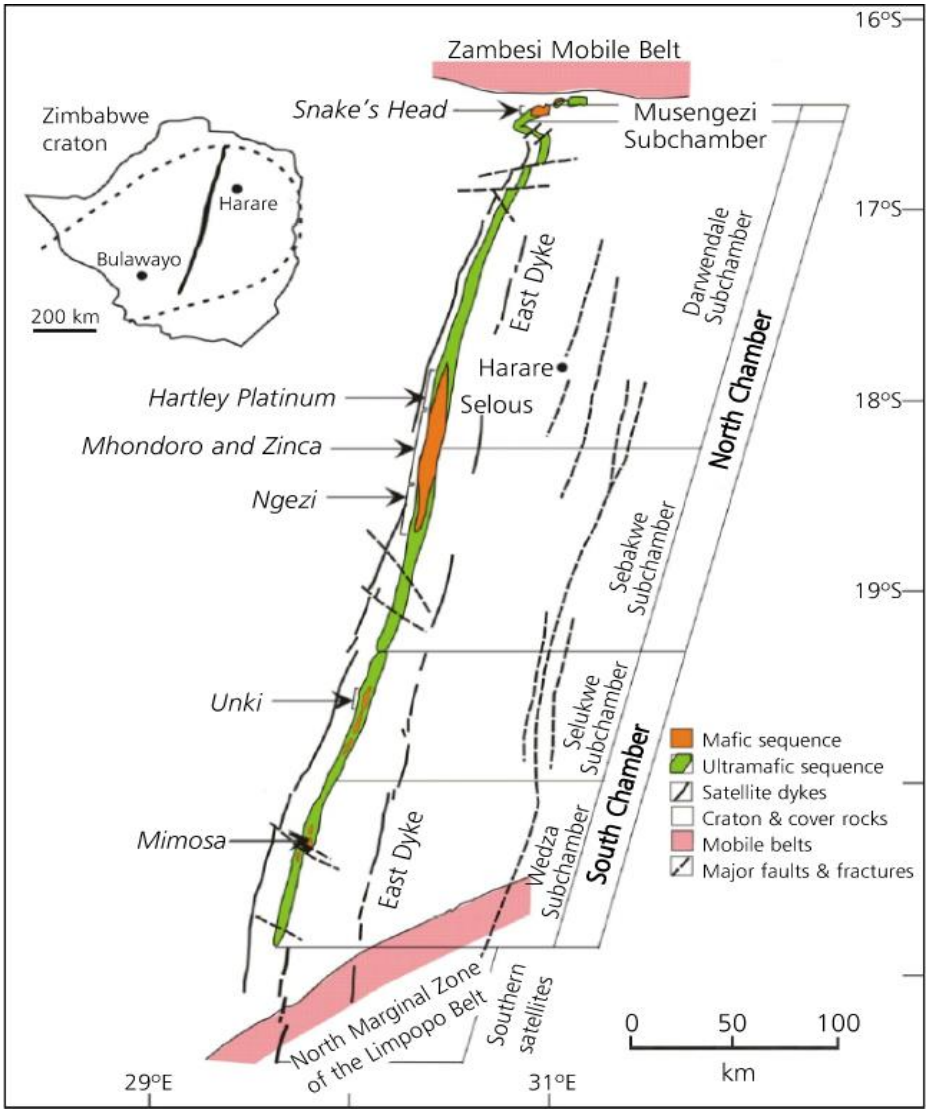

Figure 1.2: The Great Dyke (Wilson and du Toit, 2010*)*

The Great Dyke (shown in Figure 1.2) is divided into two sections along the strike, namely the North and South Chambers, with the economic PGE mineralization in the Great Dyke being stratabound and mainly found in the Main Sulphide Zone (MSZ) and the Lower Sulphide Zone (LSZ) (Oberthür *et al.*, 2003b). Ores from the Main Sulfide Zone (MSZ) in the Great Dyke are characterized by extensive oxidation and alteration resulting in numerous metallurgical challenges in recovering the PGE (Prendergast, 1990; Coghill and Wilson, 1993; Li *et al.*, 2008). The current method used in the recovery of the PGE from the Great Dyke is froth flotation. Froth flotation selectively separates hydrophobic valuable minerals such as discrete platinum group minerals (PGMs) or those platinum group elements (PGEs) associated with base metal sulfides (BMSs) from hydrophilic gangue minerals such as silicates and chromites among others. In the oxidation and alteration of ores there is a change in the nature of these PGE carriers. Several authors (Evans 2002; Oberthür *et al.*, 2013; Becker *et al.*, 2014) have shown that a large proportion of the primary PGE carriers formerly in the pristine ores, inclusive of PGMs, have been destroyed and their PGE contents are now sited either in iron hydroxides, in smectites or occur as discrete 'PGE-oxides or

hydroxides'. The relict base metal sulfides present are pyrrhotite, pentlandite and chalcopyrite, while there are low amounts of pyrite. These BMSs are enclosed within pyroxenes and plagioclase, within secondary hydrous silicates (amphiboles, talc and chlorite), within weathering products like iron and manganese oxides/hydroxides. Most of the BMS which were previously part of the pristine ore are likely to have been oxidized to iron-hydroxides often associated with smectites (Locmelis *et al.*, 2010). Additionally, the oxidation process, apart from oxidizing the BMS, results in the redistribution of Pt and Pd, with Pd being more mobile (Oberthür *et al.*, 2013; Oberthür *et al.*, 2003b; Locmelis *et al.*, 2010; Evans, 2002). This, together with the expected high grades of phyllosilicate minerals (e.g. talc, serpentine, chlorite, smectite), poses a mineralogical challenge. The deposit is therefore not being mined to its full potential as this oxidation and alteration presents a 'mineralogical barrier' (see Becker *et al.*, 2017; Bradshaw, 2014; Skinner, 1976).

The two extremes in the degree of oxidation are 1) the pristine or sulfide ore and 2) the oxidized ore. Pristine ores are mined underground at Ngezi, Unki and Mimosa after which they are subsequently treated by conventional metallurgical methods which entail grinding, milling, flotation, smelting and matte production as well as chemical refining (Oberthür *et al.*, 2013; Jones, 2005). The pristine ores have resources of approximately 2 000 Mt at an average PGE grade of 3.6 g/t (4E) (Mudd, 2012). The oxidized ores occur closer to the surface and have resources of approximately 250 Mt at an average PGE grade of approximately 3.4 g/t (4E) but are currently not being processed (Oberthür *et al.*, 2013; Implats, 2016). These oxidized ores are further split into two subsections: those that are pervasively oxidized and those that are incipiently/partly oxidized, with the latter containing relict sulfides and occurring beneath the former. Small scale operations on these oxidized ores were stopped due to low PGE recoveries (less than 50%) obtained in their concentrations using froth flotation (Evans, 2002). The low recoveries are a result of high amounts of alteration minerals including the presence of Fe-oxides and hydroxides and phyllosilicate minerals – talc, chlorite and smectite among others. The effect of oxidation and alteration on flotation of a PGE ore from the Bushveld Complex was investigated by Becker *et al.* (2014) in which low PGE recoveries were associated with the high levels naturally floating gangue, high Fe-oxide/hydroxide content and low PGM associations to BMS. However, this may not necessarily be the case for Great Dyke oxidized ores due to the marked differences in the mineralogy of the ores. It is thus imperative to investigate how the mineralogical composition of the ores affects its flotation performance.

Even though current mining activities have focused on pristine ore, the run-of-mine ore has varying degrees of oxidation (and thus phyllosilicate mineral content) and not only purely pristine material is necessarily excavated and processed at any one time resulting in ore variability. The variability in the ore composition leads to an undesirable variability in PGE recoveries and grades. This consequently affects downstream processes of the mining operation such as smelting, which is negatively impacted by high MgO content (Lotter *et al.,* 2008).

Recently there has been some renewed interest in the potential for hydrometallurgical treatment of these oxidized ores (Kraemer *et al.*, 2015). In the context of this study where flotation is a well-established method of concentration already in practice, the ability to modify operating conditions

for existing sites presents an opportunity of managing this ore variability when processing blends of pristine and oxidized ore. This may be more beneficial in comparison to the use of a new technology, which may require a lengthy period of development, large capital investment and ultimate actualization. This study therefore presents an analysis of three ores exhibiting different degrees of oxidation, together with a comparison of their flotation responses. This could lead to a better understanding of the countermeasures in flotation which would yield more constant grades and recoveries in the processing of these ores.

1.2 Problem statement

Ores from the Main Sulfide Zone (MSZ) in the Great Dyke are characterized by extensive oxidation and alteration (Prendergast, 1990; Coghill and Wilson, 1993; Li *et al*., 2008) resulting in numerous metallurgical challenges in recovering the PGE. There is therefore a need to assess the mineralogy of the ores and their relative flotation responses as well as how these responses can be managed. This study will investigate these ores to better understand and improve operations which are carried out on ores of varying composition.

1.3 Aims and objectives

This process mineralogy study aims to compare the behaviour of two pristine and one partly/incipiently oxidized Great Dyke ore focusing on their mineralogical composition, batch flotation performance and rheological characteristics. The effect of various polymeric depressants will also be evaluated with the objective of determining their ability to depress the naturally floating gangue, and mitigate any rheological complexities caused by the high concentrations of phyllosilicate alteration minerals.

Ultimately, the outcome of this study will provide deeper insight into the effect of alteration on flotation performance giving operators information which may result in improved handling of the variability in alteration mineral content commonly encountered during processing of the MSZ ores.

1.4 Scope of the study

This study focuses on understanding the effect of ore variability on the flotation performance of Great Dyke ores. The mineralogy of 3 different Great Dyke ores will be assessed and the ores' batch flotation performance and rheological characteristics compared. Two sulfide ores (one from the North and the other from the South Chamber) and one partly/incipiently oxidized ore (from the North Chamber) form the basis of the study. The intention of this study is not to further develop flotation of the Great Dyke oxidized ores, but rather to understand the effect of the variability of the composition of an ore in its processing. The choices in the experimental work are guided to mimic those applicable to the current Great Dyke operations (for example, the grind is characteristic of the operations and not ultrafine grinding as in previous more fundamental studies). Figure 1.3 illustrates a summary of the scope of this study.

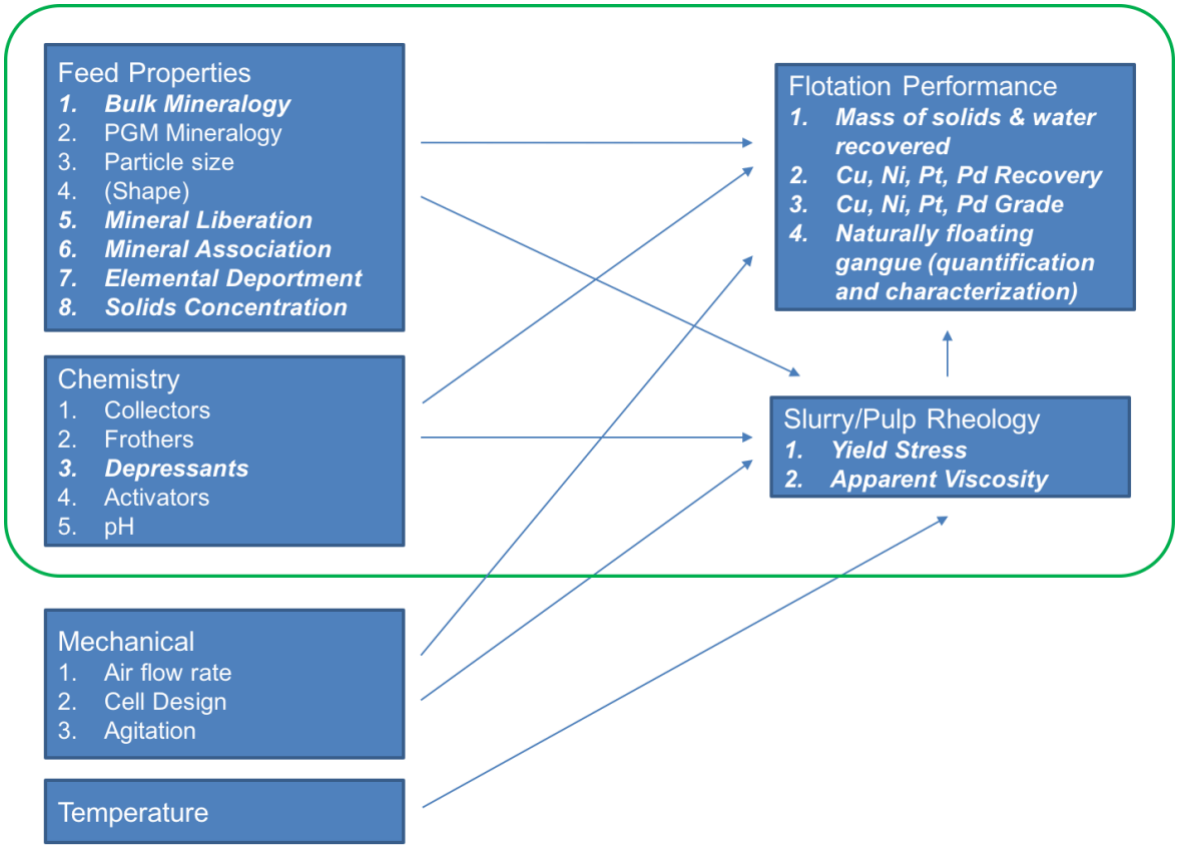

Figure 1.3: Scope of the study within the green box and work included in the study within this box is bold and italicized (e.g. *Bulk Mineralogy*).

A key contributor to the results obtained during flotation is the characteristics of the ore. The mineralogical characterization of each of the ores will be through the use of Quantitative Evaluation of Minerals by Scanning Electron Microscopy (QEMSCAN) which allows for the quantification of minerals as well as the determination of their liberation and association. The focus will be on the bulk mineralogy. Another factor that affects flotation performance is the flotation chemistry, and of interest in this study are depressants. In the experimental programme, three carboxymethyl cellulose (CMCs) depressants, with different degrees of substitution (DS), are compared in terms of their ability to depress the naturally floating gangue in flotation. The intention is not to optimize the depressant dosage, but rather to assess the effect of the different depressant types. The other reagents (that is, the collector and frother) and their dosages are kept constant throughout the flotation tests. All batch flotation tests are interrogated using a combination of copper, nickel, platinum and palladium and sulfur chemical assays, as well as measurement of entrained solids mass. Mechanical characteristics of the flotation cell are not varied in this study.

In the rheological assessment, the yield stress and viscosity will be calculated from the rheograms obtained at varying solid concentrations of each ore slurry. The same three depressants used in the flotation experiments, are assessed to determine the extent to which they alleviate the rheological complexities of these ores with high phyllosilicate mineral contents. In the rheological

investigation, the particle size distribution used is based on current plant particle size distributions, not the ultrafine sizes in which the particles are clearly within the colloidal regime.

Figure 1.4 shows the flow of the work as well as the key outputs.

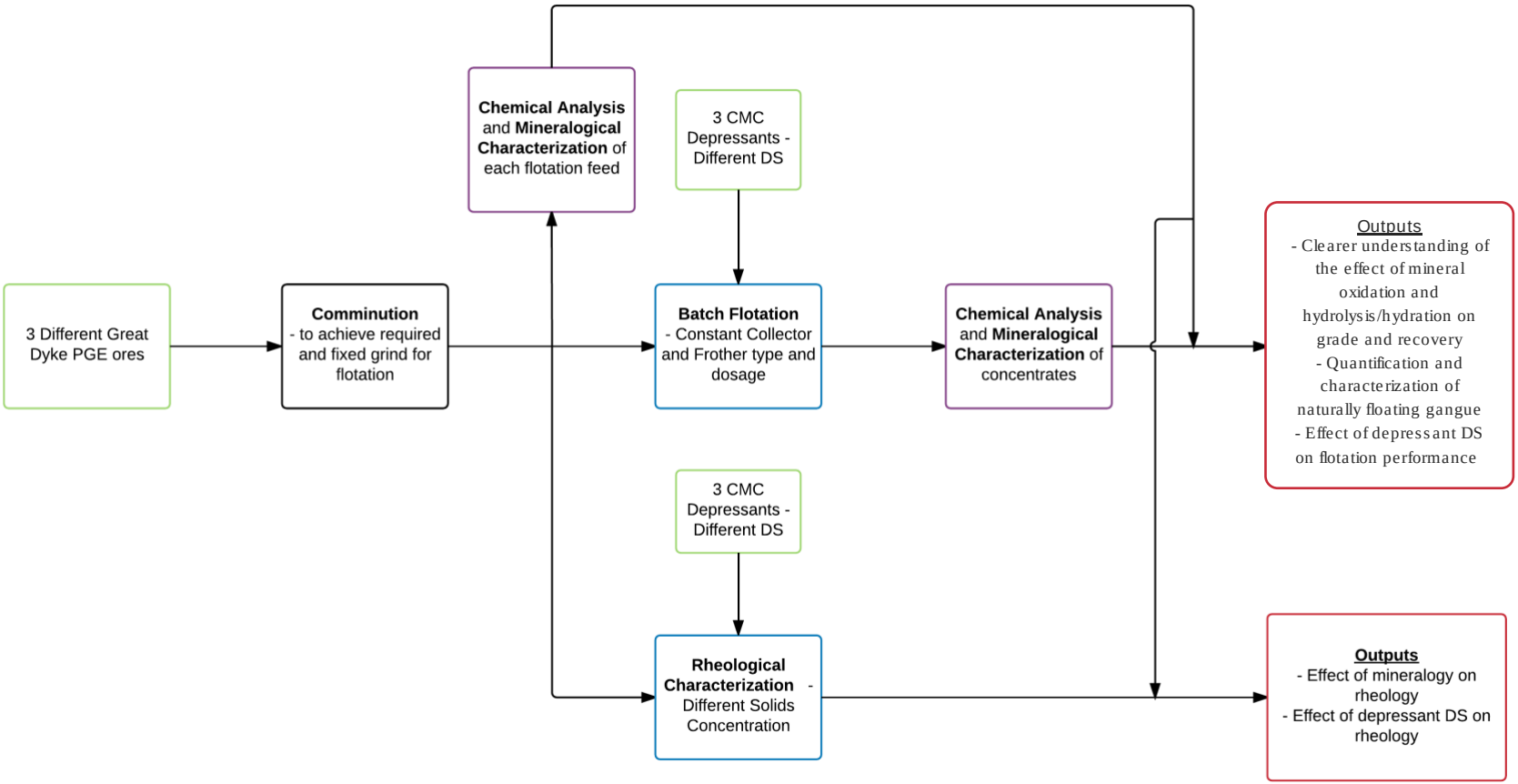

Figure 1.4: Schematic summarizing the flow of the work in the current study as well as key outputs

1.5 Dissertation Outline

After this introductory chapter comes Chapter 2 which discusses and reviews literature relevant to the current study. This is followed by Chapter 3 which details the Experimental methods used to answer the study's key questions. Chapter 4 is the Results and Discussion chapter after which the Conclusions and Recommendations are presented in Chapter 5.

Chapter 2 - Literature Review

The role process mineralogy plays in developing the optimum process parameters can never be overemphasized. It is vital to understand the mineralogy of both the valuable and gangue minerals so as to apply the most effective and profitable processing technique (Evans, 2002). Additionally, this understanding allows for the adaptation of a processing method and the design of flexible circuits which account for ore variability. The current standing of literature in process mineralogy with relation to PGE ores as relevant to this study is presented in this section.

The literature review begins with a brief description of alteration in PGE ores (Section 2.1) then an analysis of the current understanding of the characteristics of the Great Dyke PGE Pristine and Oxidized ores (Section 2.2). This is followed by Section 2.3 which details the current methods of processing the Great Dyke ores. Froth flotation with a focus on the Great Dyke ores and their mineralogy is explained in Section 2.4. This section additionally includes a review of the relationship between slurry rheology and flotation. Chapter 2 concludes with the hypotheses as well as key questions to guide the study in Sections 2.5 and 2.6 respectively.

2.1 Alteration in PGE ores

There are several types of alteration that may occur in PGE ores, some of which are oxidation, hydrolysis/hydration, silication and decarbonation, among others (Guilbert and Park, 2007). Of interest to this study are oxidation and hydrolysis/hydration. Oxidation results in the formation of oxides and sulfates from the former ferrous-ferric iron and sulfide mineralogies. Hydrolysis refers to the addition of H^+ leading to the conversion of anhydrous silicates (e.g. plagioclase) to hydrous ones (e.g. muscovite). Hydration is the addition of water to a certain mineral (for example the formation of talc from orthopyroxene as well as serpentine from olivine). Several studies have looked at alteration in PGE ores, though alteration has been loosely termed as oxidation. It may be necessary to decouple the two types of alteration (as oxidation or hydrolysis/hydration) that an ore may have undergone due to the differences in their effects on processing of PGEs as well as potential remedies to any adverse effects. Worth noting, is that these types of alteration have not been thoroughly decoupled in relation to the processing of PGE ores, which this study intends to do.

Some examples of the reactions mentioned above are shown here -

Example of Hydrolysis Reaction (Guilbert and Park, 2007):

$$\underset{\text{feldspar}}{3KAlSi_3O_8} + 2H^+(aq) \Leftrightarrow \underset{\text{mica}}{KAl_3Si_3O_{10}(OH)_2} + 6SiO_2 + 2K^+(aq) \qquad \text{(Equation 2.1)}$$

Example of Hydration Reaction (Guilbert and Park, 2007):

$$\underset{\text{olivine}}{2Mg_2SiO_4} + 2H_2O + 2H^+ \Leftrightarrow \underset{\text{serpentine}}{Mg_3Si_2O_5(OH)_4} + Mg^{2+}(aq) \qquad \text{(Equation 2.2)}$$

Example of Oxidation Reactions (Nordstram, 2011):

$$\underset{\text{pyrite}}{FeS_2} + \frac{7}{2}O_2 + H_2O \rightarrow Fe^{2+}(aq) + 2\,{SO_4}^{2-}(aq) + 2H^+(aq) \quad \text{(Equation 2.3)}$$

$$Fe^{2+}(aq) + \frac{1}{4}O_2 + H^+(aq) \rightarrow Fe^{3+}(aq) + \frac{1}{2}H_2O \quad \text{(Equation 2.4)}$$

$$Fe^{3+}(aq) + 3H_2O \rightarrow FeOH_3 + 3H^+(aq) \quad \text{(Equation 2.5)}$$

2.2 Characteristics of Great Dyke Pristine and Oxidized ores

The economic PGE mineralization of the Great Dyke lies in sulfide disseminations located in pyroxenites of the Main Sulphide Zone (Prendergast and Wilson, 1989; Wilson and Tredoux, 1990; Oberthür *et al.*, 2003; Locmelis *et al.*, 2010; Oberthür, 2011). The mineralization lies approximately 1000 m above the base of the intrusion and is characterized by relatively wide zones (approximately 1 – 3 m) of disseminated sulfides (pyrrhotite, pentlandite, chalcopyrite and pyrite) within pyroxenites (Prendergast and Wilson, 1989; Oberthür *et al.*, 1997; Maier, 2005). Sub-economic PGE concentrations are found in the Lower Sulphide Zone (LSZ) tens of meters below the MSZ and additionally within the chromite layer (Oberthür, 2011; Oberthür, 2002). As was explained in Chapter 1, the Great Dyke is split into pristine and refractory oxidized ores whose mineralogy is detailed in the following section.

2.2.1 Pristine MSZ

Since the MSZ lies within the pyroxenite (rock type rich in pyroxene) layer, the gangue of the pristine MSZ ores is mainly made up of orthopyroxene (approximately >80 vol.%), with approximately 10 – 15 vol.% plagioclase and up to 7 vol.% clinopyroxene (Oberthür *et al.*, 1997; Wilson *et al.*, 2000; Wilson, 2001; Li *et al.*, 2008). The hydrous alteration silicates present within the ores include the phyllosilicates (talc, chlorite) and amphiboles (actinolite, tremolite) and these are associated with quartz, apatite and carbonates (Oberthür *et al.*, 1997; Li *et al.*, 2008). These hydrous silicates are ubiquitous in some areas of the MSZ (Wilson *et al.*, 2001) which may result in challenges in the processing of the ores. Of particular interest to this study is talc alteration which has been found to occur in orthopyroxene microfractures and in the margins of orthopyroxene in contact with actinolite and carbonates.

The average sulfide content within the MSZ is 2% with values ranging from 0.1 – 10%. Larger sulfide grains are made up of pyrrhotite and pentlandite (Oberthür *et al.*, 1997; Oberthür, 2003a). The main sulfide minerals present are pyrrhotite, pentlandite, chalcopyrite and low amounts of pyrite (Prendergast and Wilson, 1989; Oberthür *et al.*, 1997; Oberthür *et al.*, 2003a; Li *et al.*, 2008; Locmelis *et al.*, 2010; Oberthür *et al.*, 2013). The sulfide grains mostly occur interstitial to grains of cumulus orthopyroxene and minor chromite, intercumulus clinopyroxene, plagioclase, and alteration products such as calcic amphibole, anthophyllite, magnetite, serpentine, talc, and chlorite (Oberthür *et al.*, 2013; Wilson, 2001). Pentlandite mostly forms homogenous grains within sulfide

aggregates, while chalcopyrite concentrates at the periphery of sulfide aggregates and individual pyrite crystals may be found at the margins of the aggregates (Oberthür *et al.*, 2003a).

It is well accepted that the PGM are usually associated with pyrrhotite or chalcopyrite and rarely in pentlandite (Coghill and Wilson, 1993; Wilson *et al.*, 2000, Locmelis *et al.*, 2010; Oberthür, 2011). An alternative view is that the PGM are located mainly at sulfide/silicate or sulfide/sulfide grain boundaries and rarely within primary anhydrous silicates but more likely within hydrous silicates (e.g. talc, chlorite) (Wilson *et al.*, 2000; Li *et al.*, 2008; Locmelis *et al.*, 2010). It has also been found that most of the Pd and Rh in the MSZ ores of the Great Dyke are hosted in pentlandite while Pt is mainly found in a discrete PGM (Weiser *et al.*, 1998; Oberthür *et al.*, 2000, Oberthür *et al.*, 2003a; Oberthür, 2011).

Nashwa (2007) found that the amount of talc present in the flotation feed of an ore from the Southern Chamber of the Great Dyke was 16 ± 1 %, which is similar to the value obtained by Becker *et al.* (2013). The quantitative mineralogy of the Great Dyke Pristine ore as found by Becker *et al.* (2013), which is in close agreement with findings by Nashwa (2007) is shown in Figure 2.1.

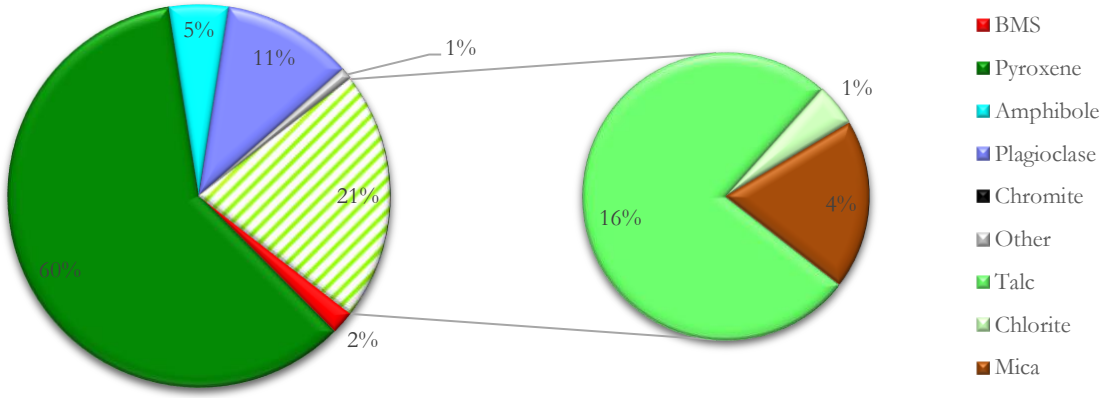

Figure 2.1: Flotation feed mineralogy obtained in a study on Great Dyke mineralogy (Becker *et al.*, 2013). The larger pie chart shows the presence of pyroxene as the major component. The smaller chart is made up of the phyllosilicates which are 21% of the feed and are subdivided into Talc (16%), Chlorite (1%) and Mica (4%). Serpentine content was negligible.

The North and South Chambers

The North Chamber of the Great Dyke has a much greater volume and is thicker than the South Chamber (Wilson, 1996; Wilson *et al.*, 2001). Additionally, the North Chamber has well developed pyroxenite layers while olivine pyroxenites predominate over the pyroxenites within the upper section of the South Chamber (Oberthür, 2011). Wilson (2001) emphasizes this point, noting that for ore from the North Chamber the percentage pyroxene is greater than 90% while in the South Chamber this ranges from 75 – 90%. There is a difference in the average PGM grain size of the two chambers (39 µm in the North chamber compared to 18.5 µm in the South chamber) and this

is expected to have implications on the processing of the ores (Oberthür, 2011). A further difference between the northern and southern chambers of the pristine MSZ is that 77% of the PGEs occur as bismuthotellurides in the northern chamber while 50% of the PGEs are sulfarsenides and arsenides (as a result of preferential combination with arsenic) (Oberthür, 2011) in the South chamber.

2.2.2 Oxidized/Supergene MSZ

An extreme level of alteration is exhibited in the near surface oxidized MSZ ore. The oxidized ores are split between pervasively oxidized and those showing incipient oxidation (Oberthür *et al.*, 2013). Oberthür *et al.* (2013) additionally noted that the pervasively oxidized ores occur closer to the surface (from the surface down to approximately 10-15 m in the case of Ngezi Mine) while those exhibiting incipient oxidation and containing some relict sulfides lie below the pervasively oxidized ores (approximately 15-30 m beneath the surface in the case of Ngezi Mine). The main constituent of the oxidized ores is again cumulus orthopyroxene (> 80 vol.%), some clinopyroxene and plagioclase (Locmelis *et al.*, 2010; Kraemer *et al.*, 2015). The primary constituents are to some extent replaced by hydrothermal products mainly talc, chlorite, tremolite and actinolite (Li *et al.*, 2008, Oberthür *et al.*, 2013). These alteration products can be seen as rims around the primary minerals, as 'bands' within minerals or patches of talc, chlorite and Fe, Mn hydroxides.

The relict base metal sulfides present are pyrrhotite, pentlandite and chalcopyrite (in approximately equal amounts), while there are low amounts of pyrite (Locmelis *et al.*, 2010). These BMSs are enclosed within pyroxenes and plagioclase, within secondary hydrous silicates (amphiboles, talc and chlorite), within weathering products like Fe and Mn oxides/hydroxides or as sulfide droplets interstitial to the primary silicates (Locmelis *et al.*, 2010). Most of the BMS that would have made up the pristine ore would have been decomposed to iron-hydroxides now often associated with smectites (Locmelis *et al.*, 2010).

There is a difference in the ores' PGM assemblages as well as redistribution of the PGEs thus affecting the processing of these ores (Locmelis *et al*, 2010; Oberthür, 2011; Oberthür *et al.*, 2013). These PGEs now occur in either iron-hydroxides, smectites or within discrete PGE oxides or hydroxides (Evans, 1994; Oberthür, 2011; Oberthür *et al.*, 2013; Becker *et al.*, 2014). According to Oberthür *et al.* (2013) most of the Pt,Pd-bismuthotellurides would have disintergrated. Some of the base metal and PGE sulfides may also be disintegrated resulting in them having released a portion of their initial base metal or PGE content. Sperrylite and cooperite/braggite grains remain as relict PGMs due to their stability. Some PGE either form secondary PGMs (in Pt/Pd oxides or hydroxides, Mn-Co hydroxides and secondary silicates). Sulfarsenides are present in pristine ores from the South Chamber but not in oxidized ores. A summary of the redistribution of Pt and Pd as presented by Oberthür *et al.* (2013) is shown in Figures 2.2 and 2.3. The oxidized ores have higher Pt/Pd ratios (2 - 5) compared to the pristine/sulfidic ores (between 1.3 and 1.7) (Stribrny *et al.*, 2000, Evans *et al.*, 2002; Oberthür *et al.*, 2013). This observation is attributed to the higher mobility of Pd compared to Pt in the supergene environment, and consequently Pd is removed from the ores (Evans, 1994; Oberthür, 2002, Oberthür and Melcher, 2005). Furthermore, S and Pd are depleted while Cu and Au are enriched (Locmelis *et al.*, 2010).

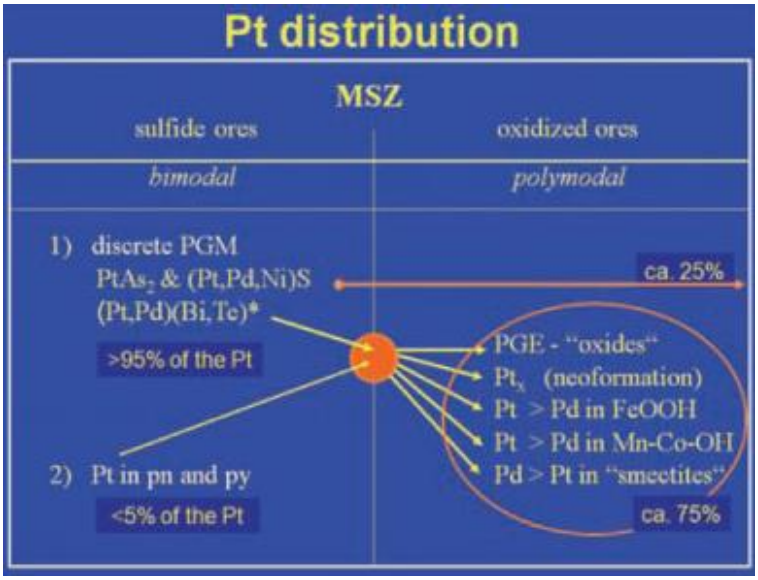

Figure 2.2: Graph summarizing trends in the distribution of Pt from pristine/sulfide ores to oxidized ores (Oberthür *et al.*, 2013). *(Pt,Pd)(Bi,Te) = (Pt,Pd)-bismuthotellurides

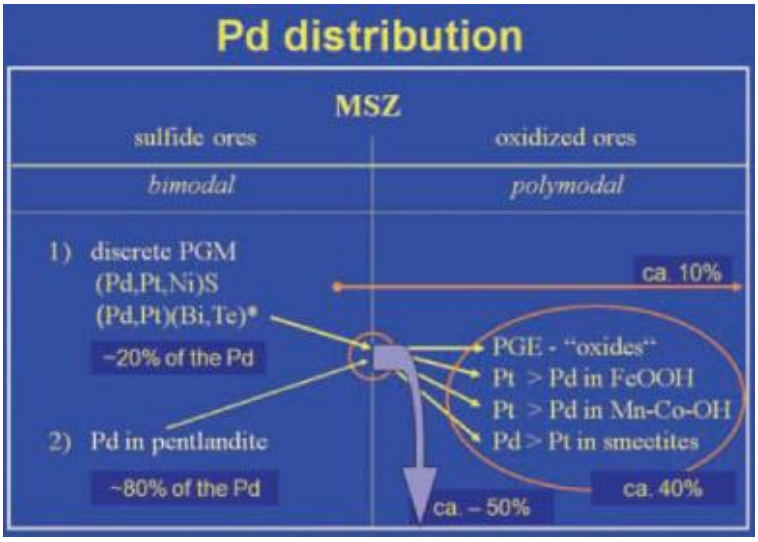

Figure 2.3: Graph summarizing trends in the distribution of Pd from pristine/sulfide ores to oxidized ores (Oberthür *et al.*, 2013). *(Pt,Pd)(Bi,Te) = (Pt,Pd)-bismuthotellurides

2.2.3 Phyllosilicates

As mentioned before, it is imperative to understand gangue mineralogy in order to be able to predict problems and improve the separation performance in mineral processing (Evans, 2002; Ndlovu *et al.*, 2013). Among the common gangue minerals of both the pristine and oxidized ores are phyllosilicate minerals. Ndlovu *et al.* (2013) note that phyllosilicates are a common accessory mineral in several mineral deposits of which the Great Dyke pristine MSZ and oxidized MSZ are no exceptions. Evidence of this can be seen in Figure 2.1, where 21% of the sampled ore is made up of phyllosilicates. Phyllosilicates are common alteration products of anhydrous primary minerals. Their structure represented by tetrahedral and octahedral layers is shown in Figure 2.4. The word *phyllos* is Greek for leaf, and phyllosilicates are so named because of their platy structure. Finding these minerals within the MSZ ores is not unexpected as these ores have been subjected

to significant late stage alteration (Prendergast, 1990; Coghill and Wilson, 1993; Li *et al.*, 2008). Phyllosilicates have the potential to affect the planning, operations and performance of a project significantly (Ndlovu *et al.*, 2013).

The specific distinguishing characteristics of phyllosilicate minerals include their colloidal particle size, anisotropic charge properties and irregular shape (Ndlovu *et al.*, 2013). Due to their high surface area to volume ratio their surface charge has a greater effect on the mineral slurry. Additionally, their small size also makes it possible for the phyllosilicates to be easily entrained (Arnold and Aplan, 1986). The distinctive morphology and electrical surface charge of clay mineral particles are key factors in their rheological behavior (Ndlovu *et al.*, 2011b).

The shape of phyllosilicate minerals is irregular (non-spherical) as many of them have a platy morphology. This leads to greater rheologically complex particle behavior (Barnes *et al.*, 1989). Additionally, non-Newtonian behavior is consistent with greater length/diameter (L/D) ratios which are characteristic of phyllosilicates (Horie and Pinder, 1979).

The edges of phyllosilicate mineral particles have a different charge to that on the faces of the particles. The faces of these minerals are considered to carry a permanent negative charge due to isomorphous substitution of higher valence cations with lower valence cations (e.g. Hendricks, 1942; van Olphen, 1951; Zhou and Gunter, 1992; Sposito *et al.*, 1999; Johnson *et al.*, 2000; Ndlovu *et al.*, 2013). Ndlovu *et al.* (2013) further suggest that the change of the charge on the basal plane with pH may be attributed to the pH dependent ionization of the silanol (Si-O-H) groups that are exposed on the surface of the minerals. The charge on the edges is thought to be as a result of the exposed hydroxyl groups thus at lower pH the edges are positively charged and the converse is true at a higher pH.

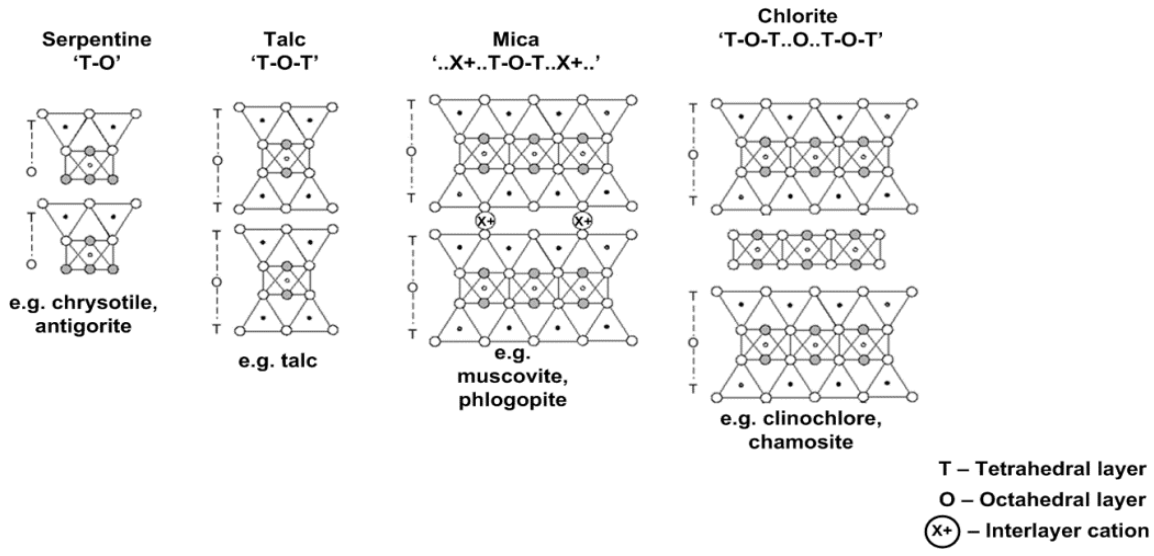

Figure 2.4: Structure of Phyllosilicate Minerals (Ndlovu, 2013)

The charge heterogeneity results in the irregular stacking of the phyllosilicate minerals. The three prevalent modes of particle interaction have been found to be edge-face (EF), edge-edge (EE) and

face-face (FF) as can be seen in Figure 2.5. Lamellar/scale-like structured aggregates are a product of FF interactions and have low yield stress, however, 3D voluminous structures which are associated with complex rheological behaviour are the result of EE and EF interactions (e.g. Johnson *et al.*, 1998; Gupta *et al.*, 2011).

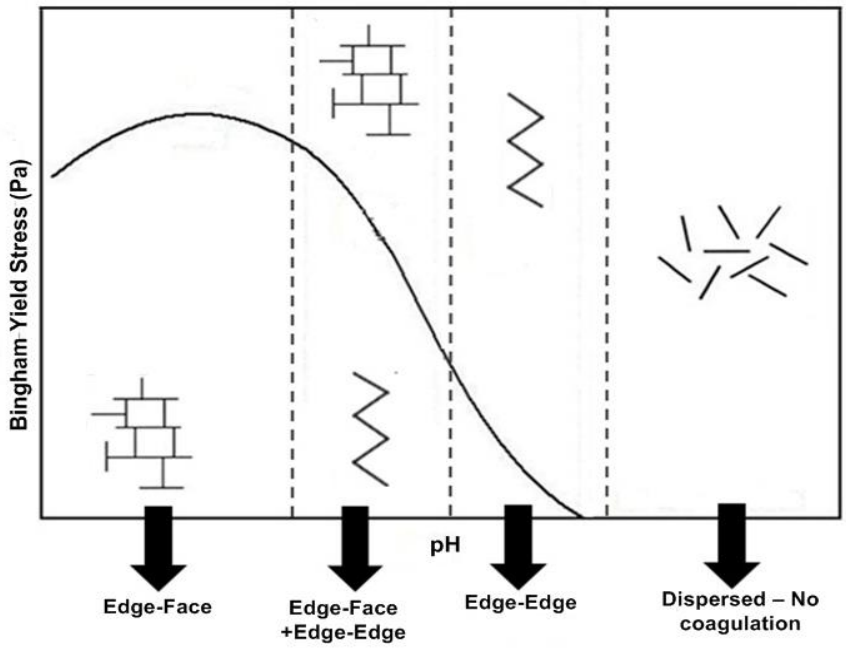

Figure 2.5: Van Olphen theory, adapted from Rand and Melton (1977) in Ndlovu (2013)

Becker *et al.* (2009) point out that the presence of talc can lead to large amounts of naturally floating gangue (NFG) reporting to the concentrate due to its association with orthopyroxene which usually makes up the bulk of the ores. The inadvertent flotation of orthopyroxene possessing talc rims due to talc's natural floatability has also been discussed by Lotter *et al.* (2008) and Jaseniak and Smart (2009). This is just one of the challenges phyllosilicate minerals pose in flotation. Some of the other challenges include effect on flotation kinetics, slime coating, higher entrainment because of increased froth stability, increased pulp viscosity which in turn increases or decreases froth stability and higher reagent consumption (Ndlovu *et al.*, 2013; Tao *et al.*, 2010; Patra *et al.*, 2010; Connelly, 2011; Farrokhpay, 2011).

2.3 Current Metallurgical processing of Great Dyke PGE resources

The metallurgical processing of sulfide PGE ores from the Great Dyke consists of crushing, grinding, and froth flotation (Evans, 2002). The PGM grains usually float along with the sulfides; as discrete PGM grains or attached to (or enclosed within) sulfide grains. Pristine MSZ ores give recoveries > 80%, whereas oxidized ore recovery is < 50% (Oberthür *et al.*, 2013). As earlier stated, attempts to process the oxidized ores have led to recoveries lower than 50% by either gravity concentration or flotation (Oberthür, 2003a). The flotation challenges include the ubiquitous presence of talc, the low concentration and fine dispersion of sulfides, poor BMS liberation as well

as the small size of the PGM grains lacking association with BMS requiring finer grinding while this would at the same time liberate more of the deleterious talc (Oberthür, 2003a; Becker *et al.*, 2014).

As a result of the low recoveries currently being obtained in the processing of the oxidized ores, Oberthür *et al.* (2013) and Evans (2002), among other authors, point out the need for novel methods to be developed for the processing of oxidized ores. This may take time however and thus there is a need to look at the currently available methods, like froth flotation (Prendergast, 1990). Prendergast (1990) and Evans (2002) highlight that novel methods would require large scale technical equipment or expensive chemicals which would not be economically viable, not to mention the lengthy processes of accepting and commissioning new methods of ore treatment.

Average Pt recoveries of between 30 and 80% have been achieved by Kraemer *et al.* (2015) in their work on oxidized ore samples from the Great Dyke. This was through the use of a multistep hydrometallurgical process that included the use of mildly acidic hydrochloric acid prior to leaching with the biogenic siderophore Desferrioxamine B. The authors do mention though that due to the corrosive nature of the pretreatment, alternative methods to heap leaching need to be considered. Despite this, flotation may be used as a concentration step prior to the leaching to reduce the processed volumes of ore.

The use of pyrometallurgy would require an ore of a very high grade (which is not the case with the Great Dyke oxidized ores) or that which has been pre-concentrated (Evans, 2002; Kraemer *et al.*, 2015). The reason for requiring ore of a high grade or that has been pre-concentrated would be to minimize the power consumption per unit metal produced at the smelter, which may be excessive when high volumes of ore are treated.

On the whole, it is necessary to individually assess mining operations, especially with the uniqueness of the Great Dyke PGE ores. Improved recoveries have been achieved through the use of clay and gangue depressants/dispersants and PGE collectors during flotation (Bulatovic, 2003; Locmelis *et al.*, 2010). It is believed that the analysis of various flotation reagent schemes, which this study intends to do, will allow improved recoveries to be attained while allowing the processing plants to use their already existing concentrators (Becker *et al.*, 2014). Though the outcome may not be that of processing the oxidized ores, it is intended that as a result of this study the processing plants would be able to more effectively handle ores of variable alteration.

2.4 Froth Flotation

Flotation is an important process in the flotation of sulfide PGE ores in order to concentrate slurries prior to smelting. It is a physicochemical process that takes advantage of the differences between valuable and gangue mineral surface properties. It consists of two phases, namely the pulp and froth phases. The hydrophobicity of a mineral surface leads to bubble-particle attachment which occurs as air is sparged through a pulp. As the bubbles rise they carry the hydrophobic minerals upwards into the froth phase. Non-selective entrainment and entrapment of particles may

occur as a result of particles reporting with the water associated with the liquid film surrounding bubbles within the froth phase. Conventional flotation (as is the case with PGE operations) is when the valuable mineral is recovered in the concentrate and reverse flotation is when the gangue/unwanted mineral(s) is recovered to the concentrate while the valuable mineral is recovered in the tails.

2.4.1 The Pulp and Froth Phases

Pulp phase

Valuable mineral extraction takes place in the pulp phase. Bradshaw *et al.* (2005) highlight the importance of creating a physically and chemically conducive environment for promoting the collision of bubbles and particles, successful attachment and transportation of the valuable minerals into the froth phase, and ensuring the unwanted particles are hydrophilic and thus are not attached to the bubbles. This physically and chemically conducive environment consists of many different parameters. These include surfactants to inhibit bubble coalescence, correct energy input for the particle size, an optimum air flow rate, correct pH and Eh for the minerals and reagents being used, amongst others.

Froth phase

The froth zone is the means by which the valuable minerals are transported to the concentrate and subsequent processing stage and this should be done without any loss of the valuable minerals in the process. According to Kawatra (2002), the structure of the froth is such that it enhances the selectivity of the overall flotation process. The structure of the froth also allows for water to drain and to ensure removal of entrained gangue. The amount of entrained gangue is proportional to the amount of water recovered during flotation (Engelbrecht and Woodburn, 1975). This therefore implies that when water recovery is lower, the amount of entrained gangue is also lower and there are higher valuable mineral grades. This makes the stability of the froth an important parameter as it affects the grade of the concentrate through the loss or retention of entrained gangue (Neethling and Cilliers, 2002a). A summary of the effect of relative froth stability on valuable mineral grade and recovery is shown in Table 2.1.

Table 2.1: Relative froth stability and its associated valuable mineral grade and recovery (Based on Bradshaw *et al.*, 2005)

Stability	Valuable Mineral Grade	Valuable Mineral Recovery
"Too stable"	Low grade because of the high amount of entrained gangue	No loss in valuable mineral recovery
"Too unstable"	High grade of valuable mineral as much of the entrained gangue is lost	Reduced recovery of the valuable mineral as there are losses due to bubble bursting and shedding of their attached valuable minerals

Wiese *et al.* (2011) noted the following as factors affecting froth stability: flotation reagent concentrations (particularly the frother), water quality, size and nature (hydrophobicity) of particles attaching at the air-water interface. It has been shown that oxidized ores high in talc produce very stable froths that lead to processing difficulties (Voyi and Wilson, 2015).

Measuring Froth Stability

Several tests for measuring froth stability have been established. These methods include air recovery, water recovery, froth rise velocity, image analysis of bubbles, among others (e.g. Barbian *et al.*, 2003; Aktas *et al.*, 2008; Barbian *et al.*, 2005; Ventura-Medina and Cilliers, 2002; Morar *et al.*, 2006; de Jager *et al.*, 2004; Zanin *et al.*, 2009). The froth stability tests fall under the categories of dynamic and static tests (Bikerman, 1973). Dynamic tests are those in which there is air input and the froth reaches a dynamic equilibrium between the rate of its rise and the rate of its decay (Barbian *et al.*, 2003; Bikerman, 1973). The static test is the one in which the froth has reached a maximum height and its rate of decay is measured while the air supply is closed and without any agitation. The dynamic method is more representative of industrial flotation cells in which an equilibrium exists between the bubble formation, drainage and bursting (Hunter *et al.*, 2007; Barbian *et al.*, 2003).

The tests can take the form of non-overflowing systems or continuous systems. Continuous systems allow the overflowing of the froth for collection of the concentrate while non-overflowing systems do not. The concentrate in this study will be assessed in the batch flotation test and thus the system used in this case does not need to allow for collection of the froth.

In the dynamic froth stability test proposed by Bikerman (1973), gas (at a specified flowrate) is passed through a column and the rise in froth or foam height measured as a function of time until it has reached its maximum height (equilibrium). Barbian *et al.* (2003) extended this test to mineral flotation froths in order to measure froth stability.

Dynamic Froth Stability Measurement

The dynamic method of measuring froth stability as developed by Bikerman (1973) was used in this study. In this method, the rise in froth height (H) is noted with time (t). After some time, the froth height ceases to increase and this is noted as maximum froth height, H_{max}. According to Bikerman (1973), the dynamic stability factor, Σ, is the ratio between the maximum volume of foam (V_f) or froth generated and the air flowrate (Q).

$$\Sigma = \frac{V_f}{Q} = \frac{H_{max} \times A}{Q} \qquad \text{(Equation 2.6)}$$

Where A = cross sectional area of the frothing column.

Barbian *et al.* (2003) noted the importance of froth rise and found that it can be modelled to Equation 2.7. Detailed steps of how this was applied are shown in the Appendix (Section 7.2).

$$H(t) = H_{max}\left(1 - e^{-\frac{t}{\tau}}\right) \qquad \text{(Equation 2.7)}$$

Where H(t) represents the froth height as a function of time (t), H_{max} is the maximum froth height achieved and τ is the characteristic average bubble lifetime.

2.4.2 Flotation Reagents

Reagents are used in flotation to alter or enhance the surface properties of either the valuable or gangue mineral. Reagents alter the pulp chemistry and enhance the desirable surface properties of minerals i.e. hydrophobicity of valuable minerals and hydrophilicity of gangue minerals, in order to improve their flotation response. The addition of reagents allows for improved flotation of the valuable minerals (collectors and activators) while reducing the amount of unwanted minerals that float (depressants). Collectors and activators improve the hydrophobicity of the valuable mineral surface while depressants cause the surface of the unwanted or gangue minerals to be hydrophilic.

Frothers are heteropolar organic compounds that aid bubble formation and stabilize the froth which is necessary for the above stated reasons. Collectors are heteropolar molecules that have a polar group that interacts with the mineral surface while the non-polar hydrocarbon chain brings about the particles' hydrophobicity (Bradshaw *et al.*, 2005). Of these the most popular collectors for BMS and PGM flotation are xanthates. It has been noted that the longer the hydrocarbon chain, the more hydrophobic the mineral surfaces and thus achieve greater recovery in the pulp zone (Taggart, 1945; Dimou, 1986; Ackerman *et al.*, 1987; Bradshaw *et al.*, 2005; Bulatovic, 2007). However, highly hydrophobic particles may have a destabilizing effect in the froth zone. This study focuses on depressants and thus these shall be investigated in more depth.

Depressants

These molecules inhibit the flotation of a particular mineral and fall into two categories, inorganic or polymeric. Inorganic depressants adsorb onto hydrophilic mineral surfaces, while polymeric ones adsorb onto mildly hydrophilic or hydrophobic mineral surfaces and render them hydrophilic (Laskowski and Pugh, 1992). The organic depressants include carboxymethyl celluloses (CMCs) and guars.

CMCs are anionic polysaccharides that are made of individual glucose units as can be seen in Figure 2.6. A property of interest when it comes to CMCs is their degree of substitution (DS) which represents the average number of carboxyl groups per monomer unit. It thus represents the extent of the negative charge on the CMCs. DS may get to a maximum of 3 though the average industrial CMCs have DSs from 0.4 – 1.2 (Board, 2002). A higher DS is thus thought to reduce the rheological complexities associated with ores possessing high amounts of phyllosilicate minerals as is expected of Great Dyke ores. This is because of the greater dispersion of mineral particles resulting from the repulsion of the more negatively charged CMCs.

Depressants are particularly used when hydrophobic gangue minerals such as talc are present (Morris *et al.*, 2002). The depressants adsorb onto the hydrophobic planes of such minerals rendering them hydrophilic. Talc is naturally floatable as a result of its inherent hydrophobicity (Dippenaar, 1978) and as its concentration in the pulp increases it has the effect of stabilizing the froth. Depressants affect froth stability in two ways: Reduce the amount of froth stabilizing gangue

in the froth, thus reducing froth stability and/or slime-cleaning of sulfide minerals due to electrostatic repulsion of slimes, producing very hydrophobic particles that destabilize the froth.

As the focus of the study will be on depressants that will combat the NFG it was necessary to focus on various depressants and their effect on flotation performance. This NFG is likely to be similar to that observed by Becker *et al.* (2009) for Merensky ore from the Bushveld Complex in South Africa due to their similar mineralogical composition. A major difference between the Merensky and Great Dyke ore samples will possibly be the greater degree of alteration of the Great Dyke samples. The NFG of these PGE ores, as earlier mentioned is mainly composed of orthopyroxene that is composite with talc or that has talc rims (Nagaraj and Brinen, 1995; Becker *et al.*, 2006; Lotter *et al.*, 2008; Becker *et al.*, 2009).

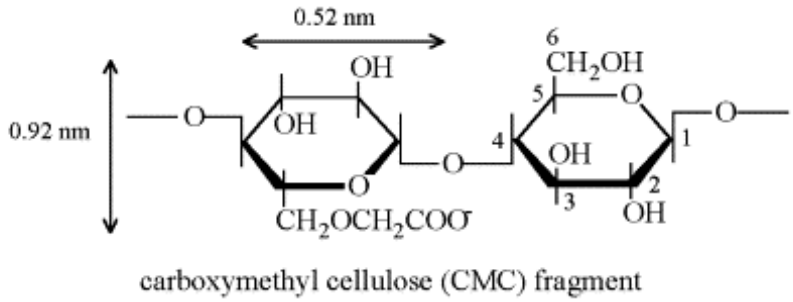

Figure 2.6: Carboxymethyl Cellulose Fragment (Morris *et al.*, 2002). The extended conformation is due to electrostatic repulsion of the anionic carboxylate groups (Kästner et *al.*, 1997)

2.4.3 Rheology and its effect on flotation

Background

Rheology is the science of deformation and flow of matter under applied stress. It is affected by the solids concentration, particle size distribution, temperature, surface charge distribution and of particular interest to this study, mineralogy. The flow curve or rheogram (a plot of shear stress against shear rate) is often used to graphically present rheological behavior. Rheological behavior is indicative of the level of inter-particle interactions or aggregation (Farrokhpay, 2012). Understanding of the rheological properties therefore allows better understanding of bubble-particle interactions in mineral slurries, with yield stress and viscosity being useful indicators of the degree of aggregation or dispersion. Slurries of high viscosity inhibit gas dispersion and slow the bubble-particle attachment rate.

Fluids exhibit either Newtonian or non-Newtonian behaviour. Non-Newtonian fluids include those that follow plastic, pseudo plastic, Bingham plastic and dilatant behaviours. As can be seen in Figure 2.7, a Newtonian fluid exhibits a linear relationship between its shear stress and shear rate. Important terms within rheological studies include yield stress and viscosity. Yield stress is the intercept of the flow curve on the shear stress axis at zero shear rate, while viscosity is the slope of the line connecting a particular point on the flow curve with the origin. It is clear that this slope is constant for fluids exhibiting Newtonian behavior but varies for those exhibiting non-Newtonian behavior. The viscosity of a non-Newtonian fluid at a chosen shear rate is thus referred to as 'apparent viscosity'.

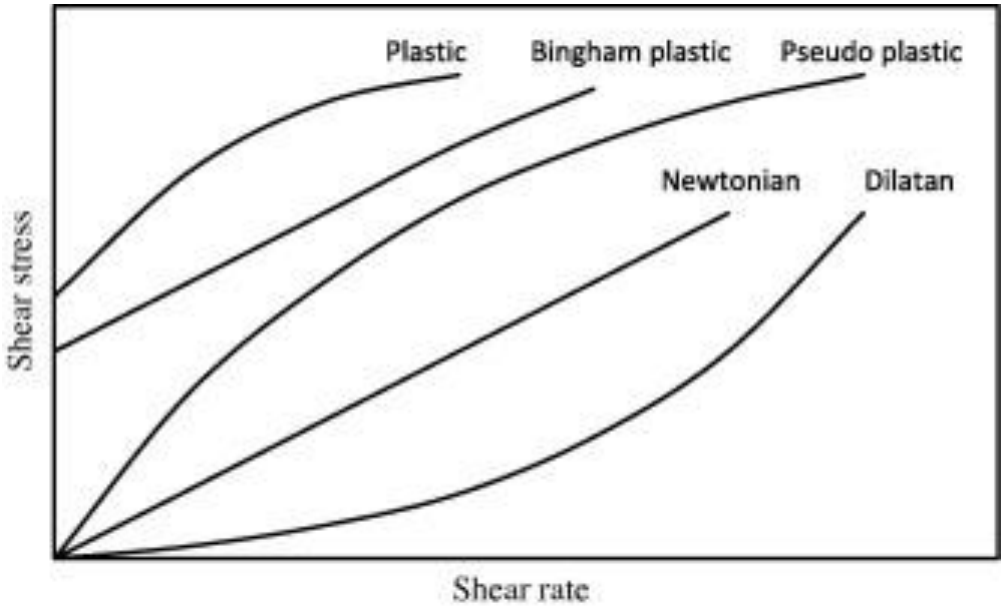

Figure 2.7: Schematic diagram of shear rate as a function of shear stress for different fluids

Mineral suspensions usually exhibit Bingham or pseudo-plastic behavior. The Bingham or Casson models are used in order to estimate the rheological properties (viscosity and yield stress) (Farrokhpay, 2011). This is due to the difficulty associated with conducting measurements at very low shear rates, resulting in the need for extrapolation using mathematical models. The above-mentioned models are as follows:

Bingham Model:

$$\tau = \tau_B + \eta_{pl} D \qquad \text{(Equation 2.8)}$$

Casson Model:

$$\tau^{\frac{1}{2}} = {\tau_B}^{\frac{1}{2}} + \left(\eta_{pl} D\right)^{\frac{1}{2}} \qquad \text{(Equation 2.9)}$$

where η_{pl} is the plastic viscosity, D is the shear rate, τ_B is the yield stress, and τ is the shear stress. (Note that the yield stress is the y-intercept of Equation 2.8).

Effect of Rheology on Flotation

Burdukova *et al.* (2006) emphasizes the extreme importance of rheological measurements stating that the efficiency of many processes depends on the rheological properties of the medium. The need for such measurements has been further amplified because of the need to grind finer to liberate valuable minerals with reducing ore grades. The rheological characteristics of particles are more pronounced at these fine sizes. Finer particles at higher solids concentration result in non-Newtonian behavior. An additional factor that affects slurry rheology is the mineralogy of the ore. Minerals such as phyllosilicates affect the rheology of the slurry and hence flotation. This

rheologically complex behavior leads to a change in the cell hydrodynamics and thus gas dispersion in flotation.

Gas dispersion is necessary for particle-bubble attachment, which is the mechanism by which flotation takes place. According to Gomez *et al.* (2003), gas dispersion defines flotation efficiency after the flotation chemistry has been established. Based on the findings of Bakker *et al.* (2010) it is expected that complex rheological behavior can lead to the formation of a 'cavern' of slurry around the impeller zone where there is poor dispersion of the tiny gas bubbles, thus leading to a decrease in gas hold-up. The above phenomenon is linked to ultrafine particles and/or ores containing minerals that are known to negatively affect rheology, an example being phyllosilicates.

Research by Zhang and Peng (2015) has suggested that an optimum viscosity exists depending on the minerals present within an ore. In their study, in spite of higher pulp viscosities corresponding to lower copper recoveries, a slight increase in pulp viscosity enhanced gold flotation but any further increase led to a decrease in its flotation. The initial enhancement in gold recoveries may be attributed to a decrease in cell turbulence. It is worth noting that free minerals (those not associated with sulfides) as well as coarse particles benefit from high pulp viscosities and aggregation as this increases the stabilization of bubble-particle aggregates (Zhang and Peng, 2015; Farrokhpay *et al.*, 2011). The need to operate at an optimum slurry rheology can however be overshadowed by other factors such as the fact that lower viscosity requires a greater dilution with water, which leads to a shorter residence time (Bakker *et al.*, 2010). Additionally, the need to use water sparingly cannot be overemphasized.

It has been found that phyllosilicate gangue minerals are major contributors to flow behavior (Burdukova *et al.*, 2008; Shabalala *et al.*, 2011). Rheology is affected by the type of phyllosilicate mineral present in the slurry (Burdukova *et al.*, 2008; Ndlovu *et al.*, 2011a, 2011b, 2014; Zhang and Peng, 2015). It is expected that in the current study there may be several different types of phyllosilicate minerals present (for example talc and chlorite) which will result in different rheological effects and thus affect flotation. Zhang and Peng (2015) found that poorly crystallized kaolinite affected viscosity more than the well crystallized variant because of its possession of more individual edges and corners resulting in greater friction (Murray and Lyons, 1956; Zhang and Peng, 2015). Additionally, the authors found that bentonite, a 2:1 structured swelling clay mineral, increased pulp viscosity more significantly than kaolinite, a 1:1 structured clay mineral. This was attributed to bentonite being a swelling clay as well.

Some rheological tests on Great Dyke slurries were conducted by Becker *et al.* (2013). The authors found that the ore from the Great Dyke presents more rheologically complex behavior when compared to UG2 ore (from the Bushveld Complex in South Africa) due to the Great Dyke's higher content of phyllosilicate minerals (talc and chlorite, 16 wt.% and 2 wt.% respectively while the UG2 sample had 2 wt.% talc and 2 wt.% chlorite). Comparing the Great Dyke feed and concentrate: The Great Dyke flotation concentrate showed high yield stress and viscosity at low solid concentrations (from 20 to 30 vol.% solids) while the Great Dyke feed exhibited this between 33 and 45 vol.% solids. This difference was attributed to particle size and mineralogical effects.

The concentrate had a finer particle size distribution (d50 of 13 μm compared to 100 μm for the feed) hence the particle surface charge effects that contribute to rheological complexity were more pronounced. The higher percent of talc in the concentrate than in the feed (32 wt.% and 16 wt.%, respectively) due to talc's floatability especially in this case where it had not been fully depressed. Rheologically complex behavior is usually attributed to particle size effects, solids concentration, surface chemistry and mineralogy. When the dominant constituent minerals (orthopyroxene and plagioclase) in the Great Dyke ore were analyzed it was found that these non-phyllosilicate minerals did not exhibit rheological complexity at solid concentrations of less than 50 vol% solids. The two reasons for the rheologically complex behavior associated with the phyllosilicates are their irregular surface charge distribution as well as irregular platy morphology (Rand and Melton, 1997).

Studies that have investigated the effect of phyllosilicates on slurry rheology agree in their findings (Becker *et al.*, 2013; Ndlovu *et al.*, 2014; Zhang and Peng, 2015). This, as was stated by Ndlovu *et al.* (2014), is that some serpentines (fibrous phyllosilicates) are the most rheologically complex, while micas are the least complex. Smectites (swelling clays) were found to have high viscosity but low yield stress at a low solids concentration, with the converse being true for the platy clays (for example, talc and kaolinite). This classification of the different phyllosilicates is shown in Figure 2.8.

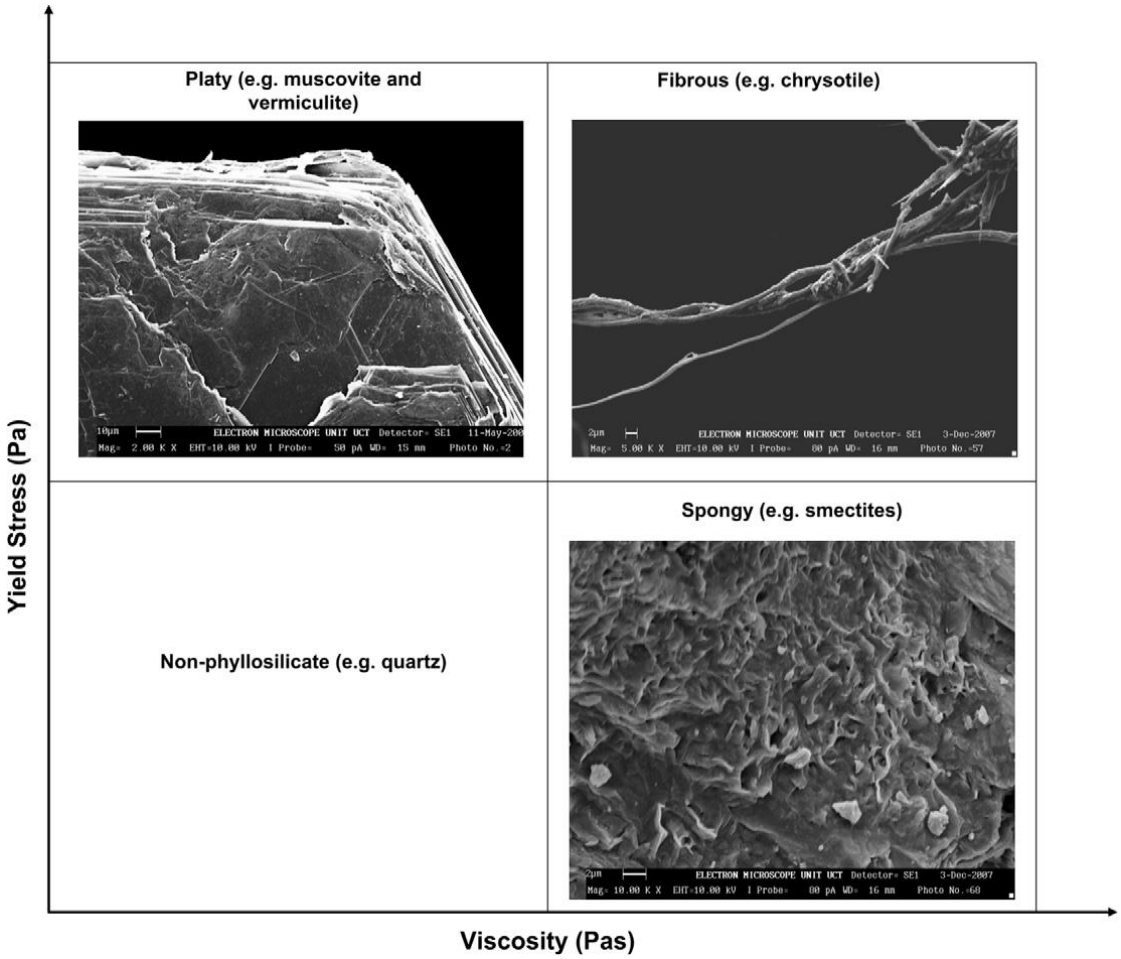

Figure 2.8: Proposed phyllosilicate mineral classification (Ndlovu *et al.*, 2011b)

Patra *et al.* (2010) and Zhang and Peng (2015) examined how cell hydrodynamics, and thus gas dispersion, were affected by a change in the rheology and the resulting effect on flotation recovery. Shabalala *et al.* (2011) focused particularly on gas dispersion and thus was able to more rigorously explain what took place with regards to hydrodynamics and gas dispersion as the rheology was altered. The findings of these studies are that an increase in viscosity leads to reduced turbulence and thus poor gas dispersion. However, Patra *et al.* (2010) believed that the bubbles would increase in size with an increase in viscosity which was found not to hold by Shabalala *et al.* (2011) who further attributed the smaller bubble size to the 'cavern of slurry' model as explained by Bakker *et al.* (2010). According to this model, stating that with higher rheological complexity and a given yield stress, the slurry seems to stick to the wall of the flotation vessel thus producing small bubbles and high gas hold-up. The results however show that for the fine particles used in these studies, a greater rheological complexity is not favourable for flotation. On the other hand, in a coarse particle study (d80 ranging from 150 to 320 μm) by Farrokhpay *et al.* (2011), the recovery of particles is not affected by a slight change in turbulence resulting from a change in rheology but rather bubble-particle detachment meaning a higher recovery may be obtained when dealing with coarse particles in a more viscous slurry. This can be explained by what had been earlier established by Xu *et al.* (2010) that a greater detachment force is required to detach particles in a more viscous mixture.

In the studies that incorporated actual flotation recoveries and related these to rheology (Farrokhpay *et al.*, 2011; Patra *et al.*, 2010; Zhang and Peng, 2015) it was noted that rheological complexity is detrimental to fine particle flotation. Schubert (2008) also noted that for fine particle flotation, as is the case for Great Dyke ores, large energy dissipation rates and low pulp viscosities are favourable for effective bubble-particle collisions (those resulting in attachment). For these fine particles better dispersion, resulting in lower apparent viscosity of the slurry is advantageous as this reduces turbulence damping which as was earlier noted, leads to reduced recoveries (Schubert, 2008). An increase in viscosity reduced flotation recoveries in the study by Patra *et al.* (2010) and for copper in the study by Zhang and Peng (2015). This implies that for fine particles, a greater viscosity is not favourable for flotation. However, in the flotation of gold, Zhang and Peng (2015) found that a slight increase in the viscosity resulted in a higher gold recovery while an additional increase lowered the recovery. The authors attributed this to the improvement in recoveries when the turbulence within the flotation apparatus had been slightly reduced while an increased damping of the turbulence adversely affected the recovery. This suggests the existence of an optimum rheological characteristic for an ore type at a given particle size distribution. The findings of Farrokhpay *et al.* (2011) show that a higher viscosity indeed led to a greater valuable mineral recovery in this coarse particle study but the effect of valuable mineral liberation could not be overlooked as attempting to float an even coarser fraction of the ore resulted in decreased recoveries.

On the whole, it was found that flotation performance is affected by pulp rheology which in turn varies with the particle size distribution and mineralogy. There also seems to be an optimal viscosity for the flotation of ores to achieve best recoveries. It is expected that for Great Dyke

ores in this study, which have fine flotation feed particle sizes, increases in viscosity would be detrimental to flotation recoveries.

2.4.4 Flotation reagents affecting rheology

The advantage of reduced pulp viscosities is that of increased collision rates, improved transport of particles into the froth zone and thus faster flotation kinetics (Schubert, 2008). This necessitates the use of chemical compounds known as dispersants that reduce rheological complexities of the slurry. Dispersants work through effecting electrostatic and/or steric repulsion of the particles, as well as reducing the hydrophobicity of particle surfaces in the slurry (Schubert, 2008; Pawlik, 2005). Electrostatic repulsion is a result of dispersants inducing surface charge (of the same sign) on particles that is sufficiently high for the particles to repel each other (Schubert, 2008; Pawlik, 2005). Steric repulsion is when a polymer adsorbs onto the surface of the particles and the molecules of the polymer form mechanical/flocculation barriers that keep solid particles at bay and renders their attractive forces negligible (Schubert, 2008; Pawlik, 2005; Napper, 1977). Increasing the wettability of particles in a slurry therefore results in a reduction of the formation of aggregates of hydrophobic particles (Schubert, 2008; Pawlik, 2005; Pawlik *et al.*, 1997). It has been noted that depressants have a dispersive effect and this is discussed in the following section. Considering the already complex pulp systems (consisting of liquid, solid and gas as well as ions and reagents dissolved in the liquid), the use of a depressant that would have dispersive properties would be an added advantage. This is in comparison to adding a dispersant that could further complicate the pulp system.

The effect of depressant type on rheology and flotation

A depressant with a high degree of substitution (DS) would seem to favour the flotation of ores rich in talc and other phyllosilicate minerals which influence rheological complexity. However, it has been noted that their high DS could be detrimental to flotation recoveries and grades. Anionic depressants are stronger dispersants than non-ionic ones as a consequence of the increased negative electrical charge of the interacting particles (repulsive forces) upon adsorbing the anionic polymers as well as the steric effect of the polymer molecules (Pawlik, 2005; Burdukova *et al.*, 2007; Schubert, 2008). This negative charge results in repulsive forces dominating over interparticle attraction leading to a higher dispersion and lower yield stress of the suspension (Pawlik, 2005; Burdukova *et al.*, 2006). However, as the degree of substitution increases there is greater intra- and intermolecular electrostatic repulsion which leads to the depressant being less densely packed on the mineral surface, which has been found to directly correlate with mineral hydrophilicity (Mierczynska-Vasilev and Beattie, 2010). Morris *et al.* (2002) found similar results and notes that talc depression is greatest when repulsion is minimum. It therefore seems there is a tradeoff between dispersion and the effectiveness of a depressant.

2.5 Hypotheses

The following was hypothesized based on the literature review:

- The more oxidized ore sample(s) from the Great Dyke will exhibit lower valuable metal (Cu, Ni, Pt and Pd) recoveries due to the oxidation of the former host minerals of these valuable metals. This oxidation when ubiquitous could have even led to the disintegration of the valuable minerals and thus resulting in a new mineralogy. The oxidation and new mineralogy hinders or makes collector attachment impossible and renders the minerals containing these metals non-recoverable using the typical flotation reagent suite.
- The greater the phyllosilicate alteration mineral content of an ore the lower the grade and recovery of valuable minerals (using the same reagent suite) as a consequence of the higher amount of NFG within the ore as well as the rheological complexities associated with these phyllosilicate alteration minerals.
- Using a depressant with a higher degree of substitution (DS) at the same dosage decreases the rheological complexity of a mineral slurry as a result of the increased negative electrical charge of particles in the slurry due to CMC adsorption. The reduction of rheological complexity could lead to greater recoveries due to the presence of an advantageous hydrodynamic environment for flotation, though a tradeoff exists between dispersion and the effectiveness of a depressant due to intermolecular electrostatic repulsion affecting how much of the depressant is adsorbed on the mineral surface.

2.6 Key Questions

In line with the hypotheses, the following key questions have been formulated:

- How have alteration reactions affected the mineralogy of these ores and what is the effect of this alteration on batch flotation performance (Cu, Ni, Pt and Pd grade and recovery) and the ores' slurry rheology?
- What is the composition of the NFG of the different ores and how does this relate to each ore's feed mineralogy?
- What is the effect of using a depressant with a higher DS on the rheology and flotation performance of the ores and why?

Chapter 3- Experimental Details

The following experimental programme was used for both the assessment of each of the ore's mineralogical characteristics and metallurgical performance so as to allow for the linking of these two. The ore samples, experimental methodology, and analytical equipment used within this study are described.

A summary of the experimental programme is given in Section 3.1 after which the ore samples and their preparation are described in Section 3.2. The methods used in characterizing the ores are detailed in Section 3.3. Section 3.4 outlines the batch flotation tests performed, followed by an outline of the rheological characterization in Section 3.5. Unless otherwise stated, all experiments were conducted in the Centre for Minerals Research, Department of Chemical Engineering at the University of Cape Town.

3.1 Experimental Programme

A detailed summary of the work done on each ore is shown in Figure 3.1. Thereafter, Table 3.1 follows with the details of how the work was subdivided into two phases. In the first phase of the experimental work the South Chamber sulfide ore was tested. The same tests were then conducted on the North Chamber sulfide and partly-oxidized ores in the second phase. All sample preparation was performed while wearing the appropriate personal protective equipment.

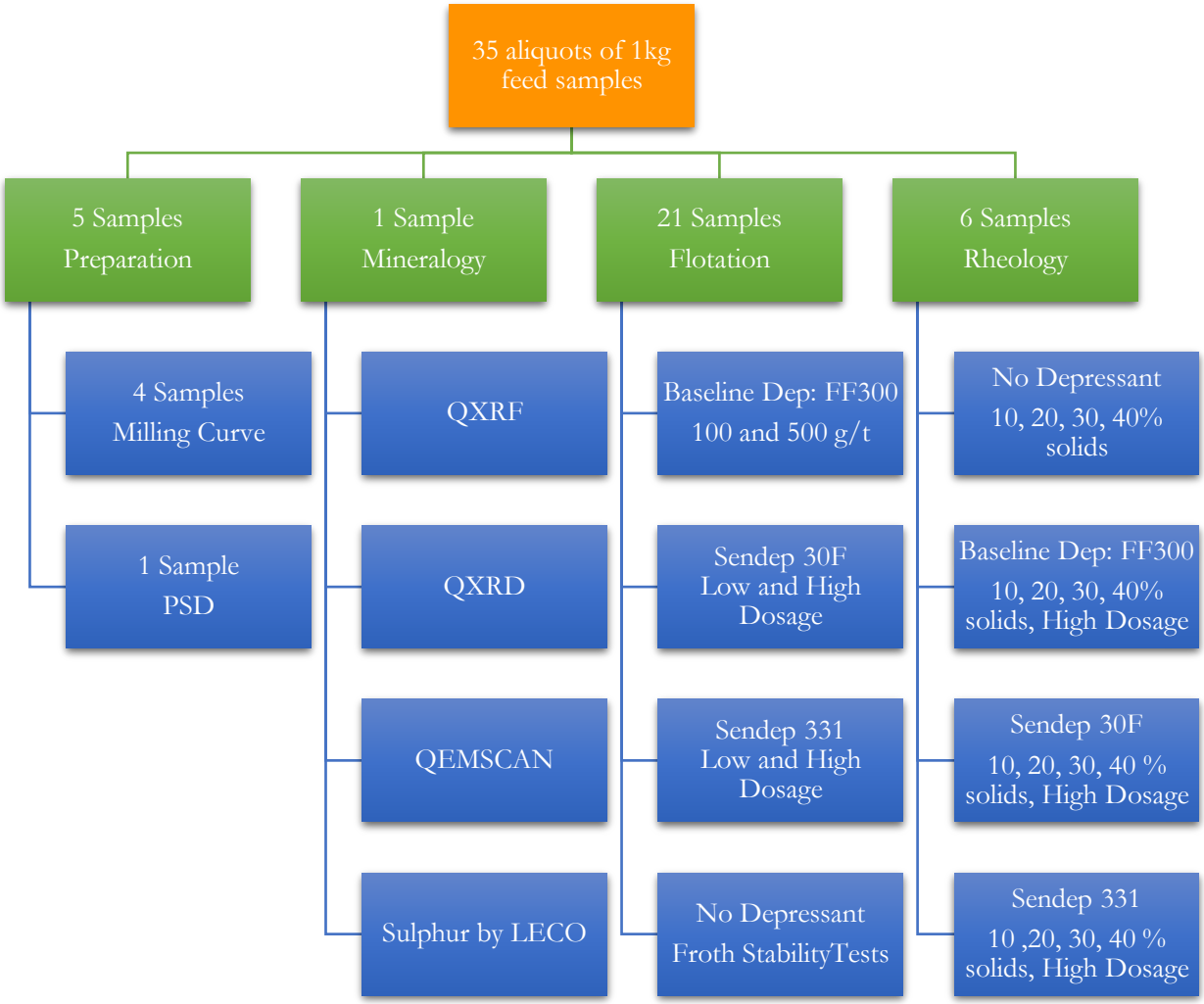

Figure 3.1: A summary of the experimental procedure used to test the mineralogical composition, batch flotation performance and rheological characteristics of each ore.

Table 3.1: Summary of the 2 phases of the experimental work

Phase	Task	Measurements/ Outcome	Equipment
Phase 1 South Chamber Pristine Ore	Sample Preparation	1 kg aliquots of the feed	Rotary Splitters
	Mineralogical characterization of flotation samples	Feed bulk mineralogy, (Gangue, BMS and PGMS) with a focus on their mode of abundance, liberation and association.	QEMSCAN, QXRD, QXRF
	Batch Flotation Tests	Depressant type, grade, recovery, degree of entrainment	Modified Leeds 3 L float cell
	Rheology Tests	Apparent viscosity and shear rate at varying solid volumes, depressant type	AR1500EX TA rheometer
Phase 2 North Chamber Pristine and Partly Oxidized Ores	Sample preparation	Same as for South Chamber Pristine Ore	
	Mineralogical characterization of flotation samples		
	Batch Flotation Tests		
	Rheology Tests	Apparent viscosity and shear rate at varying solid volumes, with and without baseline depressant type	AR1500EX TA rheometer
Phase 3 All 3 Ores	Froth Stability Tests	Maximum froth height, froth stability factor/coefficient	20 cm Diameter Frothing Column

3.2 Ore Samples and Sample Preparation

Three 100 – 150 kg ore samples, MIM-S (Mimosa Sulfide), ZP-S (Zimplats Sulfide) and ZP-O (Zimplats Incipient Oxide) were obtained from different locations (North and South chambers) along the Great Dyke. Two underground 'pristine'/sulfide ores that are currently processed by Mimosa and Zimplats are labelled MIM-S and ZP-S. Zimplats also supplied a partly-oxidized ore from an open-pit source that was labelled ZP-O. The sulfide ores were grey in colour, while the oxidized ore was red in colour as a result of the richer Fe-oxide/hydroxide content. These were

prepared by crushing to a size of 100% passing 3 mm, which is the state in which the samples were received. On arrival at the Centre for Minerals Research laboratories at the University of Cape Town (UCT), each of the ore samples were blended, riffled and split using a rotary sample splitter into representative 1 kg portions using a Dickie and Stockler rotary splitter. The splitting of the ore samples in this way was done to minimize the variation in the composition between the samples for each of the tests conducted on them. Additionally, the spinning riffler reduces the group and segregation error if the topsize of the particle size distribution has been matched to Gy's safety Line (Gy, 1979; Lotter and Fragomeni, 2010). This splitting method also reduces the relative standard deviation of the average valuable mineral grade.

Each of the 1 kg samples was then milled to 65% passing 75 µm (resulting in a similar particle size distribution shown in Figure 3.2) in a 1 kg stainless steel rod mill. The mill was charged with 20 stainless steel rods of varying diameter (6 x 25 mm, 8 x 20 mm and 6 x 16 mm), at 66 wt.%, solids using synthetic plant water (Wiese *et al.,* 2005). The grind of 65% was selected based on the existing flowsheets from Great Dyke operations. All milling and batch flotation experiments were conducted using synthetic plant water made from distilled water and the addition of various chemical salts (supplied by Merck). The composition of the water simulated that of a South African platinum concentrator as reported by Wiese *et al.* (2005) is shown in Table 3.2. The divalent cations within the plant water are essential for the effective adsorption of the depressants onto talc (Khraisheh *et al.,* 2005).

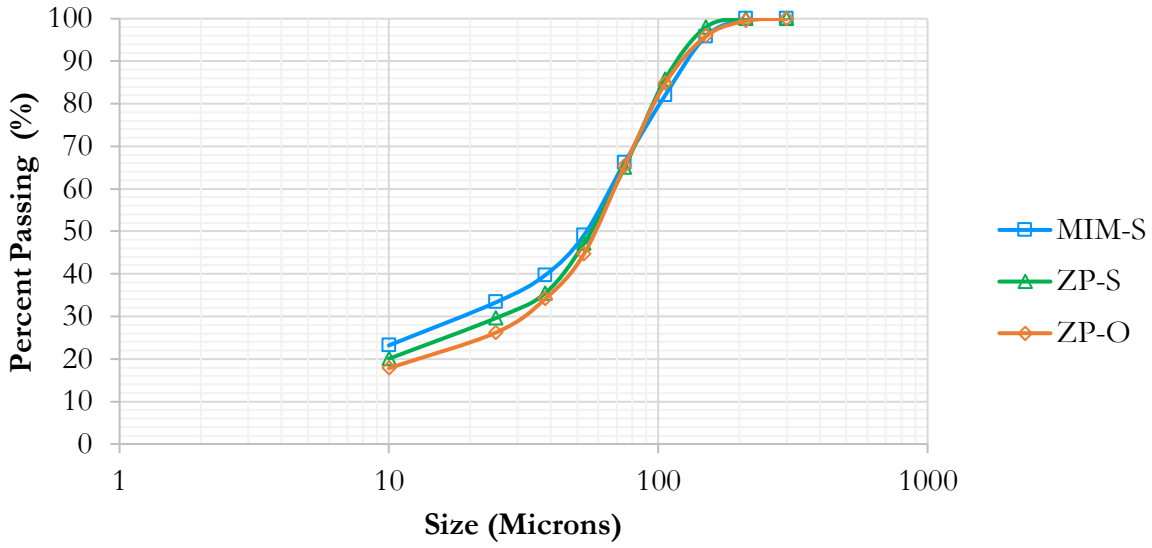

Figure 3.2: Particle Size Distributions of the flotation feed of the 3 ores at a grind of 65% passing 75 µm.

Table 3.2: Synthetic plant water constituents (from Wiese *et al.*, 2005). TDS: total dissolved solids

Ion	Ca^{2+}	Mg^{2+}	Na^{+}	Cl^{-}	SO_4^{2-}	NO_3^{-}	NO_2^{-}	CO_3^{2-}	TDS
Concentration (ppm)	80	70	153	287	240	176	-	17	1023

3.3 Ore characterization – QEMSCAN, XRF and XRD

After screening the mill product into various size classes, bulk mineralogical composition, sulfide liberation and association of the different Great Dyke feed samples were determined using Quantitative Evaluation of Minerals by SCANning Electron Microscopy (QEMSCAN) analysis on an FEI QEMSCAN 650F. From the sized samples based on the PSD, 4 g samples were split out using a rotary splitter. These 4 g samples were then split (using a Quantachrome microriffler) into 1 g aliquots for QEMSCAN blocks (3 blocks were prepared per size fraction). The blocks were then prepared through mixing of the aliquots with graphite and resin. Upon curing, a printed label (including the sample name, size and number) was added to the back of the mould and set in some additional resin and allowed to cure. Once completely cured the blocks were polished. Polishing was done in a series of grinding and polishing steps until the final 1 µm polish. The samples were then dried in an oven. The quality of the final polish was checked using an optical microscope after which the samples were carbon-coated using an Emitech carbon evaporator. The carbon coat is needed to diffuse electrons off the surface of the sample when they are in the QEMSCAN. All QEMSCAN analyses were run at 25kV, 10 nA using the analysis routines as given in Tables 3.3 and 3.4.

Table 3.3: QEMSCAN analysis routines

Measurement	Description	Sample Type	Information Obtained
Particle Mineralogical Analysis - PMA	two-dimensional mapping analysis tool which is ideal for liberation analysis and is often used where gangue characterization is required	MIM-S, ZP-S, ZP-O feed in these 4 size fractions • -25 µm • +25/-53 µm • +53/-75 µm • +75 µm	Bulk Mineralogical Composition of the Ore, Mineral Liberation and Association
Sulfide Mineral Search - SMS	increases analysis efficiency and focuses on target minerals	MIM-S, ZP-S, ZP-O feed in these 4 size fractions • -25 µm • +25/-53 µm • +53/-75 µm • +75 /-300 µm	Base Metal Sulfide Mineralogy

Table 3.4: QEMSCAN Conditions – Field Size, Pixel Size and Particle Count. All analyses were at 25 kV

	Size Fraction (μm)	Field Size (μm)	Pixel Size (μm)	BMS Particle Count		
				MIM-S	ZP-S	ZP-O
PMA (Feed)	-25	300	1	30 800	65 400	34 300
	+25/-53	750	2	21 500	39 100	19 400
	+53/-75	1000	3	16 800	35 300	14 300
	+75/-300	1500	4	7 800	17 800	12 100
PMA (Concentrates)	+38/-75	1000	3	6 310	6 130	5 570
SMS - Sulfide Minerals Search (Feed)	-25	300	1	7 380	4 300	7 840
	+25/-53	750	2	1 990	1 340	1 860
	+53/-75	1000	3	1 900	1 030	1 180
	+75/-300	1500	4	1 200	1 950	1 380

To ascertain that the mineralogical data provided by QEMSCAN was accurate, validation of the bulk mineralogy of the various samples was done using quantitative X-ray Diffraction (XRD) and X-ray Fluorescence (XRF). Bulk samples (10 g each) were prepared for quantitative XRD with a McCrone micronizing mill, then analyzed on a Bruker D8 Advanced powder diffractometer with Vantec detector with Co source. Phase quantification was performed by Rietveld refinement with the Bruker Topas software. For quantitative XRF the Panalytical Axios Wavelength dispersive XRF with Rh tube with natural element standards was used. The validation was through comparison of chemical assay data from XRF to that calculated by QEMSCAN based on its mineral identification protocol. Figure 3.3 shows the assay reconciliation representing the elemental QEMSCAN results to those obtained through XRF analysis. Good parity is shown based on these graphs therefore the mineral list being used in QEMSCAN strongly correlated to the elements present within the ores. Loss on ignition, as determined by QXRF was also a key input in determining the hydrous mineral content and thus data validation.

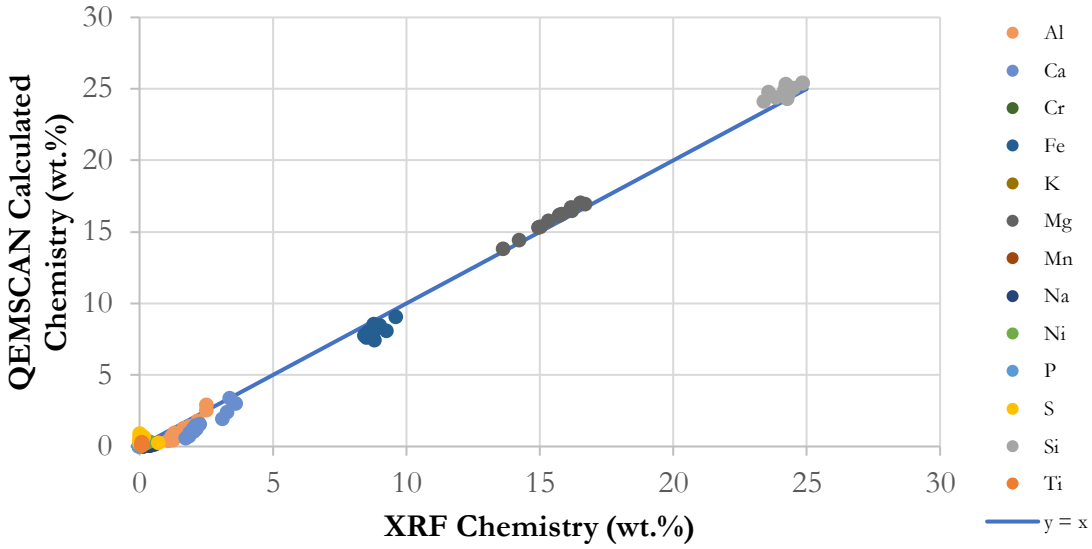

Figure 3.3: Graph showing assay reconciliation for all 3 ores

3.4 Batch Flotation Tests

Reagents chosen were based on those currently used on Great Dyke PGE operations. All the flotation reagents used in this study were supplied by Senmin International (Pty) Ltd. The depressants of interest were characterized at the Centre for Minerals Research, Polymer Characterization Laboratory at the University of Cape Town and the results are given in Table 3.5. The major differences in the depressant types were their purity and degrees of substitution (DS). FinnFix300 (FF300) and SenDep30F (SD30F), possessed similar DS at 0.7 and 0.8, respectively, while SenDep331 (SD331) possessed a higher DS at 1.1. To cater for differences in the purity of the depressants, the dosages used were on an active content basis. For the collector (sodium isobutyl xanthate) and the frother (SasFroth 200); the dosages used were 300 g/t and 75 g/t respectively, which were chosen based on the existing flowsheets from Great Dyke operations.

Table 3.5:Depressant Characteristics

	FinnFix300	SenDep30F	SenDep331
Molecular weight (g/mol)	251 000	284 000	266 000
Purity (%)	97.6	58.6	62.1
Insoluble content (%)	1.4	1.5	0.8
Polydispersity	7.0	6.6	5.6
Degree of Substitution	0.7	0.8	1.1

As part of this study was aimed at understanding and comparing the flotation behaviour of the 3 ores there was need for the quantification of the naturally floating gangue which required the determination of a 'high' and 'low' depressant dosage (Wiese, 2009). The 'low' dosage is that at which the froth is manageable, with the amount of floating gangue being larger than the amount of entrained gangue. The 'high' dosage is that at which the floating gangue is fully depressed and recovery of any gangue to the concentrate is a result of entrainment or due to composite sulfide-

gangue particles (Bradshaw *et al.*, 2005; Wiese, 2009). Preliminary batch flotation tests were thus performed to determine the 'high' and 'low' depressant dosages. The results of these investigation are shown in the Appendix (Section 7.6), with the low dosage being determined at 100 g/t and the high at 500 g/t, which were then used for the batch flotation test work.

For batch flotation tests, the collector was added to the mill charge prior to milling. The milled slurry from the sample preparation stage was transferred to a modified Leeds 3 L batch flotation cell and made up with synthetic plant water to attain a solids concentration of 35% by mass. The impeller speed was set at 1200 rpm and pulp level was controlled manually. Air supply was maintained at 7 L/min and froth height was kept constant at 1 cm. A feed sample was taken before the commencement of the flotation procedure. The depressant was added to the slurry in the flotation cell and a conditioning time of 2 minutes was allowed. The frother was then added and allowed a conditioning time of 1 minute after which the air supply was opened. Four concentrate samples were collected by scraping the froth every 15 seconds into a collecting pan. The concentrate/froth was collected for the following time intervals: 0 – 2 min (concentrate 1 - C1), 2 – 6 min (C2), 6 – 12 min (C3) and 12 – 20 min (C4). A tailings sample was also collected after each flotation test. The amount of water recovered was measured during each of the tests. These tests were performed in duplicate.

Each of the flotation feeds, concentrates and tailings were filtered, dried and weighed prior to analysis. Batch flotation tests at each condition were conducted in duplicate and the standard error calculated. Each of the dried flotation feed, concentrate and tailings samples were analyzed for Cu, Ni and S. The concentrate samples for tests at the same conditions were combined for Pt and Pd analysis due to the comparatively larger sample quantity required for these PGE analyses. The copper and nickel content analysis was measured on powdered samples using a Bruker S4 Explorer XRF Spectrometer, while sulfur analysis was done using a LECO DR 423 sulfur analyzer. Pt and Pd were concentrated by fire assay and analyzed by Inductively Coupled Plasma Optical Emission Spectrometry (ICP-OES) at an external laboratory.

The results of all batch flotation tests were analyzed by comparing their solids mass and water recoveries, as well as Cu, Ni, S, Pt, Pd grade and recoveries. In addition, the amount of floating gangue was determined using the method described by Wiese (2009) and further elaborated in the Section 4.3.2. The +38/-75 µm fraction of the flotation concentrates, representing a particle size range more characteristic of recovery by true flotation (Savassi, 1998) was additionally mineralogically assessed so as to determine the nature of the naturally floating gangue.

Froth Stability Tests

Froth stability column tests were used to gain an understanding of whether any differences in the flotation response were due to differences in the stability of the flotation froths. The column used in this study is made of Perspex and has a diameter of 200 mm and a height of 1 m. There are 4 ceramic frits at the base of the column through which air is bubbled.

For the froth stability tests, the collector was added to the mill charge prior to milling. The milled slurry was transferred into a feed tank and synthetic plant water added to attain a solids concentration of 35% by mass. The frother was then added and allowed to condition for 1 minute. The air inlet was opened slightly to avoid the settling of slurry and clogging up of the frits when the slurry was added into the column. Thereafter, a peristaltic pump was used to feed the slurry into the column up to the 200 mm mark from the base of the column. The agitator was started to allow for homogenous mixing of the slurry but ensuring a quiescent slurry surface. Simultaneously, the stop watch was started, the air supply opened and maintained at 24 L/min and the froth height noted every 5 seconds until a level where the froth was no longer rising denoting H_{max}, the maximum froth height. These tests were performed in duplicate.

3.5 Rheology

Rheological measurements of the various flotation samples were conducted as a function of solids volume concentration. The suspensions were made up using synthetic plant water (Table 3.2). The concentrations were varied from 10% to 40 % vol. solids in increments of 10 %, and in narrower increments of 5% as the slurry became more viscous and difficult to manage. The measurements were performed using an AR1500EX TA rheometer (manufactured by Thermal Analysis, Germany) with a standard vaned rotor geometry. All tests were conducted in a shear rate controlling regime, with shear rates ranging from 10/s to 400/s. The resulting rheograms were analyzed in order to establish rheological behavior after which the Bingham Model was used. The viscosities reported in this study are apparent viscosities taken at a shear rate of 160 /s which typifies the shear rate in a mechanical flotation cell (Shabalala *et al.*, 2011). All measurements were run in triplicate and the standard error calculated. The same tests were applied to pure talc (Texas Talc) with a d50 of 5 μm. This d50 was determined using a Malvern Mastersizer (Malvern, UK).

Chapter 4 - Results and Discussion

The results and discussions of this study are presented in this chapter. In order to understand the relevance of certain details of key mineralogical measurements, mineralogical findings are presented after initial flotation results since they facilitate the interpretation thereof. The feed characteristics are given in Section 4.1 followed by the rheological properties of the ores in Section 4.2. The batch flotation performance results and their interpretation using solids and water recoveries, mass of gangue recovered, valuable metal recoveries as well as base metal sulfide liberation and association is given in Section 4.3. Section 4.4 closes off this chapter with the decoupling of alteration reactions that take place in PGE ores. Actual results are given in the Appendix.

4.1 Feed Characterization of the ores

The feed ore samples were assessed mineralogically and chemically to allow for an understanding of what would contribute to differences in flotation responses, if any, given the use of a uniform reagent suite for all three ores. The minerals referred to as altered silicates include phyllosilicates as well as any hydrous silicates that are formed as a result of reactions acting on the primary anhydrous silicates.

4.1.1 Bulk Mineralogy

As can be seen from Table 4.1, all three ores are pyroxene rich, with ZP-O having the highest amount (85%) compared to 81% in ZP-S and 74% in MIM-S. MIM-S was found to be the richest in plagioclase (7.1%) versus 3.2% and 2.7% in ZP-O and ZP-S, respectively. MIM-S and ZP-S have similar amounts of phyllosilicates (approximately 10%), with ZP-S having a slightly higher talc content. ZP-O had the lowest phyllosilicate content (5.3%). No smectite was present in the ore samples. Due to the comparatively low altered silicates content, the ZP-O sample seemed to be the least altered of the three ore samples. ZP-O, however, was expected to be the most alteration mineral-rich due to it having been labelled as a partly oxidized ore, having a visibly distinct reddish colour (indicative of Fe-oxides/hyroxides) compared to the grey colour of the other ore samples. Additionally, this sample having been sampled closer to the surface, had been expected to have been the most exposed to low temperature alteration of anhydrous minerals like orthopyroxene. The lower percentange of pyroxene and a higher percentage of phyllosilicates in MIM-S and ZP-S, however, points towards the alteration of orthopyroxene with the formation of phyllosilicates (paticularly talc) along the grain boundaries and cleavage planes of orthopyroxene (Becker *et al.*, 2009). Talc and orthopyroxene are of interest due to their contribution to the amount of floating gangue. Important to note yet again is that the values given by QEMSCAN were validated against XRD and XRF including a calculation of the amount of hydrous silicates present based on loss on ignition (LOI) thus giving confidence to the results. XRD and XRF results are shown in Sections 7.1.1 and 7.1.2 of the Appendix.

Table 4.1: Bulk mineralogy of the 3 ore samples from QEMSCAN (wt.%). Ni-sulfides and Cu-sulfides primarily constitute of pentlandite and chalcopyrite, respectively. 'Other sulfides' are mainly made up of galena while a major constituent of 'Other' is quartz.

	MIM-S	ZP-S	ZP-O
Ni-sulfides	0.5	0.3	0.2
Cu-sulfides	0.4	0.3	0.3
Pyrrhotite	0.5	0.2	0.1
Pyrite	0.1	0.1	0.3
Other sulfides	< 0.1	< 0.1	< 0.1
Olivine	1.8	1.4	1.3
Orthopyroxene	64.9	78.2	81.9
Clinopyroxene	8.5	2.7	3.3
Serpentine*	0.1	0.2	0.1
Talc*	8.4	9.1	4.9
Chlorite*	1.3	0.6	0.3
Mica*	0.5	0.2	0.1
Amphibole	3.8	1.8	1.5
Plagioclase	7.1	2.7	3.2
Calcite	0.2	0.3	0.0
Chromite	0.2	0.3	0.2
Fe oxides / hydroxides	0.9	0.9	1.6
Other	0.9	0.8	0.5
Total	100.0	100.0	100.0

* Phyllosilicate minerals

The greatest percentage of BMS were in MIM-S (1.5 %), with ZP-O and ZP-S containing similar amounts (0.9 %) as shown in Figure 4.1. MIM-S is richest in pyrrhotite, followed by Ni-sulfides (mainly pentlandite), Cu-sulfides (mainly chalcopyrite) and lastly pyrite (and other sulfides). Though having comparable overall amounts of BMSs, ZP-S is richer in pyrrhotite while ZP-O is richer in chalcopyrite and pyrite.

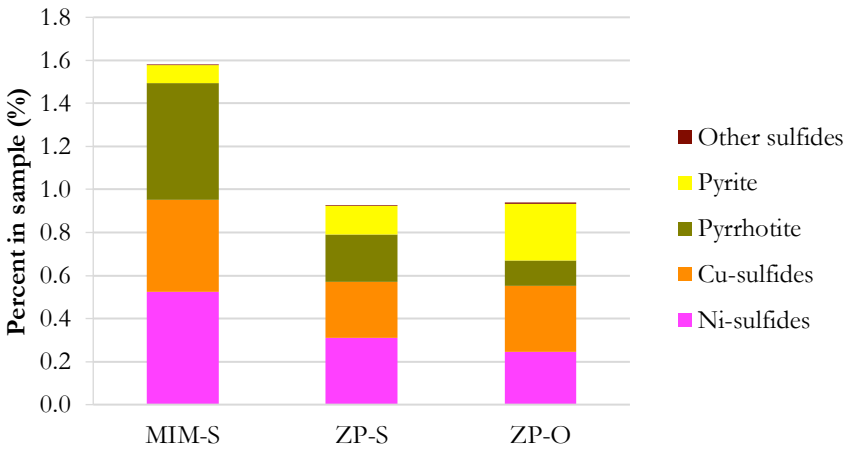

Figure 4.1: Base Metal Sulfide (BMS) Content of the 3 ore samples. Ni-sulfides and Cu-sulfides primarily constitute of pentlandite and chalcopyrite, respectively. 'Other sulfides' are mainly made up of galena.

The Fe-oxide/hydroxide content of ZP-O is almost double that of the other 2 ore samples (Table 4.1). This is a result of the oxidation of sulphides and is likely what justifies the name "oxidized" (/partly in this case), rather than its content of silicate alteration minerals (which come about as a result of hydrolysis). The results in Figure 4.1 point towards the fact that a so-called "oxidized" ore sample, ZP-O in this case, may not necessarily have a lower BMS content than a pristine one (ZP-S). It would have been expected that the ZP-O sample would have a lower BMS content due to the depletion of the BMS to form Fe-oxides and hydroxides (Oberthür *et al.*, 2003b), however, these findings indicate that ZP-O exhibits incipient oxidation rather than oxidation of the pervasive type.

4.1.2 Feed Chemical Assays

To further distinguish differences between the 3 ore samples their feed elemental Cu, Ni, Pt and Pd were analyzed and are shown in Table 4.2.

Table 4.2: Valuable Element (Cu, Ni, Pt and Pd) Feed Grades and Pt/Pd Ratio.

	Cu (%)	Ni (%)	Pt (g/t)	Pd (g/t)	Ratio (Pt/Pd)
MIM-S	0.14	0.27	1.64	1.29	1.26
ZP-S	0.08	0.20	1.45	1.19	1.22
ZP-O	0.14	0.27	2.08	0.91	2.29

Of interest is that the Pt feed grade of the oxidized sample was found to be higher than that of the other pristine samples, while its Pd grade was lower. The Pt:Pd ratio for the former is 2.3 compared to one in the region of 1.2 for the latter samples. As was earlier noted a greater Pt:Pd ratio is one of the distinguishing characteristics of an oxidized PGE ore and is due to the mobilization of Pd during oxidation of the ore (Evans, 2002; Oberthür, 2003b; Oberthür *et al.*, 2013). The Pt:Pd ratio and composition of ZP-O is similar to that reported by Oberthür *et al.* (2013) and Kraemer *et al.* (2015) in their work on oxidized PGE ores from the Great Dyke. This similarity points towards ZP-O ore sample being representative of Great Dyke oxidized PGE ores despite not being rich in alteration silicates in comparison to the ores from the Bushveld Complex that were analyzed by Becker *et al.* (2014).

4.2 Rheology

As a preliminary check to assess whether any differences in the flotation responses would have been due to the rheological complexities associated with the individual ore types, rheological assessments were conducted and the results presented in Figures 4.2, 4.3 and 4.4. Figure 4.2 shows the fitting of linear trendlines to rheograms confirming Bingham plastic behaviour of the slurries (Figure 2.7). The coefficient of correlation for fitting the data to a straight line are all above 97%. Figures 4.3 and 4.4 show the yield stress and apparent viscosity of the ore samples upon varying solids content in the slurries, with and without a depressant. The determination of yield stress is shown in Section 7.5.2 of the Appendix. A sample of Texas Talc was included in the comparison to show its exhibition of high rheological complexity and to assess whether any of the samples analyzed in this study behaved in a similar way. Yield stress results for an orthopyroxene sample

(d50 = 11 µm) from a study by Becker *et al.* (2013) are also included in Figure 4.3 for comparison. The error bars for the rheological test work results are too small to be visible on these graphs. These tests were done in triplicate as was mentioned in the Experimental Section of this study.

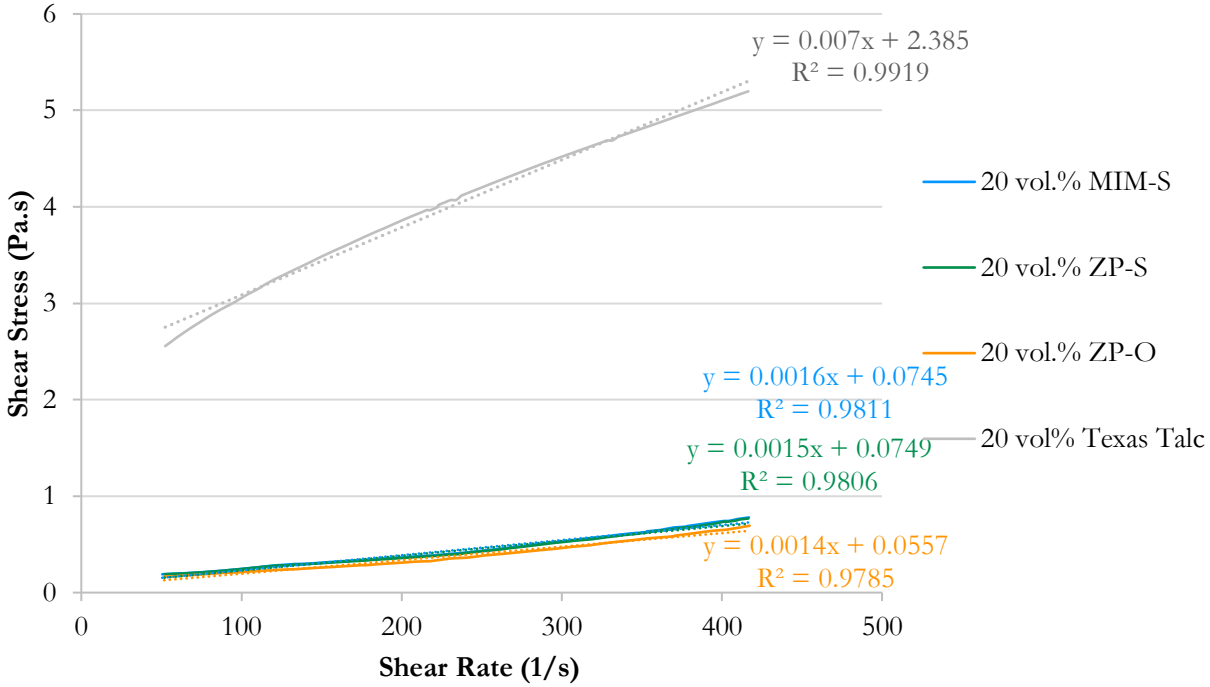

Figure 4.2: Rheogram showing Bingham plastic behavior of slurries in comparison with Texas Talc. The y-intercept of each straight line fit to the data is the yield stress.

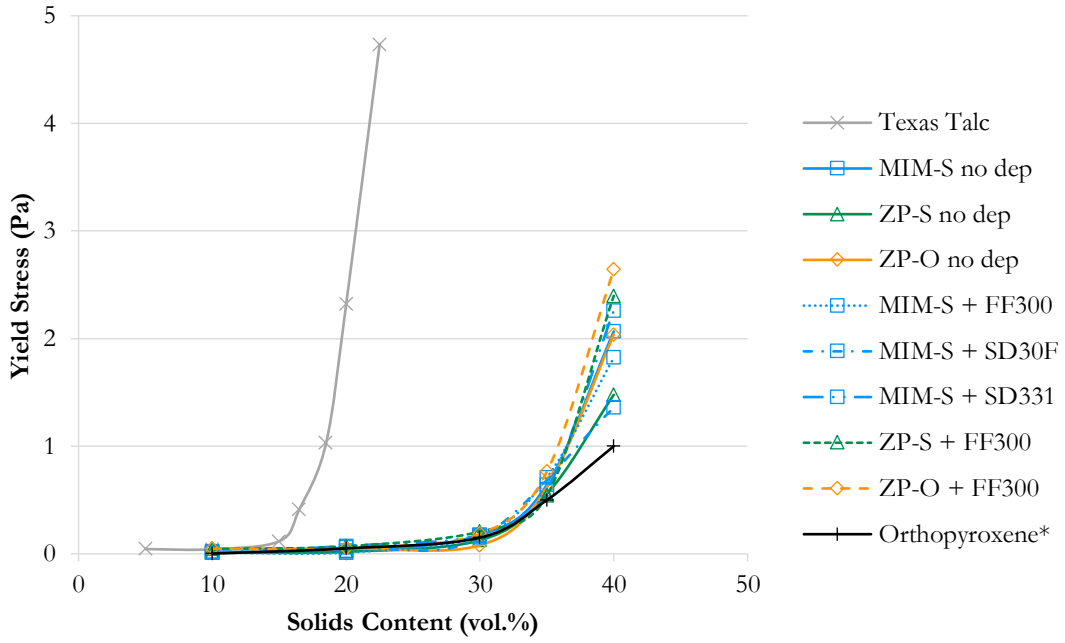

Figure 4.3: Yield stresses at varying solids concentrations for the 3 ore samples with and without a depressant. *(Orthopyroxene Yield Stress from Becker *et al.* (2013)) (The tabulated results used to plot this graph are in Section 7.5 of the Appendix.)

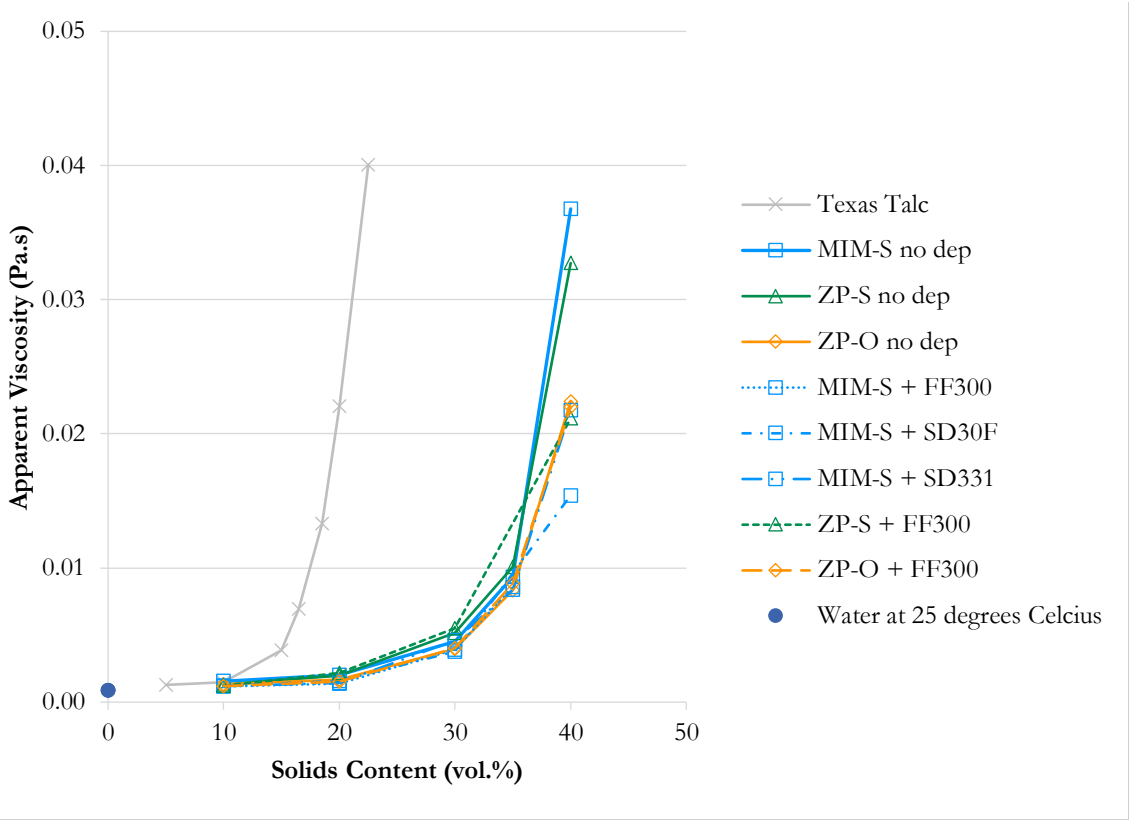

Figure 4.4: Apparent viscosities at varying solids concentrations for the 3 ore samples with and without a depressant. (The tabulated results used to plot this graph are in Section 7.5 of the Appendix.)

When comparing the yield stress and apparent viscosity against solids concentration of the 3 ore samples at feed grind (Figures 4.3 and 4.4, respectively) it was noted that the graphs followed the same trend with the point of inflection lying between 30–35 vol.% solids. (The point of inflection denotes solids concentrations around which an ore begins to manifest rheological complexity). The reason for the similarity in the three ore samples' rheology is likely due to the largely similar bulk mineralogy, which is dominated by pyroxene. This is illustrated by the point of inflection for a pure orthopyroxene sample (Becker *et al.*, 2013) lying within the same region as that of the 3 ore samples, that is 30–35 vol.% solids, whereas the inflection point of a pure talc sample lies between 15 and 16 vol.% solids. Despite the more oxidized ore sample having a lower phyllosilicate (including talc) content its rheological response was similar to the pristine ore samples. It seems the effect of the minerals that result in greater rheological complexity is buffered by the larger amounts of minerals with a more regular surface charge distribution and morphology like orthopyroxene, resulting in similar rheological characteristics. The dispersing effect of the CMCs was not observed in this work as adding them did not alter the rheological complexity of the samples and resulted in points of inflection within the same region.

On the whole these observations showed that any differences in the batch flotation response would unlikely be as a result of differences in the rheologies of the ores.

4.3 Batch Flotation Performance

In the assessment of the metallurgical performance of the ores the masses of solids and water recovered (reflecting the availability of floatable material and stability of the froth) were examined. This was followed by an assessment of the mass of naturally floating gangue, froth stability test results as well as the key indicators of valuable mineral recoveries through the elements Cu, Ni, Pt and Pd. The error bars shown on the graphs represent standard error.

Worth noting from the outset is that there was no observed trend when it came to the difference in the flotation responses of the 3 ore samples when the depressant type was changed. This can be seen in Table 4.3 and is graphically illustrated in Figure 4.5 (mass of solids and water recovered) as well as Figures 4.6, 4.7, 4.8 and 4.9 (which show the cumulative Cu, Ni, Pt and Pd Grades, and Recoveries, respectively). The similarity in the responses upon changing the depressant type is likely due to the depressants not significantly affecting the rheology of the mineral slurries as discussed in Section 4.2. The depressants are comparatively effective in depressing the talc and associated minerals. Something to consider is that the effect of the depressants on rheology is a secondary effect and does not mean that the depressants were ineffective. A greater difference may have been observed in the presence of greater percentages of talc at which depressant-talc interactions would have been more pronounced.

Changing from a depressant dosage of 100 g/t to 500 g/t resulted in an average loss of Cu, Ni, Pt and Pd recovery of 12%, 13%, 12% and 10%, respectively. Because of the absence of an observed trend upon changing the depressant type, the following discussions mainly focus on the differences in the flotation responses of the 3 ore samples rather than the effect of the depressant type. The focus will be on tests with FF300 at a dosage of 100 g/t as this allows for a comparison of the ores' flotation behaviour without the full depression of the floating gangue. Additionally, this dosage also makes possible the assessment of the concentrate mineralogy of which an understanding of the naturally floating gangue is essential and forms a core part of this study. It is worth noting that a 100 g/t depressant dosage would be too low for actual Great Dyke operations based on the current reagent schemes, but still serves the purpose of allowing for an understanding of the flotation behaviour. At the 500 g/t dosage there may even be some depression of the valuable minerals and this dosage was only used to allow the determination of the amount of floating gangue (See Section 4.3.2). FF300 was chosen for this comparison as it is the depressant currently being used on the Great Dyke operations.

Table 4.3: Batch flotation results for the 3 ore samples upon changing both depressant type and dosage. These include: Cumulative mass of solids recovered, mass of water recovered as well as Cu, Ni, Pt and Pd cumulative grades and recoveries.

Ore	Depressant Type	Depressant Dosage (g/t)	Mass of Solids Recovered (g)	Mass of Water Recovered (g)	Copper		Nickel		Platinum		Paladium	
					Recovery (%)	Grade (%)	Recovery (%)	Grade (%)	Recovery (%)	Grade (g/t)	Recovery (%)	Grade (g/t)
MIM-S	FF300	100	211	1360	87.4	0.63	67.0	0.89	86.7	6.01	84.4	4.38
		500	25.4	386	73.3	3.64	52.2	5.42	72.6	46.0	70.5	36.0
	SD30F	100	235	1380	88.3	0.58	65.2	0.68	89.9	6.23	88.5	4.90
		500	36.7	603	75.3	2.74	53.6	3.86	80.3	39.0	79.9	34.0
	SD331	100	232	1420	88.3	0.58	69.5	0.85	88.4	6.43	86.8	4.92
		500	29.2	456	74.5	3.20	53.2	4.72	75.4	43.0	70.1	29.0
ZP-S	FF300	100	198	1610	82.9	0.37	54.2	0.53	85.9	6.84	85.7	5.00
		500	34.7	721	74.4	1.81	47.1	2.86	75.4	33.0	79.7	30.0
	SD30F	100	197	1620	82.8	0.37	54.7	0.59	86.6	6.61	87.0	5.46
		500	34.5	727	72.9	1.75	44.7	2.59	75.1	31.0	78.2	27.0
	SD331	100	218	1690	79.5	0.26	52.1	0.46	86.9	6.11	88.3	5.28
		500	36.5	919	72.6	1.64	44.9	2.62	74.6	28.0	74.9	23.0
ZP-O	FF300	100	140	1600	68.7	0.72	46.2	0.95	77.3	11.1	62.1	3.63
		500	36.8	997	59.0	2.24	35.6	2.76	68.3	39.0	56.4	13.7
	SD30F	100	151	1560	73.1	0.69	52.6	0.98	78.9	10.9	66.2	3.84
		500	32.8	940	57.4	2.30	32.7	2.61	65.1	42.0	53.0	15.5
	SD331	100	157	1650	70.4	0.64	49.2	0.90	74.2	10.0	56.4	3.38
		500	33.2	917	57.5	2.21	32.4	2.53	64.0	42.0	50.6	15.6

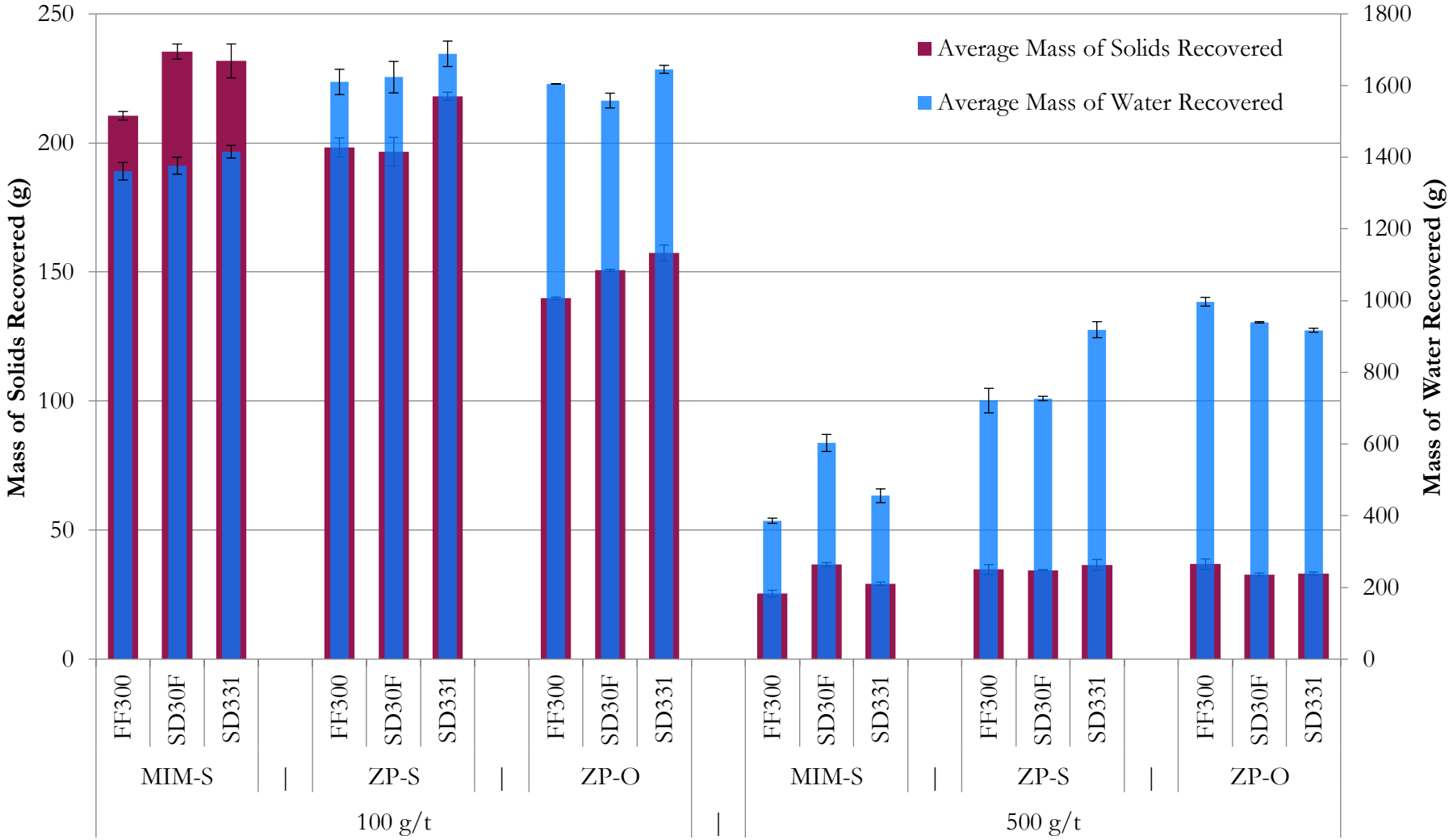

Figure 4.5: Total Mass and Solids Recovered for the 3 ores while varying depressant type and dosage. The error bars shown on the graphs represent standard error.

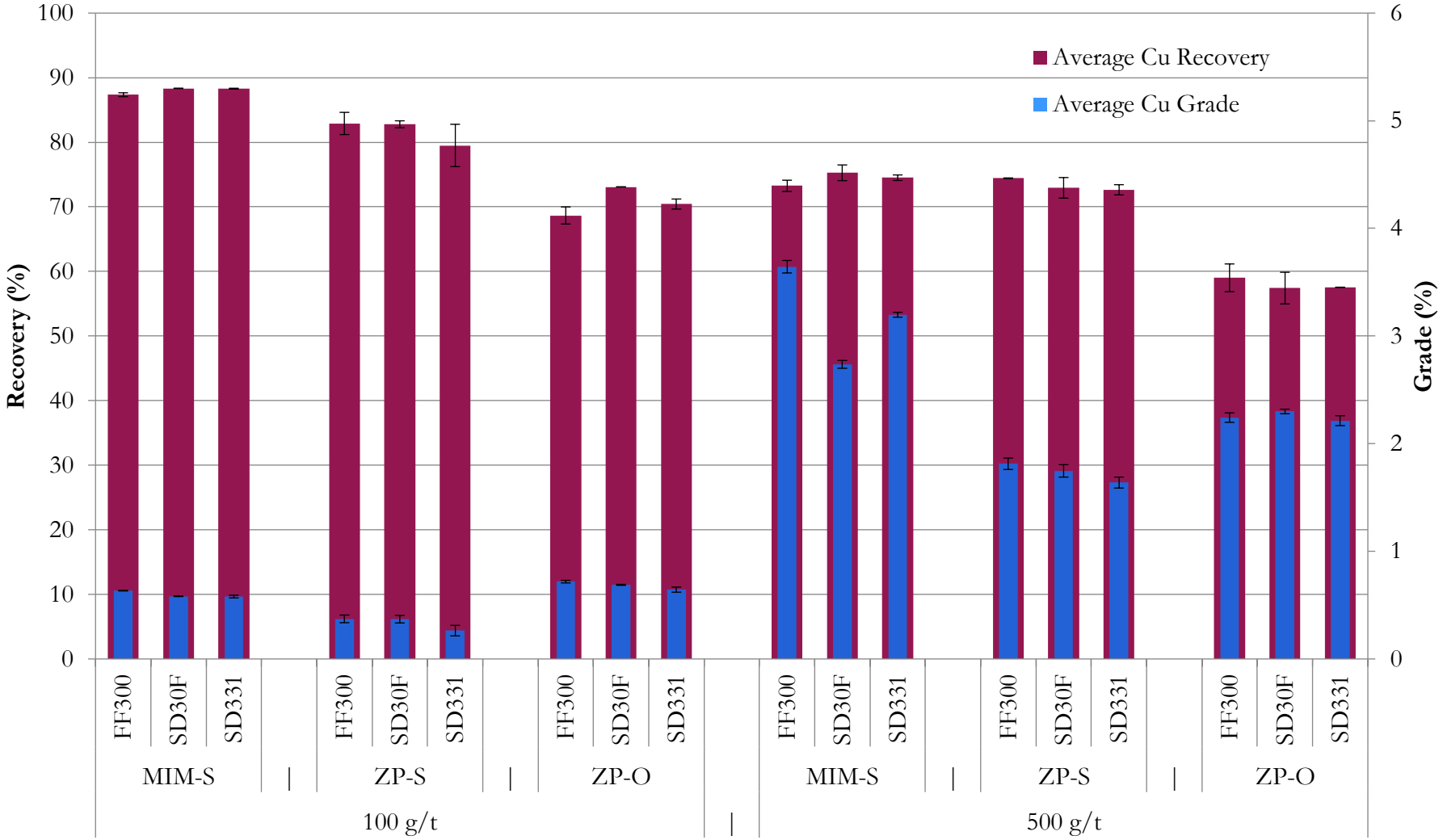

Figure 4.6: Cu Recovery and Grade for the 3 ores while varying depressant type and dosage. The error bars shown on the graphs represent standard error.

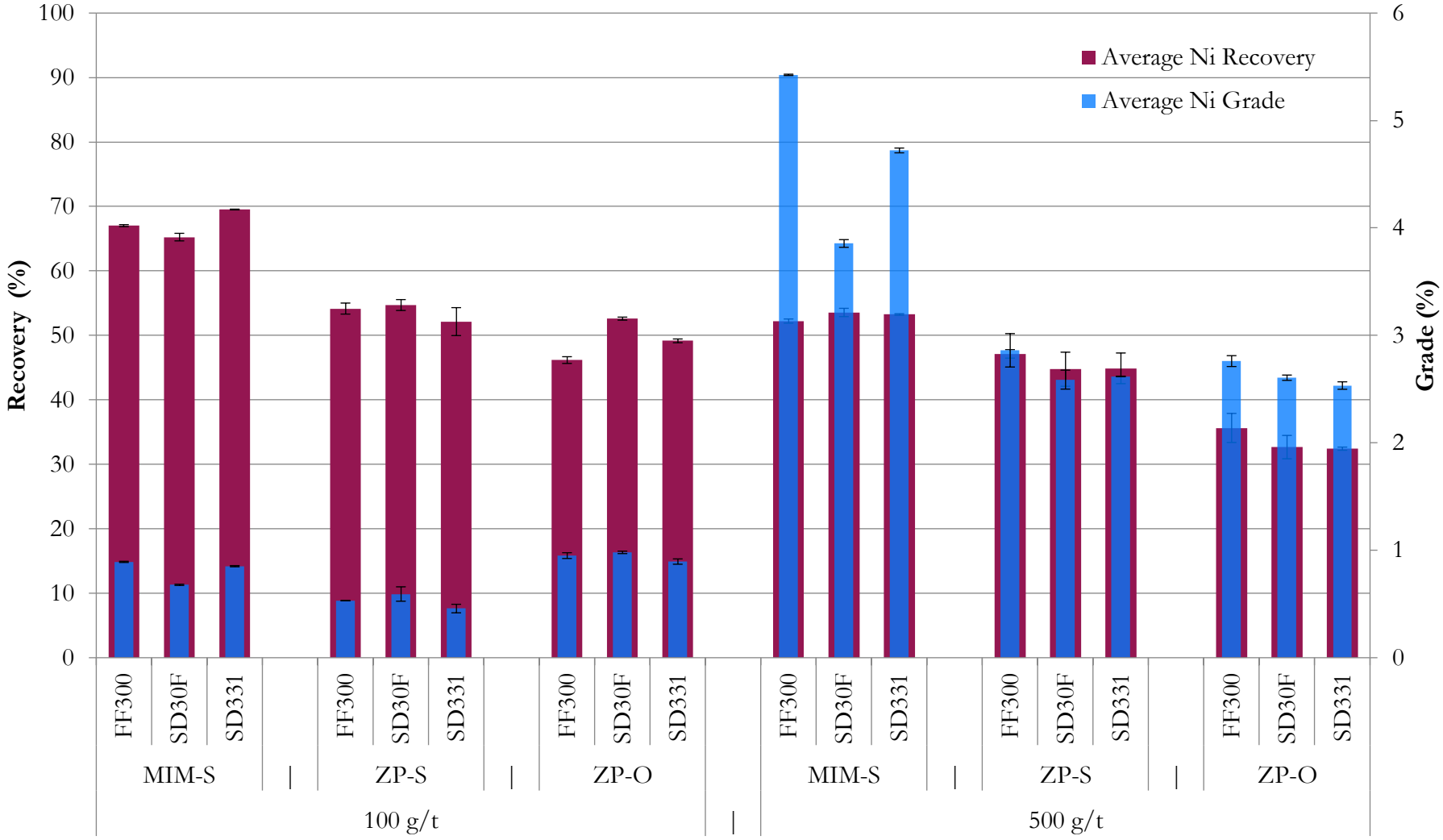

Figure 4.7: Ni Recovery and Grade for the 3 ores while varying depressant type and dosage. The error bars shown on the graphs represent standard error.

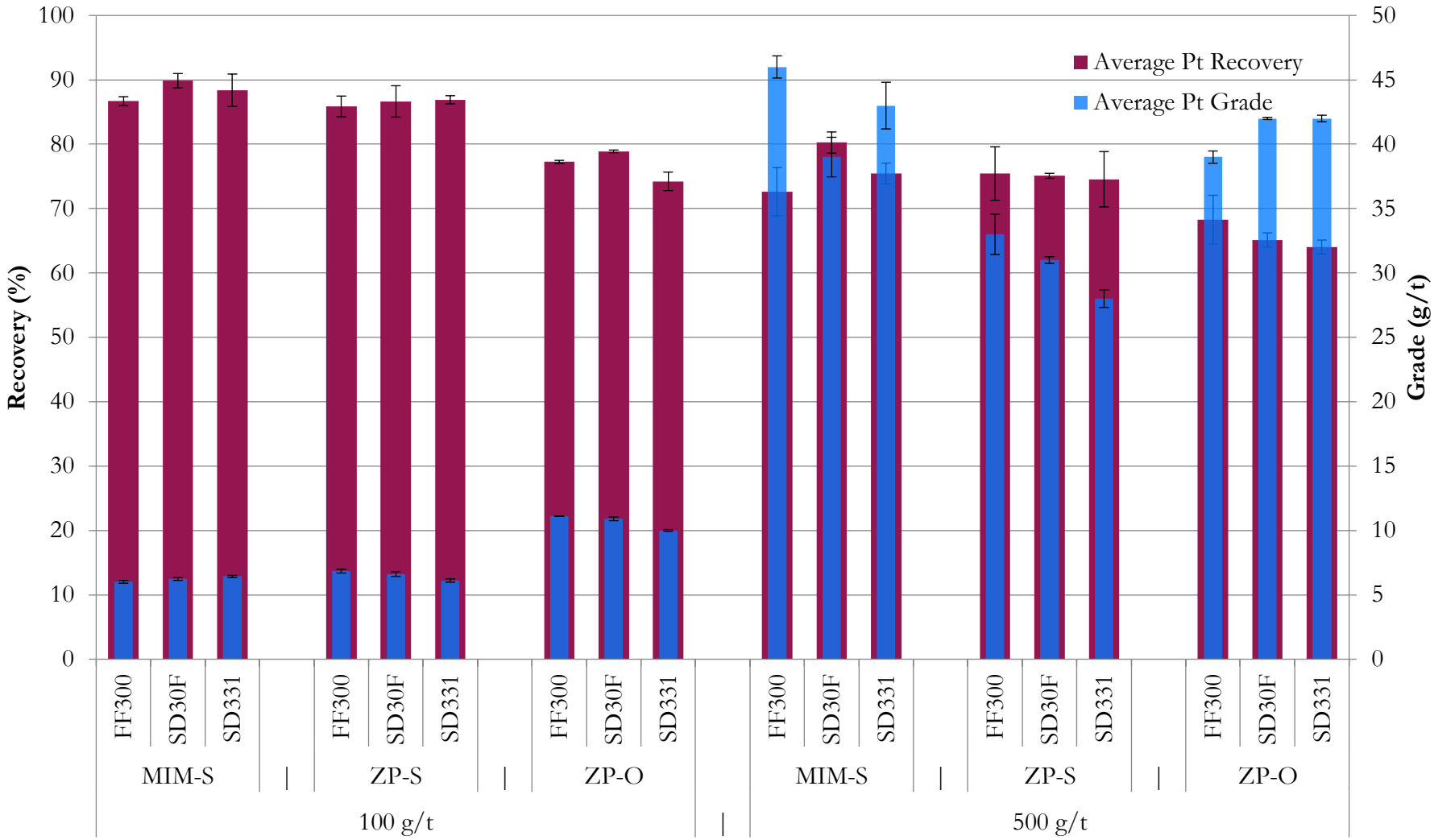

Figure 4.8: Pt Recovery and Grade for the 3 ores while varying depressant type and dosage. The error bars shown on the graphs represent standard error.

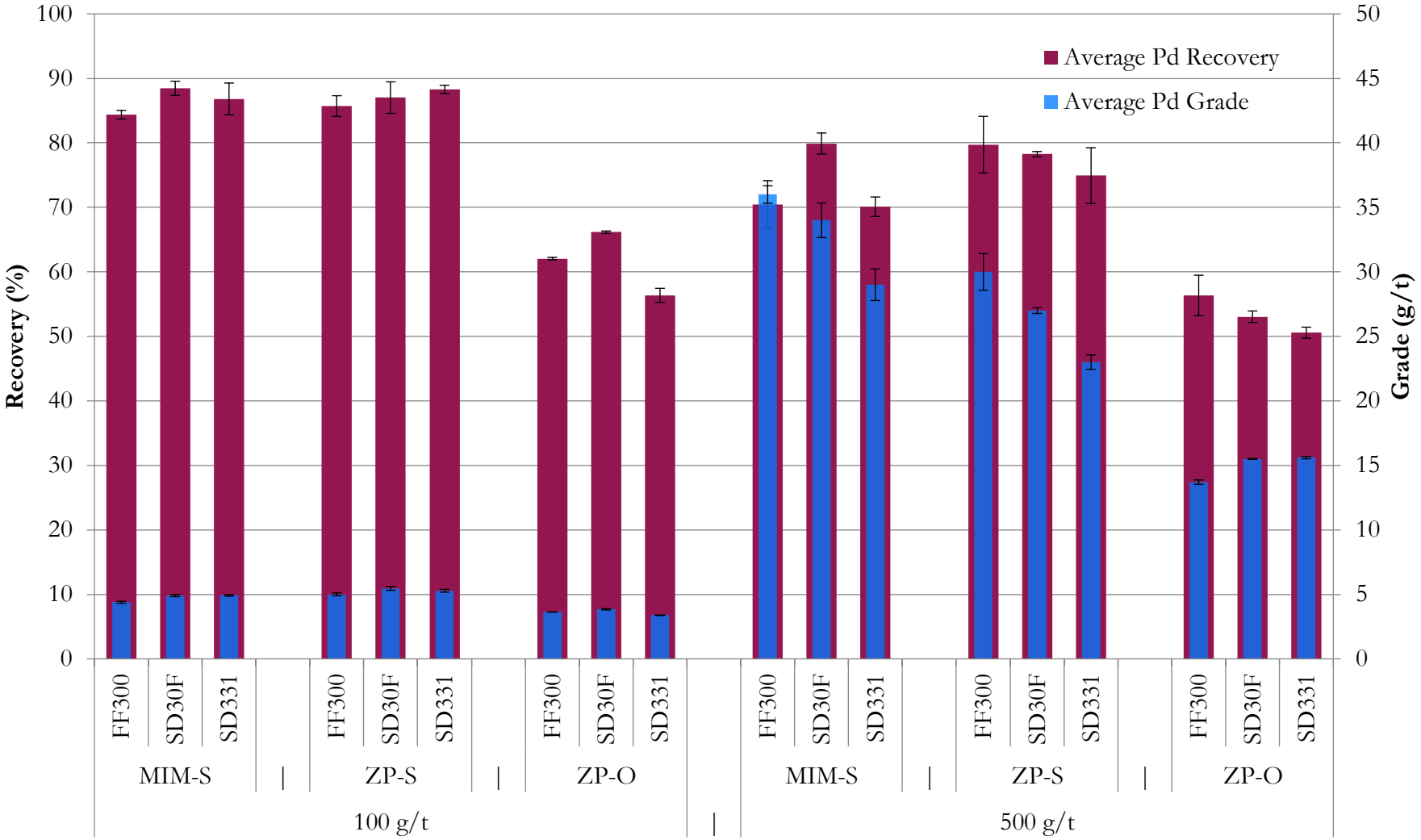

Figure 4.9: Pd Recovery and Grade for the 3 ores while varying depressant type and dosage. The error bars shown on the graphs represent standard error.

4.3.1 Mass of Solids and Water Recovered

The mass of solids and water recovered give an indication of the flotation response of the ores in terms of absolute masses that were recovered. Additional insight with regards to froth stability can be gained from these results. Figure 4.10 shows the cumulative mass of solids and water recovered in the flotation of the 3 ore samples. Most notable and expected is the higher mass of solids recovered at the lower depressant dosage. It can also be seen that the tests run at the high depressant dosage (500 g/t) generally have the same cumulative mass of solids recovered. MIM-S had the least amount of water recovered, followed by ZP-S and lastly ZP-O. At the low dosage (100 g/t) the solids recovered were in the following order: MIM-S>ZP-S>ZP-O, while MIM-S had the least amount of water recovered, with ZP-S and ZP-O having similar amounts.

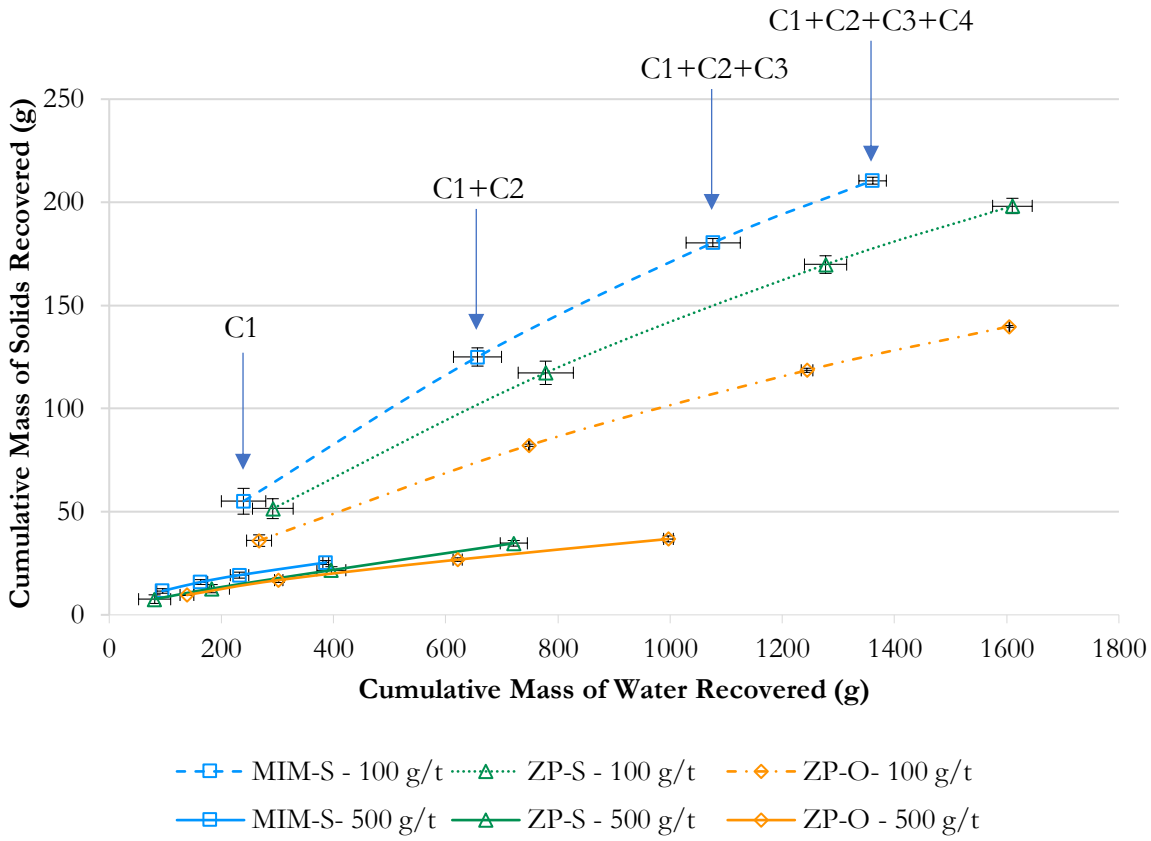

Figure 4.10: Cumulative mass of solids and water recovered in batch flotation tests with varying depressant type and dosage for each of the 3 ore samples. The error bars shown on the graphs represent standard error.

At the lower depressant dosage the higher amount of solids recovered per unit water in the tests with MIM-S could be due to the fact that it contains higher amounts of floatable material, as a result of having a BMS content higher than the other two ore samples and a talc content comparable to that of ZP-S. The higher mass of solids recovered in tests with MIM-S and ZP-S could be linked to a higher froth stability resulting from the higher amounts of hydrophobic material which stabilize the froth (the greater froth stability of MIM-S was visibly apparent during the batch flotation tests and froth stability tests - Section 4.3.3). Figure 4.11 shows a picture taken during the batch flotation tests of the 3 ore samples using FF300 at a 100 g/t dosage. The pristine

ore samples (MIM-S and ZP-S) show a more stable froth in comparison to the more oxidized ore sample (ZP-O).

It is suggested that the lower solids recoveries observed in the tests with ZP-O, in spite of having a similar BMS content to that of ZP-S, could be as a result of the lower amount of the naturally floating talc. In addition, the floatability of the BMS was lower for the ZP-O as was shown in Figure 4.6 and Figure 4.7.

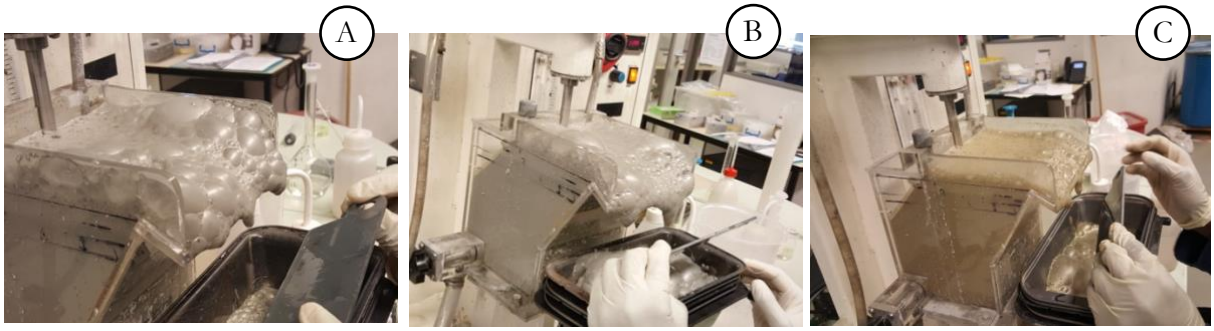

Figure 4.11: Differences in the froth observed during the batch flotation tests on the 3 ores after 1 minute of floating at the low depressant dosage. A: MIM-S, B: ZP-S and C: ZP-O.

4.3.2 Naturally Floating Gangue

To further compare the flotation response of the ores, the amount of floating gangue for each of the ores was calculated based on the method to quantify the amount of floating gangue (Wiese, 2009) and is shown in Figure 4.13. In this method, the total mass of gangue (that is, the full concentrate mass excluding sulfide minerals) was plotted against the amount of water recovered for all the tests. The slope of the line is equivalent to an 'entrainability factor' (See Figure 4.12 and Table 4.4) that was then used to calculate the amount of entrained gangue using Equation 4.1. The total mass of gangue less the mass of entrained gangue gave the amount of floating gangue (Equation 4.2). The detailed calculation is shown in the Appendix (Section 7.2).

$$Mass\ of\ Entrained\ Gangue = Mass\ of\ Total\ Water\ Recovered \times Entrainability\ factor \quad \text{(Equation 4.1)}$$

$$Mass\ of\ Floating\ Gangue = Mass\ of\ Total\ Gangue - Mass\ of\ Entrained\ Gangue \quad \text{(Equation 4.2)}$$

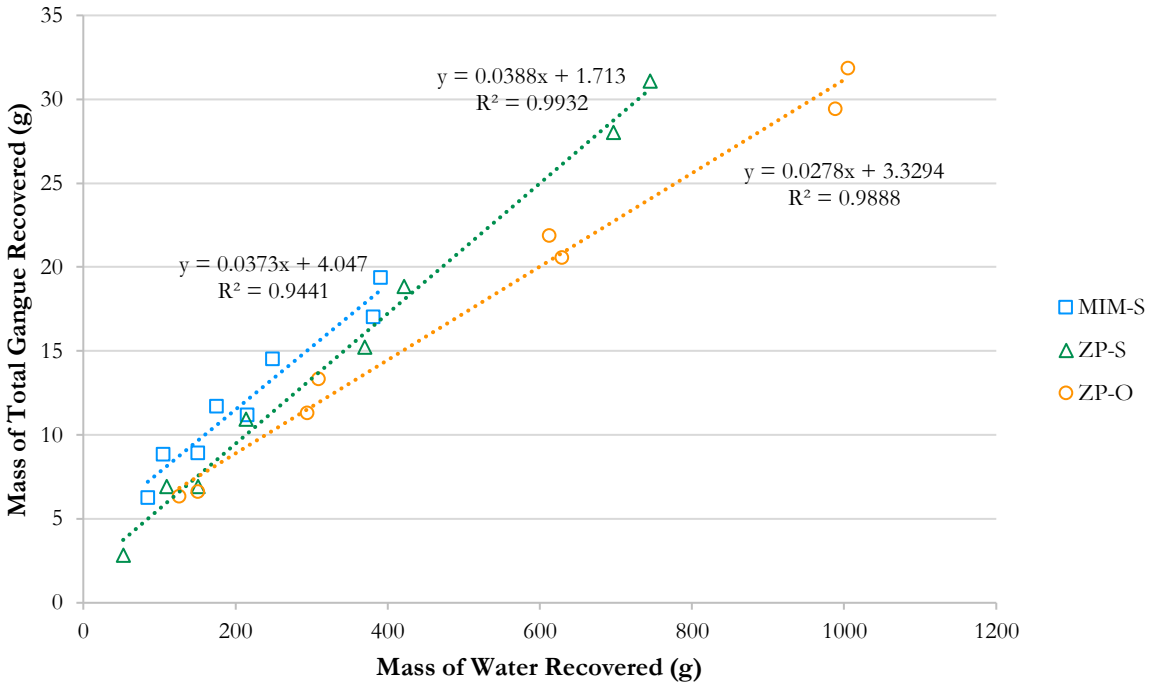

Figure 4.12: Mass of total gangue recovered versus mass of water recovered in batch flotation tests with the 3 ore samples so as to determine the entrainment factor for use in calculating the amount of naturally floating gangue.

Table 4.4: The entrainability factors of the different ores from the mass of total gangue recovered versus mass of water recovered (Figure 4.12).

	MIM-S	ZP-S	ZP-O
Entrainability Factor	0.0373	0.0388	0.0279

Entrainability factors for tests on MIM-S are similar to those of ZP-S and are higher than those of ZP-O. Additionally, this points towards MIM-S and ZP-S having the most stable froth as a result of the greater amount of entrained gangue which has a froth stabilizing effect. Had the entrained gangue been fully liberated, the lines of fit would have gone through the origin (Neethling and Cilliers, 2002b) but this is not the case here. This indicates that some of the gangue is associated with BMSs. Because the BMSs are naturally floatable a small amount of the gangue reports to the concentrate by true flotation rather than entrainment resulting in the lines of best fit (in Fig 4.12) not going through the origin.

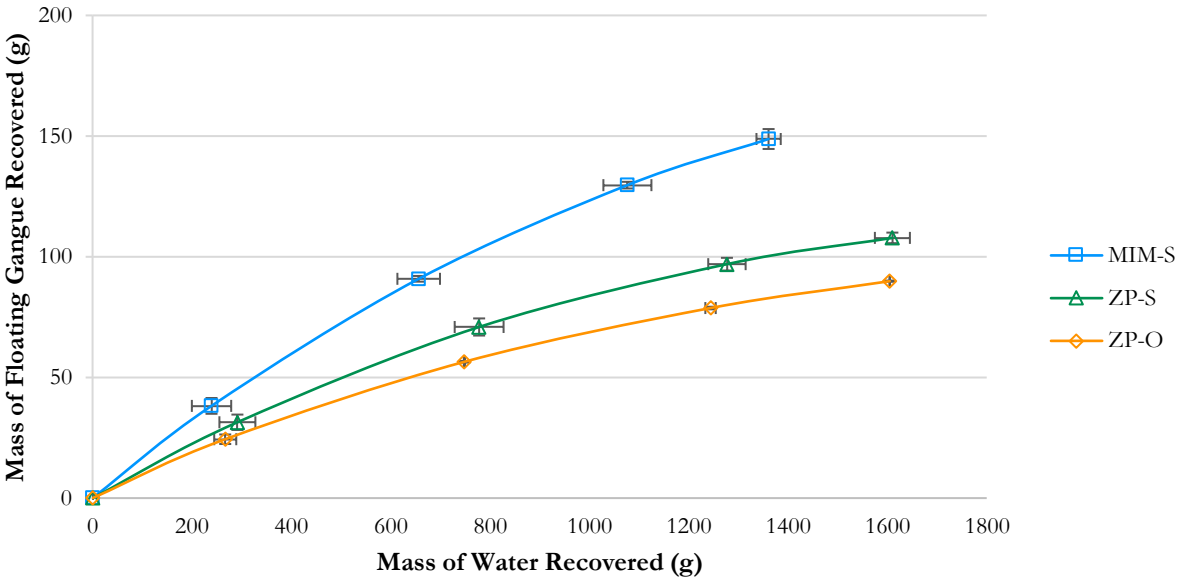

Figure 4.13: Cumulative Mass of Floating Gangue Recovered against Cumulative Mass of Water Recovered. The error bars shown on the graphs represent standard error.

MIM-S had the highest amount of naturally floating gangue (NFG). This was followed by ZP-S and lastly ZP-O. This was also the order of decreasing mass pull. It would have been expected that ZP-S would have the highest amounts of NFG of the 3 ore samples due to its higher orthopyroxene content (with a talc content comparable to that of MIM-S) since the greatest contribution to NFG has been attributed to the occurrence of composite orthopyroxene and talc particles (Becker *et al.,* 2009). The presence of these composite orthopyroxene and talc particles for the ore samples in this study is shown in Figure 4.14.

A mineralogical analysis of the batch flotation concentrate material in the +38/-75 µm size class was performed in order to gain insight on the characteristics of the naturally floating material. (The +38/-75 µm size class represents a particle size range more characteristic of recovery by true flotation (Savassi, 1998)). Such an analysis would give a better understanding of the differences between the ore samples as why there were differences in the ores' flotation response, if any. Through this analysis, it was noted that despite MIM-S containing lower amounts of talc in the concentrate (Table 4.5 and Figure 4.14) implying that it would have been expected that this ore would have a lower amount of NFG than ZP-S, this was not the case. A simplified mineral list was used is reported in Table 4.5 and the full one can be found in the Appendix (Section 7.2.1 – Table 7.9). Through liberation and association analysis it was observed that the talc in the MIM-S concentrate was locked (less than 30 % liberated) and lay within pyroxene grains (Figure 4.15). In this study, liberation refers to the area percent that is exposed while surface association is related to the perimeter of the grain or particle under investigation. This meant that it would be harder for a depressant to act on this locked talc compared to the liberated talc in ZP-S. Increasing the depressant dosage may, in such a case, lead to the loss of recovery of valuable minerals instead of an improvement of the grade. This is because high depressant dosages adversely affect valuable mineral recoveries. Further to this, an analysis of the talc grain size distribution within the same

size fraction showed that the talc in the MIM-S concentrate was more finely disseminated than that in ZP-S (Figure 4.16). The implication of this is that even lower amounts of this talc finely dispersed in pyroxene grains are able to result in the inadvertent flotation of the pyroxene associated with it thus resulting in greater amounts of NFG.

The mineralogy results of the feed were then analyzed yet again to assess the predictability of the flotation response based on the talc liberation (Figure 4.17) and grain size distribution (Figure 4.18). It was noted that MIM-S had 53 wt.% locked talc while ZP-S and ZP-O had 43 and 37 wt.% respectively. The talc grain size distributions in the feed samples were however almost identical. Based on these findings one may not be able to predict the sample that would have a higher amount of floating gangue as can be seen in the analysis of the concentrates.

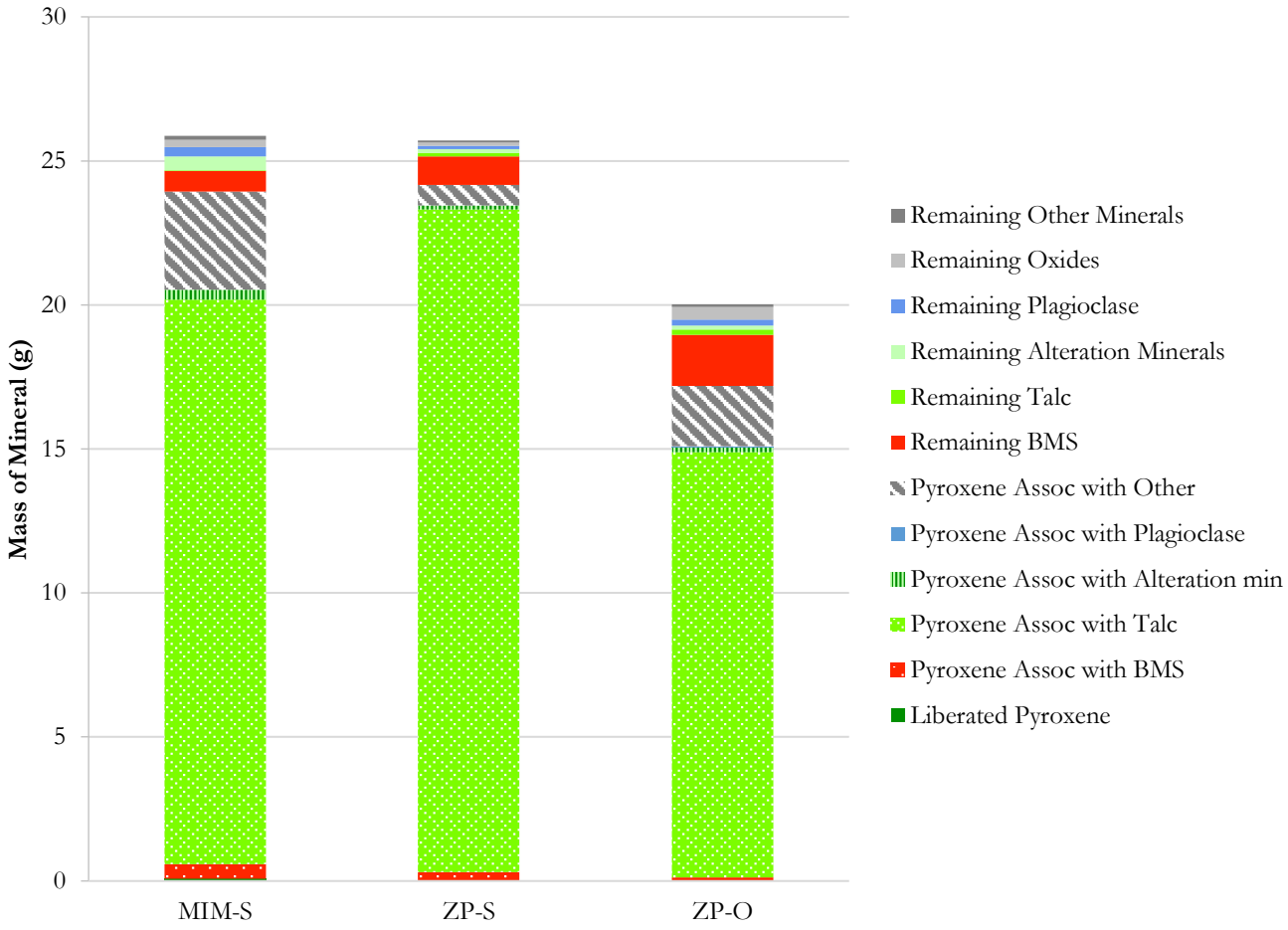

Figure 4.14: Mass of minerals in the in the -75/+38 µm fraction of the batch flotation concentrates of the 3 ores. (Assoc is short for Associated; e.g. Pyroxene Assoc with BMS = Total Mass of Pyroxene Associated with BMS + Mass of BMS in these composites. Remaining BMS = Mass of BMS not within these Pyroxene-BMS Composites. 'Other' is mainly composed of quartz. The tabulated results used to plot this graph are in Section 7.2 of the Appendix.)

Table 4.5: Simplified mineralogical composition of +38/-75 µm fraction of the batch flotation concentrates analyzed by QEMSCAN.

	Mass in MIM-S (g)	Mass in ZP-S (g)	Mass in ZP-O (g)
BMS	0.9	1.2	2.0
Pyroxene	18.8	18.1	12.1
Talc	1.4	3.2	3.3
Alteration minerals*	1.7	1.3	0.6
Plagioclase	0.6	0.2	0.3
Oxides	2.2	1.5	1.6
Other	0.3	0.2	0.2
Total	**25.9**	**25.7**	**20.0**

* Alteration minerals here include Serpentine, Chlorite, Mica and Amphibole

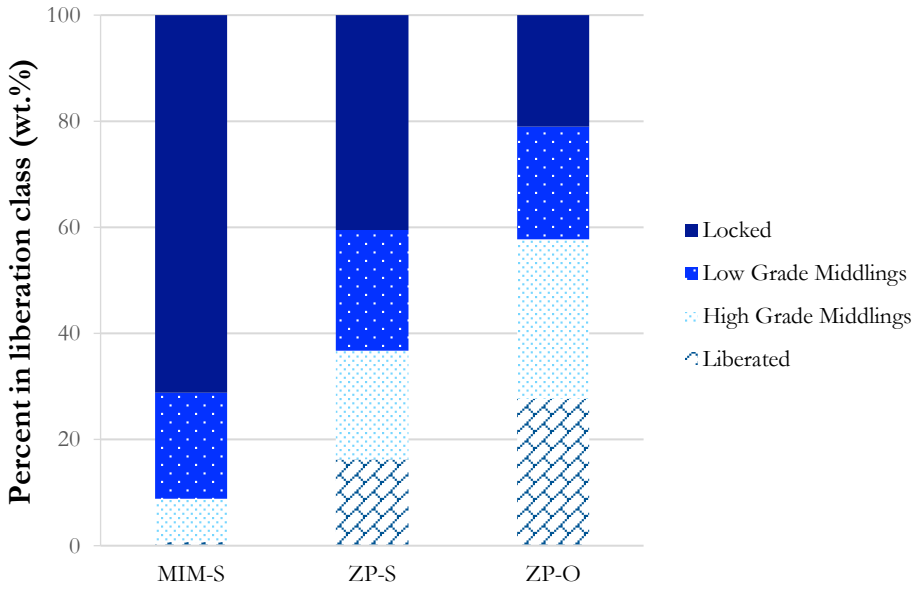

Figure 4.15: Talc liberation in the +38/-75 µm fraction of the batch flotation concentrates. Liberated: Area % Talc > 90, High Grade Middlings: 90 ≥ Area % Talc > 60, Low Grade Middlings: 60 ≥ Area % Talc > 30, Locked: Area % Talc < 30. (The tabulated results used to plot this graph are in Section 7.2 of the Appendix.)

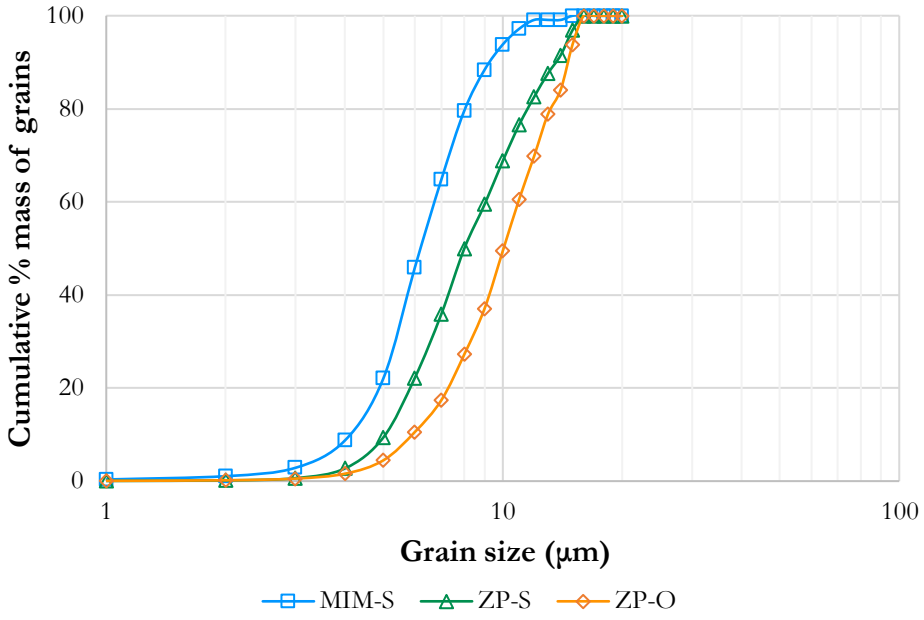

Figure 4.16: Talc Grain Size Distribution in the -75/+38 µm fraction of the batch flotation concentrates. Number of grains analyzed (N) = 4619 for MIM-S, 3787 for ZP-S and 5155 for ZP-O. (The grain sizes were calculated using equivalent circular diameter)

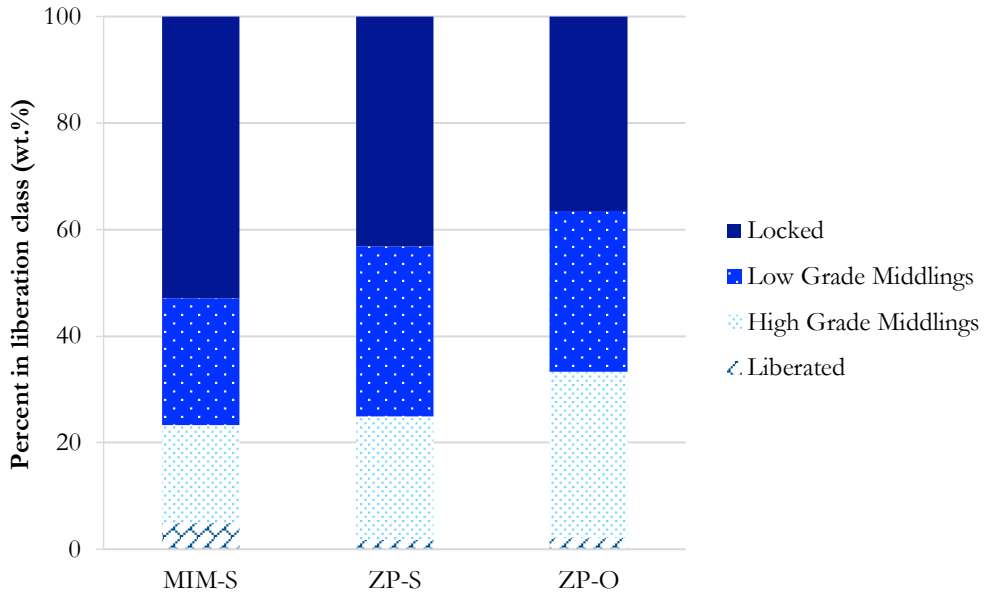

Figure 4.17: Talc liberation in the feed ore samples. Liberated: Area % Talc > 90, High Grade Middlings: 90 ≥ Area % Talc > 60, Low Grade Middlings: 60 ≥ Area % Talc > 30, Locked: Area % Talc < 30. (The tabulated results used to plot this graph are in Section 7.2 of the Appendix.)

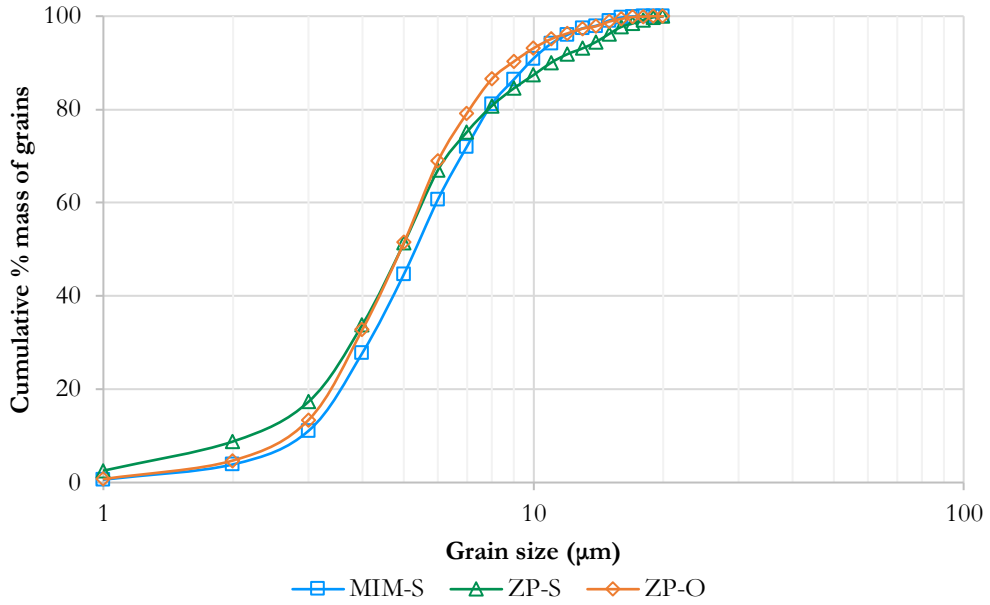

Figure 4.18: Talc Grain Size Distribution in the feed ore samples. Number of grains analyzed (N) = 47 555 for MIM-S, 61 801 for ZP-S and 47 424 for ZP-O. (The grain sizes were calculated using equivalent circular diameter)

4.3.3 Frothing Column Tests

In order to establish the contribution of froth stability to the flotation response, frothing column tests were conducted and the results are presented in Figure 4.19 and Table 4.6. It had been earlier postulated that the higher mass of solids recovered for MIM-S could be due to the higher froth stability observed in the tests with this ore sample and this was indeed seen to be the case in froth stability tests. The difference in the froth stabilities is likely to be more pronounced at industrial scale – that is when the froth is not in a froth limited system as in the batch flotation and frothing column tests.

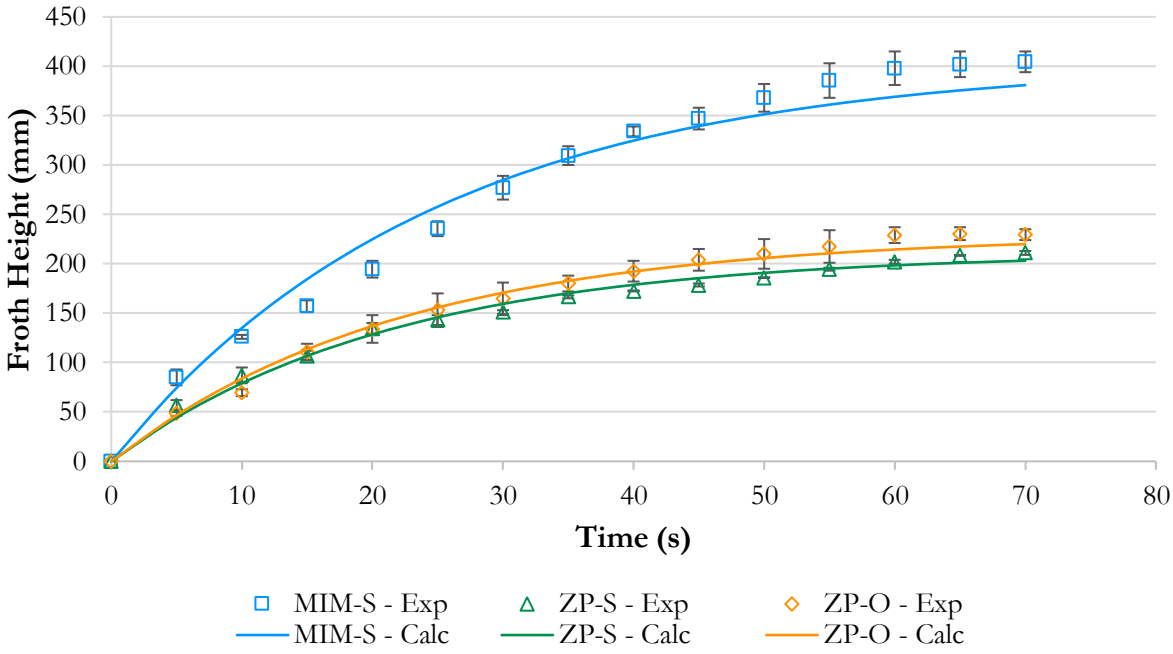

Figure 4.19: The rise in froth height with time for the 3 ore samples. (Exp denotes the experimentally attained froth height while Calc denotes the theoretical one). The error bars shown on the graphs represent standard error.

The maximum froth height attained with MIM-S was almost two times higher than that obtained with the other ores. ZP-O had the second highest and lastly ZP-S. This corresponds to the stability coefficients shown in Table 4.6 which indicate that MIM-S had the highest froth stability followed by ZP-O and ZP-S, respectively. The higher amount of BMS and NFG present in MIM-S could be one of the reasons contributing to its higher froth stability compared to ZP-S since MIM-S and ZP-S have similar amounts of floating gangue as was described in Section 4.3.2.

Table 4.6: Maximum observed froth height and stability coefficient for the 3 ore samples

	H_{max} (mm)	Stability Coefficient (s)
MIM-S	405	31.8
ZP-S	211	16.6
ZP-O	230	18.0

4.3.4 Concentrate Recoveries, Grades and Kinetics

Recoveries and Grades

The copper, nickel, platinum and palladium grades and recoveries representing the metallurgical performance of the ores at 100 g/t depressant dosage are presented in this section (Figure 4.20 A and B). The most important feature of these results is the consistently lower recoveries achieved by ZP-O for all four metals. Possible reasons for this will be discussed here. For Pt and Pd there was only sufficient sample to do cumulative grades and recoveries therefore kinetic curves for these elements cannot be shown.

For Cu, the recoveries for the pristine ores are between 82% and 88% but less than 70% for the more oxidized ore. For Ni recovery, 67%, 54% and 46% for MIM-S, ZP-S and ZP-O respectively. Pt and Pd recoveries for the pristine ore samples were in the range 84-87% while Pt recovery is 77% and Pd recovery is 62% for the more oxidized ore sample. Cu, Ni, Pt and Pd grades for MIM-S were 0.6%, 0.9%, 6 g/t and 4 g/t respectively. For ZP-S, they are 0.4%, 0.5%, 7g/t and 5 g/t respectively. Finally, ZP-O concentrate grade of Cu = 0.7%, Ni = 0.95%, Pt = 11g/t and Pd = 4g/t.

MIM-S consistently showed the highest and ZP-O the lowest Cu, Ni, Pt and Pd recoveries. The low recovery of ZP-O can also be linked to its lower BMS feed grade. The reasonably high recoveries of Pt and Pd in the case of MIM-S and ZP-S suggest a strong association of the Pt and Pd bearing minerals with base metal sulphides. However this seems not to be the case for ZP-O. Additionally, ZP-O's significantly lower Pd recoveries may be a result of the mobilization of the Pd during the oxidation of the ore, resulting in a lower Pd feed grade which leads to lower Pd recoveries. The more oxidized ore sample having lower recoveries but a similar BMS content to ZP-S warranted an analysis of the BMS liberation and association which is discussed in Section 4.3.5. On the whole, the Ni recoveries are lower than Cu recoveries across the tests, as expected. This is a result of the non-recoverable, non-sulphide Ni occuring in silicate gangue minerals such as olivine, pyroxene, chlorite or smectite.

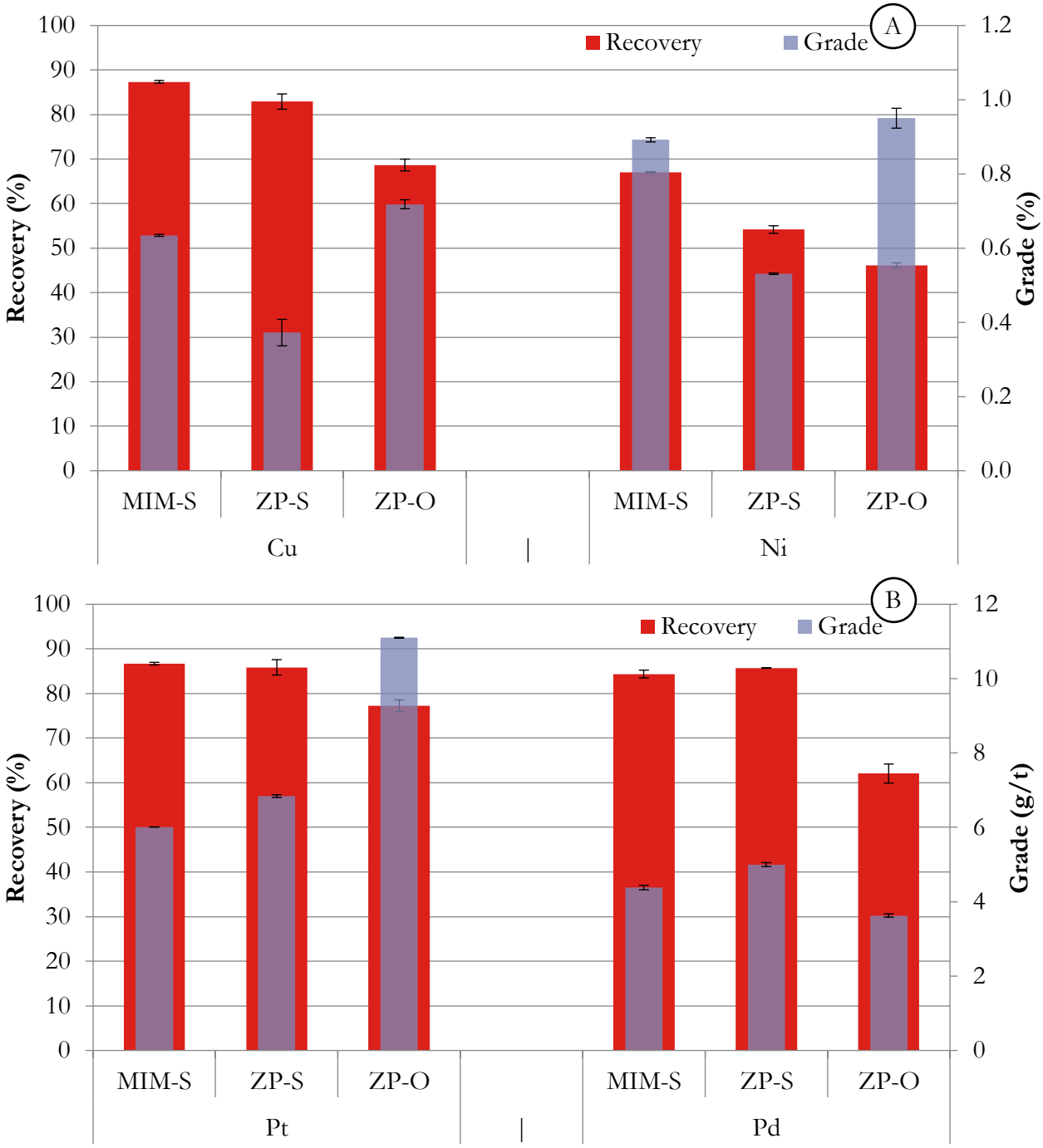

Figure 4.20: Cumulative Cu and Ni (A), Pt and Pd (B) recovery and grade in batch flotation tests at 100 g/t depressant dosage for each of the 3 ore samples. Note the difference in y axis scale for grade between Cu-Ni and Pt-Pd. The error bars shown on the graphs represent standard error.

The effect of head grade and oxidation on the recoveries of ZP-O is discussed in this section. The effect of head grade should be examined since it is well known that flotation recovery increases with increasing head grade (Napier-Munn, 1998). However, in this case, the poor recoveries experienced by ZP-O appear not to be related to the head grade since an examination of Table 4.2 shows that ZP-O has the highest grades of Pt and Ni and similar grade of Cu to MIM-S, yet the recoveries for all these metals are consistently lower for ZP-O. A possible explanation for this lies

in differences in mineralogy between pristine and oxidized PGM ores. A notable difference between the pristine and oxidized ores is in their PGM assemblages and the distribution of PGEs (Locmelis *et al.*, 2010; Oberthür, 2011). Several authors (Hey, 1999; Evans, 2002; Oberthür *et al.*, 2013; Becker *et al.*, 2014) have shown that a large proportion of the primary PGE carriers formerly in the pristine ores, inclusive of PGMs, has been destroyed and their PGE contents are now sited either in iron hydroxides, in smectites or occur as discrete 'PGE-oxides or hydroxides' and PGE-neoformations. This exacerbates the recoveries (especially those of Pd) for the more oxidized ore. Oberthür *et al.* (2013) noted that most (Pt,Pd)-bismuthotellurides would have been disintegrated. Some of the sulfide minerals would have disintegrated as well and released some of their base metal and PGE content and these are replaced by Fe-oxides/hydroxides (Evans *et al.,* 1994; Evans, 2002; Oberthür, 2011; Oberthür *et al.*, 2013; Becker *et al.,* 2014). Some PGE in the oxidized ores form secondary PGMs (in Pt/Pd oxides or hydroxides, Mn-Co hydroxides and secondary silicates). These changes reflect what potentially results in the lower recoveries when it came to the flotation of the more oxidized ore sample (ZP-O) due to the non-floatable nature of the secondary PGE carriers on which conventional xanthate flotation collectors do not work.

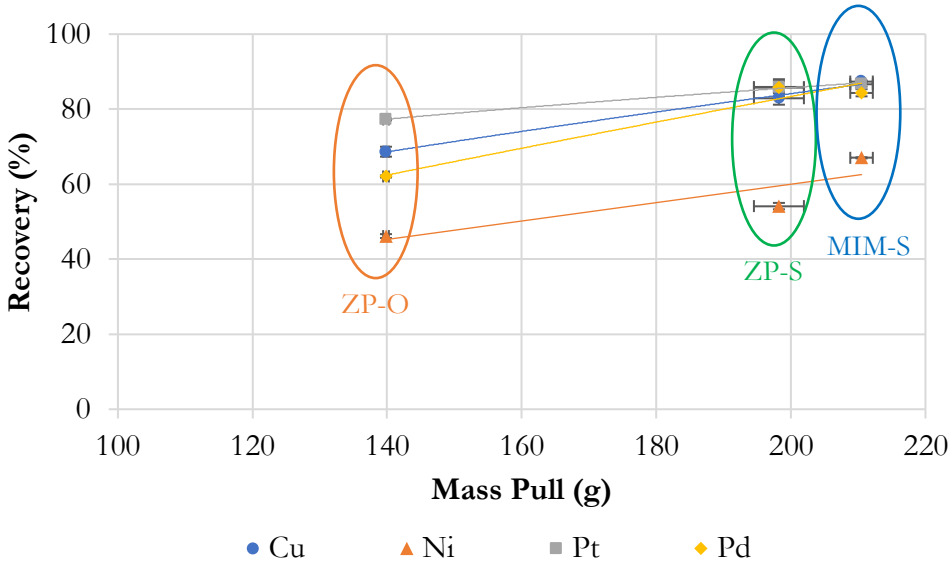

Figure 4.21: Recovery of Cu, Ni, Pt and Pd as a function of mass pull for all three ores at 100 g/t depressant dosage. The error bars shown on the graphs represent standard error.

Another point worth noting is the differences in mass pull between the different ores under the same cell operating and reagent conditions. It is well known that increases in mass pull result in an increase in recovery, with a simultaneous decrease in grade. The increase in grade that is usually associated with a decrease in mass pull is noted in Figure 4.20 A and B. ZP-O generally has the highest concentrate grades for all metals, except for Pd, where the head grade was significantly lower. The increase in mass pull resulted in a dilution of the concentrates for MIM-S and ZP-S, resulting in lower grades. Figure 4.21 shows the recovery of Cu, Ni, Pt and Pd as a function of mass pull. This shows that the flotation recovery generally follows the expected trend of increasing recovery with mass pull. Figure 4.21 also shows that ZP-O has a significantly lower mass pull than MIM-S and ZP-S. Reasons for this will be discussed in Sections 4.3.2 and 4.3.5. However, this data

suggests that, if operating conditions were optimized to increase the mass pull for ZP-O, increases in recovery may be realized, although this would be at the expense of grade.

Flotation Kinetics

In order to determine the kinetics of Cu and Ni in the batch flotation tests of the 3 ores, the Klimpel Flotation Model (Equation 4.3) was applied (Klimpel 1980). These results are presented in Figures 4.22 and 4.24 as well as Tables 4.7 and 4.8.

$$R(t) = R_{max}\left[1 - \frac{1}{kt}(1 - e^{-kt})\right] \qquad \text{(Equation 4.3)}$$

Where R is the theoretical recovery [%] at a certain time, t [min], R_{max} is the maximum recovery [%] and k is the kinetic rate constant [min^{-1}].

The Klimpel Flotation Model is based on the premise that not all particles in a flotation cell will be recovered by flotation despite the amount of time they spend in a flotation cell. It was selected due to it being regarded as one of the two most successful flotation models, the other of which is the distributed rate constant model that is appropriate for a bank of flotation cells and/or a complete plant unlike the Klimpel Model, which is suitable for single flotation cells as is the case in this study. Several authors (e.g. Xu, 1998; Vinnett *et al.*, 2015) also noted this first order kinetic model as the most widely used and adequate for modelling batch processes though other models have been formulated.

From Figure 4.22 as well as the constants in Table 4.7, it can be noted that when it came to the floatability of Cu, MIM-S outperformed the other two ores. It had both a higher maximum recovery (R_{max}) and rate constant (k). This was expected due to the higher Cu feed grade (Table 4.2) which serves as a driving force for the kinetics. On comparing ZP-S and ZP-O, however, it can be seen that the kinetics of the former are faster in spite of ZP-O having a higher Cu feed grade as kinetics are a function of the number of floatable particles in the feed which are potentially going to collide with bubbles and float (Schuhmann, 1942). This points towards a difference in the mineralogy or location of the Cu within the more oxidized ore sample. Since chalcopyrite is the main Cu bearing mineral within these 3 ores there is a likelihood that it is either not as well liberated or has experienced some oxidation in the more oxidized ore resulting in the lower recoveries and slower kinetics. Additionally, Figure 4.23 shows that there are significantly higher amounts of secondary Cu minerals, for example; covellite, chalcocite and chrysocolla, which will contribute to the slower kinetics of the Cu present in the ZP-O sample as these minerals are not readily floatable with the current SIBX collector (e.g. Grobler *et al.*, 2005; Lee *et al.*, 2009). Lee *et al.* (2009) obtained similar results in the comparison of the flotation kinetics of sulfide and oxide Cu ore samples. Chalcopyrite's higher floatability can also be seen in the higher amount of Cu reporting to the concentrate as chalcopyrite in the ZP-O concentrate than that in the feed, with a reduction in the amount of covellite and chalcocite (Figure 4.23).

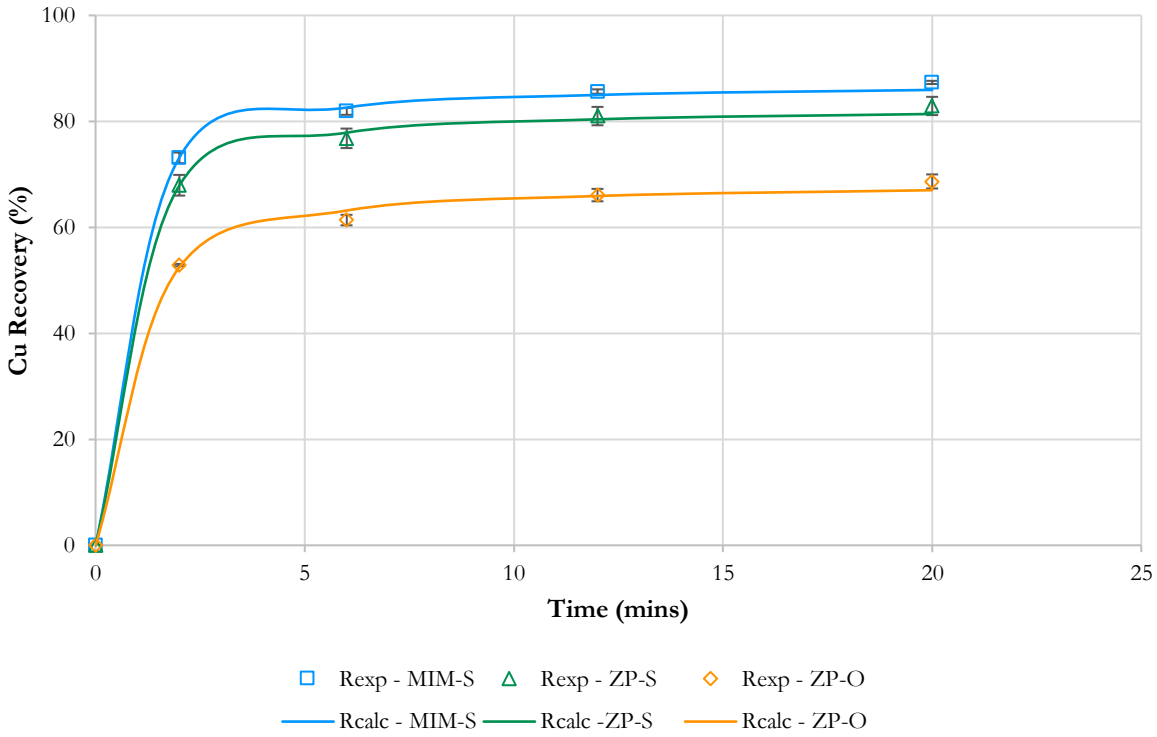

Figure 4.22: Cumulative Cu Recovery with time for the 3 ore samples. (Rexp is the recovery from the experiment while Rcalc is the modelled recovery)

Table 4.7: Maximum Cu recovery and flotation rate constant for the 3 ore samples

	R_{max} (%)	k (min^{-1})
MIM-S	86	3.1
ZP-S	81	2.7
ZP-O	67	2.1

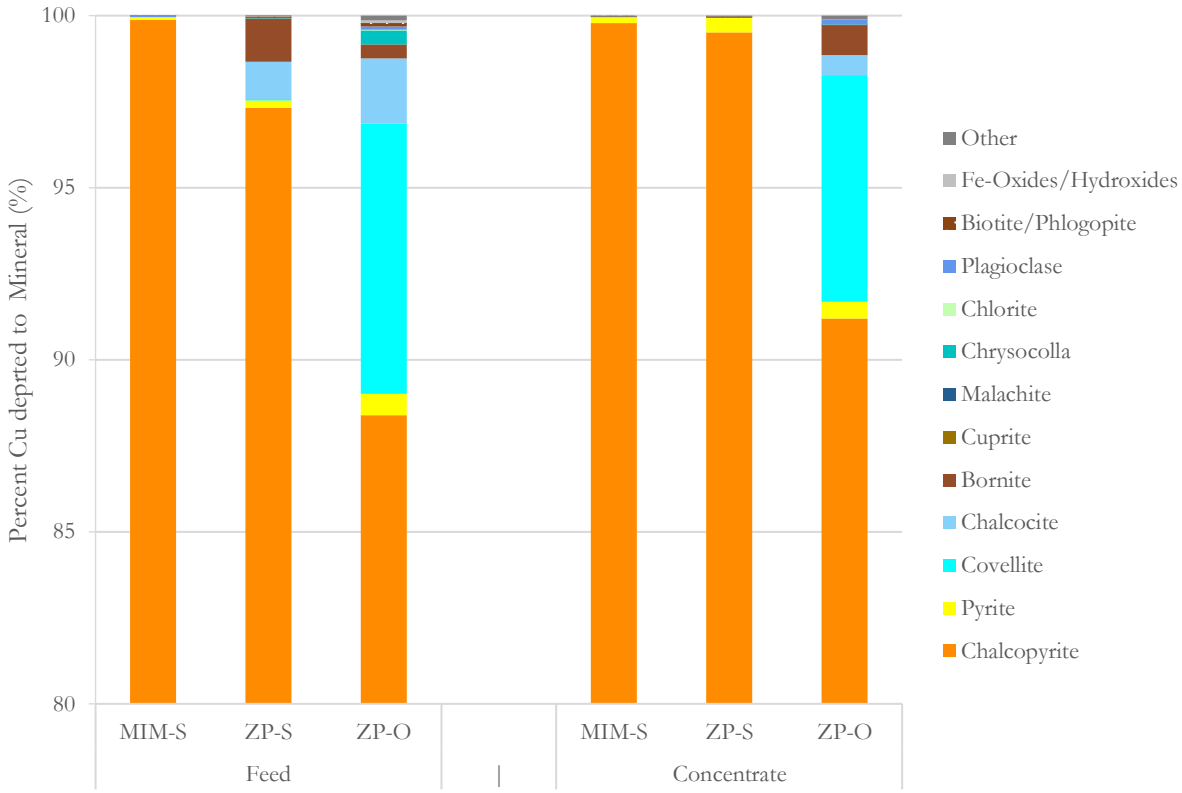

Figure 4.23: Cu deportment in the feed and the -75/+38 µm fraction of the batch flotation concentrates of the 3 ore samples. (Note that the y-axis starts at 80%. The tabulated results used to plot this graph are in Section 7.1 of the Appendix.)

Moving on to Ni and particularly focusing on the pentlandite content of the ores (due to the presence of some Ni bearing gangue minerals) it is again noted, from Figure 4.24, that MIM-S had the fastest kinetics of the 3 ore samples. This is likely due to MIM-S sample's higher Ni-sulfide feed grade (Figure 4.1). Pentlandite is the main floatable material hosting Ni in these PGE ores. ZP-S and ZP-O have similar Ni-sulfide feed grades (Figure 4.1) but the maximum recovery of Ni in ZP-S is higher than that in ZP-O while ZP-O has slightly faster kinetics (Table 4.8). This is again likely to be an issue of the oxidation of the Ni containing sulfides (further discussed in Section 4.3.5). Slower Ni flotation kinetics would have been expected for ZP-O due to the presence of Ni in secondary sulfide minerals like millerite and violarite in higher proportions than in the other ores (Figure 4.25) which the collectors may not have been designed to attach to. However, the larger proportion of Ni present as millerite in the ZP-O concentrate than in the feed, points towards potentially favourable conditions being present for its recovery through flotation. Further to this, Smith *et al.* (2011) indicate that millerite is strongly floatable, almost as much as pentlandite. However, violarite (which forms on pentlandite's cleavage planes), is slightly less floatable than pentlandite and may negatively affect its flotation (Chanturiya *et al.*, 2004) which is likely one of the reasons for ZP-O's poorer Ni recovery. It is however likely that despite MIM-S and ZP-O having similar Ni feed grades (notice the difference in amounts of Ni-sulfides shown as pentlandite in Table 4.1), there is a greater amount of Ni present in non-floatable silicates which adversely affects its flotation performance (Schuhmann, 1942).

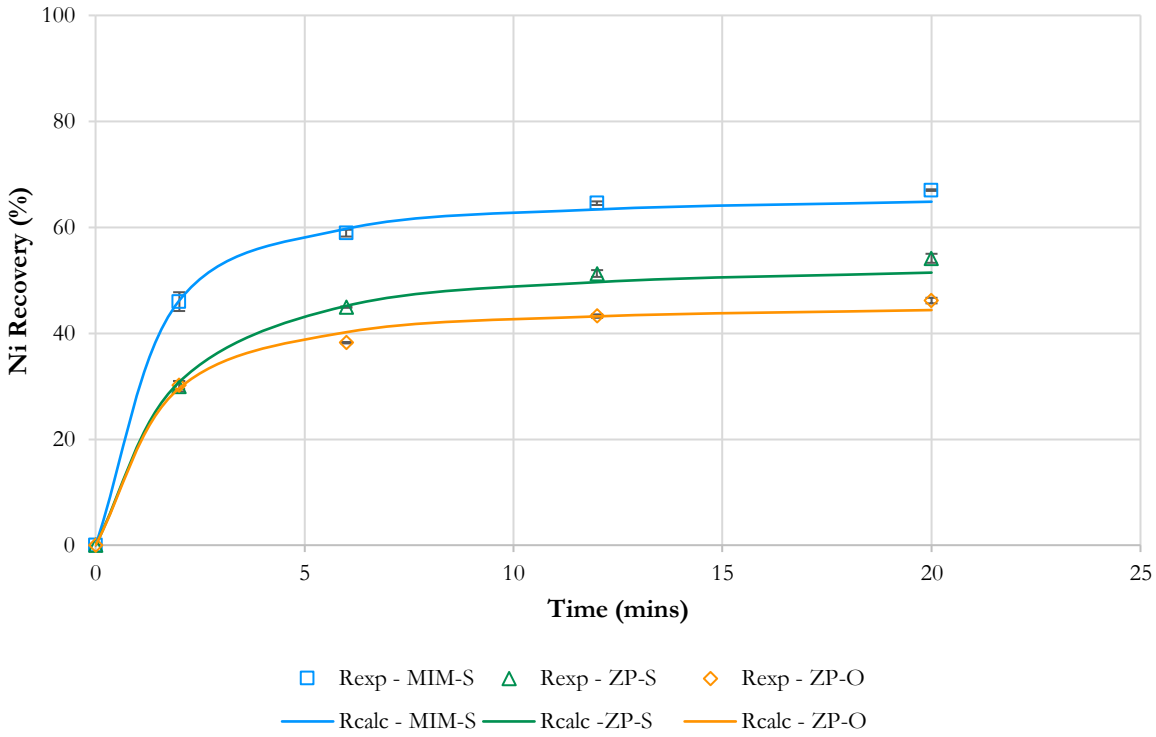

Figure 4.24: Ni Recovery with time for the 3 ore samples. (Rexp is the recovery from the experiment while Rcalc is the modelled recovery)

Table 4.8: Maximum Ni recovery and flotation rate constant for the 3 ore samples

	R_{max} (%)	k (min^{-1})
MIM-S	65	1.5
ZP-S	51	1.0
ZP-O	44	1.3

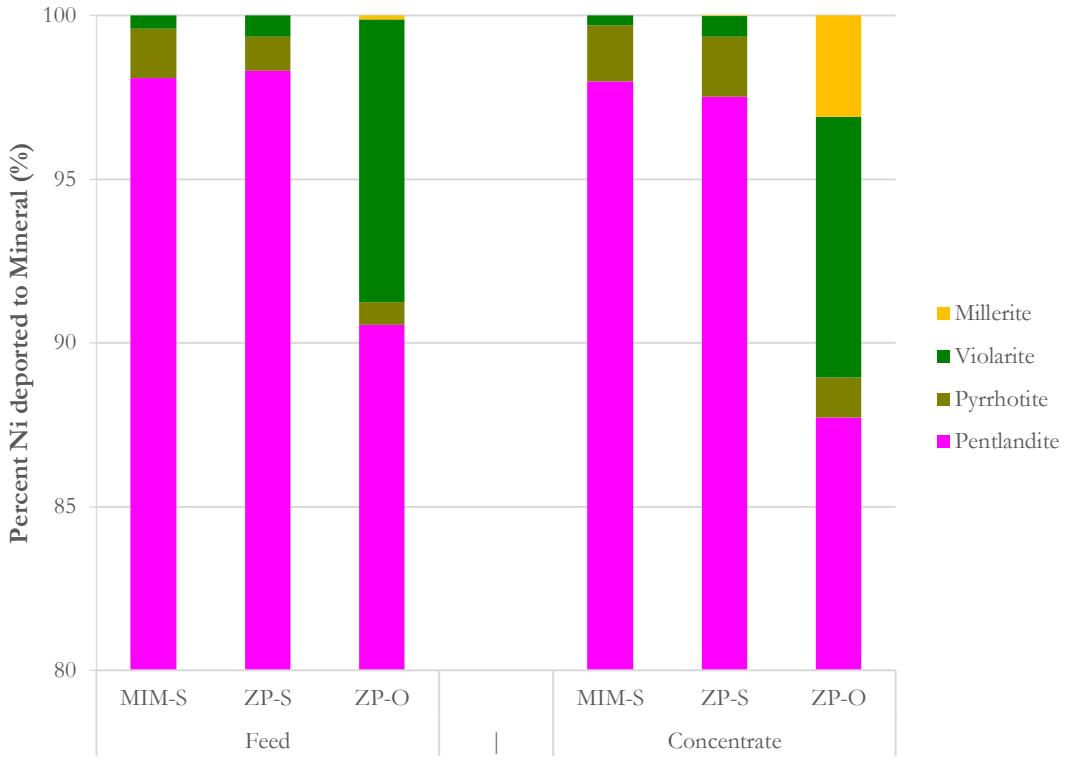

Figure 4.25: Ni deportment in the feed and the -75/+38 µm fraction of the batch flotation concentrates of the 3 ore samples. (Note that the y-axis starts at 80%. The tabulated results used to plot this graph are in Section 7.1 of the Appendix.)

4.3.5 BMS Liberation and Association

An understanding of BMS liberation and association is quintessential in gaining insight into batch flotation performance. In this study, liberation refers to the area percent that is exposed while surface association is related to the perimeter of the grain or particle under investigation. Greater BMS liberation would result in a greater likelihood of the BMS being recovered to the froth as a result of a greater surface area being available for attachment of particles to the air bubbles as they rise to the froth. On the other hand, greater BMS association with Fe-oxides/hydroxides results in the recovery being undesirably affected especially in the case where the BMS minerals are locked within the Fe-oxides/hydroxides.

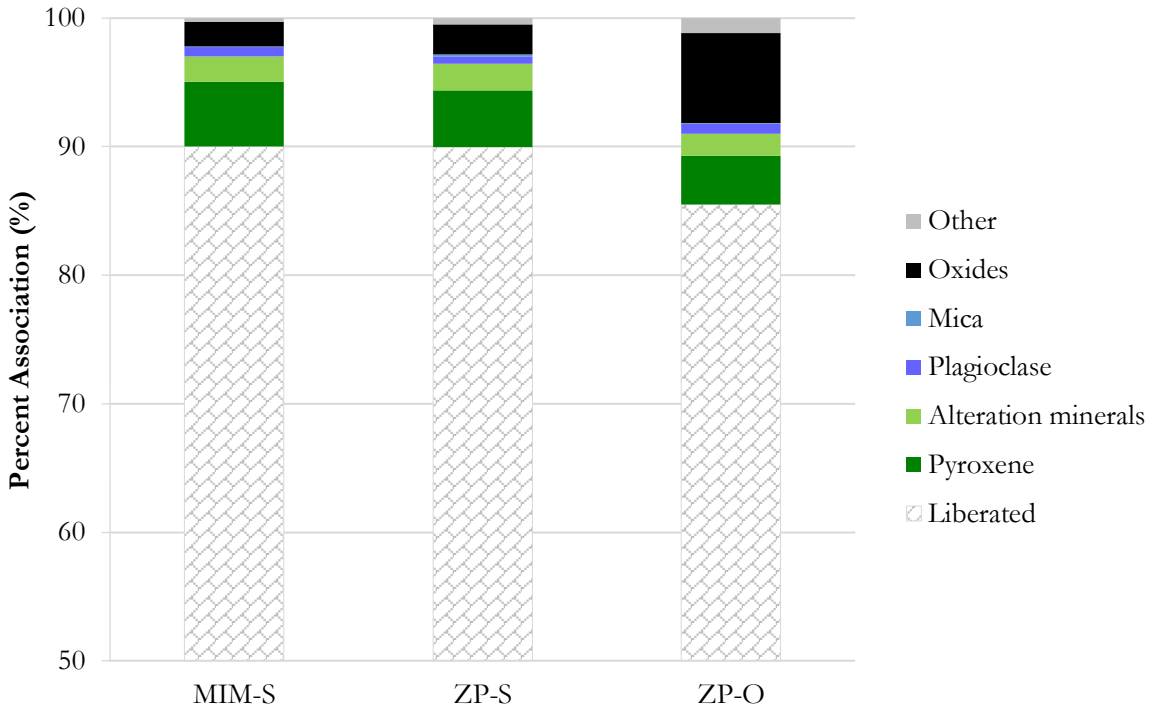

Figure 4.26: Base Metal Sulphide liberation and associations in the 3 ore samples. Liberated BMS: Area % BMS > 90. (Note that the y-axis starts at 50%. The tabulated results used to plot this graph are in Section 7.1 of the Appendix.)

As can be seen in Figure 4.26, the liberation of BMSs is similar for the pristine ore samples, (almost 90 wt.%), while 86 wt.% of the BMSs are liberated in the more oxidized sample. (Liberated material is that with an area % greater than 90 % in a particular grain). The BMSs in ZP-O are therefore only slightly less liberated than those in the pristine samples but this difference is worth noting due to the difference in flotation recoveries as described in Section 4.3 (An average of 15%, 15%, 8% and 24% difference in Cu, Ni, Pt and Pd recoveries, respectively, between the pristine and oxidized ore samples, with the more oxidized ore having the lower recovery). However, BMSs present in the ZP-O have greater association with Fe-oxides/hydroxides which negatively affect the flotation performance as a result of reducing the BMS floatability (Figure 4.26). The higher amount of oxides present in ZP-O (Table 4.1) and the greater BMS association to these oxides adversely affects their floatability. This is seen in the lower mass pull and Cu, Ni, Pt and Pd recoveries. Newell *et al.* (2006) also noted the presence of BMS-oxide composites on a Bushveld Complex oxidized ore.

Further to this, QEMSCAN/SEM images (Figures 4.27 A and B) show the existence of some Fe-oxide/hydroxide rims on the edges of BMS grains in ZP-O. Figure 4.28 shows the same for discrete PGM grains. The rimming (or presence of an oxide layer), which could even be at the nanometer scale, adversely affects the flotation and lowers BMS and PGM recoveries of an ore sample as it affects the attachment of reagents onto the surface of the valuable minerals and hinders mineral bubble attachment. This was also noted by Li *et al.* (2008) and Newell *et al.* (2006) in their work and is likely to be the case for ZP-O in this study. Since the rimming could be at the

nanometer scale it may not be fully detectable by QEMSCAN analysis which means that this rimming may be more prevalent than the current mineralogical analysis suggests.

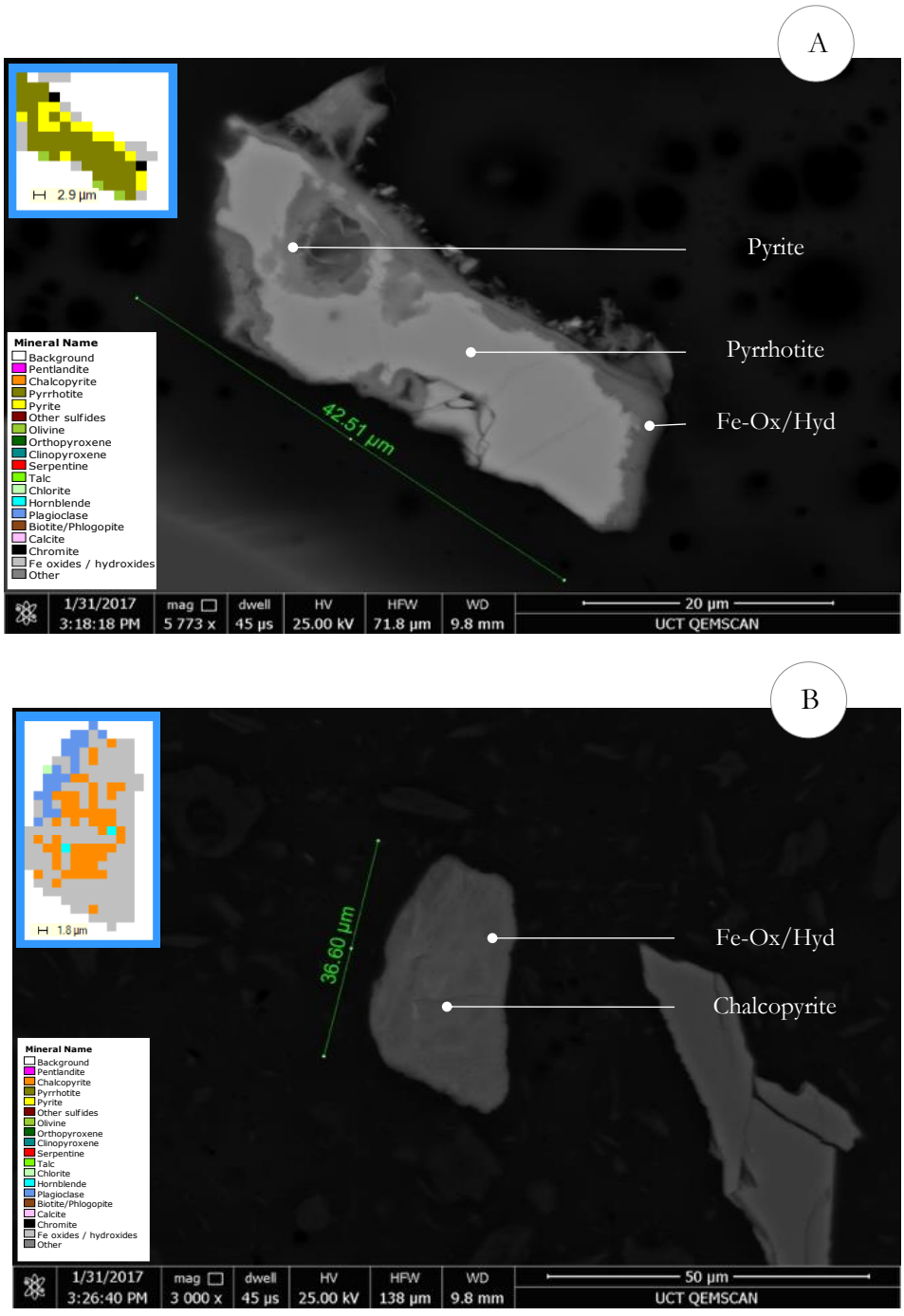

Figure 4.27: BSE and QEMSCAN False Colour Image of (A) composite particle of Pyrrhotite and Pyrite rimmed by Fe-Oxide/Hydroxides from the oxidized ore sample (ZP-O). (B) Locked Chalcopyrite grain rimmed by Fe-oxide/hydroxide from the oxidized ore sample (ZP-O). The QEMSCAN False Colour Images (in the top left corner of each of the BSE images) and the key provide an indication of the location of the different minerals on the particles of interest.

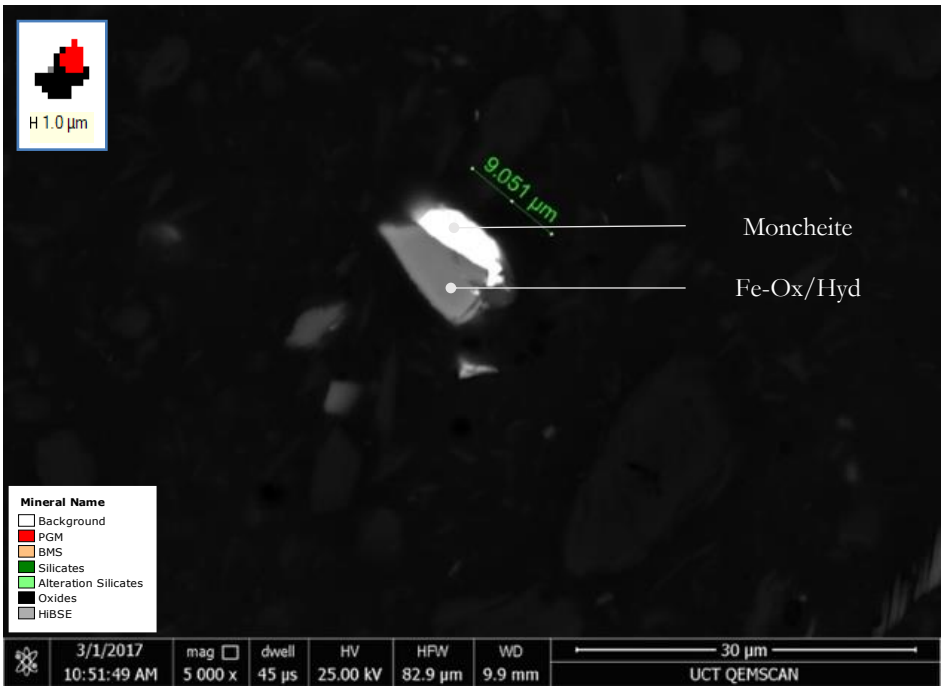

Figure 4.28: BSE and QEMSCAN False Colour Image of Moncheite (Pt-Bismuthotelluride) associated with Fe-Oxide/Hydroxide from the oxidized ore sample (ZP-O).

4.4 Disambiguation of alteration nomenclature in PGE ores

The importance of decoupling the terms that refer to alteration was noted in this study. A summary of the different types of alteration (oxidation and hydrolysis/hydration) and their potential effects on processing of ores is given in Figure 4.29 and explained in this section.

Oxidation, the type of alteration exhibited by the ores of the Great Dyke as noted in the studies by Evans (2002), Oberthür *et al.* (2003, 2013), Locmelis *et al.* (2010) and the current study, acts on the valuable minerals, that is the PGMs and BMSs. Oxidation destroys sulfides (Ni,Cu,Fe) and PGMs to certain degrees and leads to redistribution of Ni, Cu, PGE in the ores. It results in the partial to complete oxidation and disintegration of the PGMs and BMSs which affects the attachment of reagents to these minerals as most collectors are mineral specific. Even when partial oxidation occurs the surface of the mineral would not necessarily be the same thus affecting collector attachment. PGMs are additionally no longer associated to the BMS which are mostly targeted by collectors in the recovery of PGMs (Oberthür *et al.*, 2013). The PGMs, especially the fine ones, therefore become harder to recover. Base metals (BMs) and PGE also get redistributed and are no longer located where they would have been expected (in the BMSs or former PGMs), especially shown in the mobilization of Pd (Evans, 2002; Oberthür *et al.*, 2013). This results in new mineralogy and therefore conventional reagents not being able to attach to these. On the whole, these effects on the valuable minerals result in lower recoveries of these pay metals. In this case altering the depressant type or dosage may not yield improvements in the recovery of the valuable minerals but there would be need for new strategies (for example, the use of a different collector) to target these oxidized minerals or recover them based on their new mineralogy.

Hydrolysis/hydration, on the other hand, acts on the silicate minerals. It mostly results in the formation of large percentages of phyllosilicates, an example of which is talc. This has an effect on the amount of naturally floating gangue (Nagaraj and Brinen, 1996; Becker *et al.*, 2009; Lotter *et al.*, 2008; Jaseniak and Smart, 2009) as well as the rheology (e.g. viscosity) of an ore's slurry (Burdukova *et al.*, 2007; Ndlovu *et al.*, 2011b; Becker *et al.*, 2013). Higher amounts of naturally floating material lead to lower grades as well as the need for greater amounts of reagents to depress the gangue (Wiese, 2009; Becker *et al.*, 2014). Rheological complexity resulting from the higher amounts of phyllosilicates could then affect both the concentrate grade and recovery of an ore (Schubert, 2008; Bakker *et al.*, 2010; Patra *et al.*, 2010; Shabalala *et al.*, 2011; Farrokhpay *et al.*, 2011; Zhang and Peng, 2015). Both types of alteration were observed by Becker *et al.* (2014) in their work on a PGM ore from the Bushveld Complex in which there were high amounts of oxides as well as talc in the feed, this implies that the different types of alteration are not mutually exclusive. The changing of a depressant type and dosage could in this case improve the flotation performance as this reduced the amount of the naturally floating gangue reporting to the concentrate. Overall, the alteration of the gangue or silicate minerals (remembering that these make up approximately 98% of the processed material from Great Dyke ores) through hydrolysis/hydration mostly has an effect on the concentrate grade rather than the recovery.

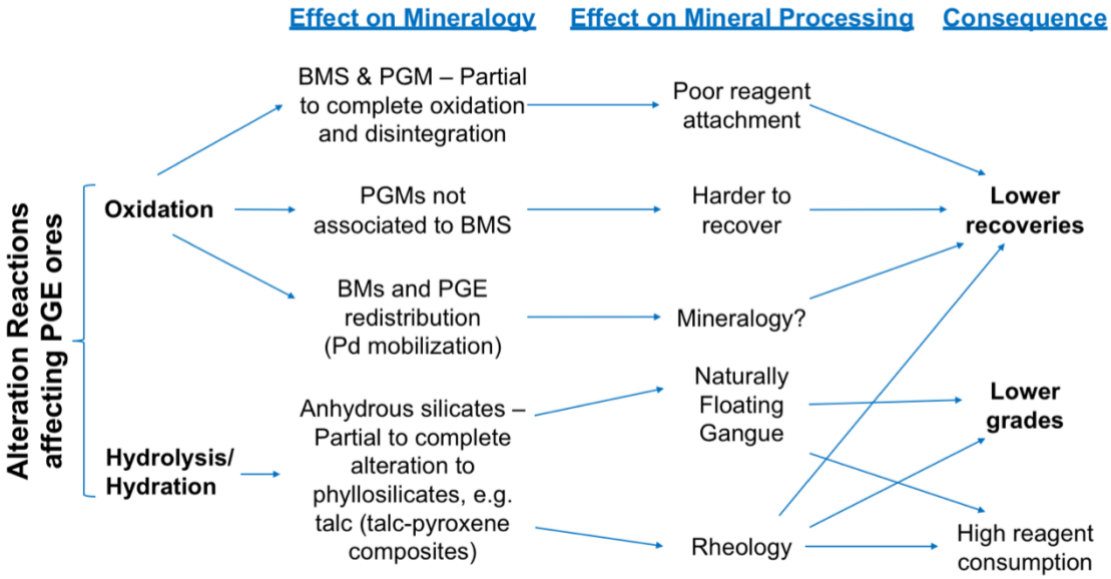

Figure 4.29: Potential challenges arising from alteration of PGM ores, based on the findings of Evans *et al.* (1994), Evans (2002), Oberthür *et al.* (2003, 2013), Newell *et al.* (2006), Locmelis *et al.* (2010), Becker *et al.* (2014) and the current study.

It is worth noting that the 'loose' use of terminology may be misleading in that a so-called "oxidized" ore may have undergone a type of alteration called hydrolysis/hydration which acts on the silicate gangue minerals and not necessarily oxidation of the valuable minerals. The alteration exhibited by ZP-O was of the oxidation type and thus the use of a different type of depressant in an attempt to curb poor flotation performance would be (and was) futile since the problem lies, not in the gangue, but in the valuable minerals.

Chapter 5 - Conclusions and Recommendations

This study has shown the effects of differences in the mineralogy of 3 ores on their rheological characteristics and batch flotation performance, with the use of 3 different depressants varying in their degree of substitution.

As had been hypothesized, the more oxidized ore sample (ZP-O) had markedly lower flotation recoveries than the pristine ones (MIM-S and ZP-S). This was attributed to the oxidation of these valuable minerals resulting in the presence of Fe oxides/hydroxides which render the valuable minerals non-recoverable as the oxides and hydroxides are not recoverable with the current flotation reagent suite, among other reasons. Relatively small differences in bulk and BMS mineralogy were found to lead to large differences in flotation recovery. The more oxidized ore sample's lower recoveries were additionally attributed to the potential rimming of the BMS particles. An understanding of the PGE/PGM mineralogy would add to this work and result in a better understanding of the behaviour of Pt and Pd, particularly in the more oxidized ore. The main mineralogical differences noted for ZP-O were:

- Lower phyllosilicate content (5% in comparison to 10%), which was unexpected in a so-called oxidized ore.
- Higher Pt/Pd ratio (2.3 versus 1.3)
- Slightly higher oxides (1.6% compared to 0.9%)
- Slightly lower BMS liberation (86% compared to 90%)
- Slightly greater association of BMS with oxides (12% versus 5%)
- Oxide rimming of BMS particles

The hypothesis that the greater phyllosilicate alteration mineral content of an ore results in lower grade and recovery of valuable minerals (using the same reagent suite) as a result of the higher amount of NFG within the ore, as well as the rheological complexities associated with these phyllosilicate alteration minerals, was partially disproved. This was shown through the decoupling of the two alteration reactions, oxidation and hydrolysis/hydration. Noting that oxidation acts on the valuable minerals and thus lowers valuable mineral recovery while hydrolysis/hydration acts on the silicate minerals and mainly affects grade. The effect of the presence of higher amounts of the naturally floating phyllosilicate mineral, talc, was noticed in the higher mass of solids recovered for the pristine ores (affecting the valuable mineral grades) compared to ZP-O. It had been previously assumed that a more 'oxidized' ore generally meant one that is both richer in oxides and hydrous silicates, but this was not the case. The effect of talc grain size distribution, liberation and association was also discussed, noting that a more finely disseminated and locked (unliberated) talc mineralogy resulted in greater amounts of NFG. The effect of the amount of phyllosilicate minerals in affecting the rheology of the slurries seemed not to be noticeable in the case of the ore samples analyzed, which exhibited different amounts of these phyllosilicates. This was attributed to the dampening of any rheological complexities due to

the greater proportion of non-rheologically complex silicates, like orthopyroxene. It is recommended that Great Dyke operators limit solids concentrations to below 30-35 vol.% (approximately 60-65 wt.% solids at a specific gravity of 3.3) which is the region after which rheological complexity starts to increase exponentially. This will help avoid or reduce processing challenges associated with the rheological complexity that arises at concentrations beyond these. Worth noting, however, is that solids concentrations in flotation are lower than the values above, but these concentrations may be present in other sections of the circuit (e.g. comminution). An awareness of the potential problem this could pose, coupled with monitoring the solids concentration will prove worthwhile when there are some inconsistencies in plant performance.

With regard to depressants, it had been hypothesized that using a depressant with a higher degree of substitution (DS) at the same dosage decreases the rheological complexity of a mineral slurry as a result of the increased negative electrical charge of particles in the slurry upon adsorbing the CMC. This was not observed in the tests with these Great Dyke ore samples, again due to the dampening effect of the minerals that reduce complex rheological characteristics that are in greater proportion than the phyllosilicates that lead to rheological complexity. Further to this, it is clear that changing depressant type does not result in grade or recovery improvement for an ore that has undergone oxidation, rather than hydrolysis/hydration, as the challenge lies not in the gangue but with the valuable minerals. However, all three depressant types tested in this study performed their primary role of depressing the gangue comparably well but did not exhibit the added benefit of acting as a dispersant in this case.

Additionally, the ambiguity of the use of the term 'oxidized' was elaborated upon in this study. Some ores could have undergone alteration of the oxidation type (as seen in the current study) while others could have undergone hydration/hydrolysis, though these types of alteration are not mutually exclusive. Oxidation acts on the valuable minerals and leads to reduced recoveries while hydrolysis/hydration acts on the silicate gangue minerals and results in reduced concentrate grades.

It is recommended that future work be conducted analyzing the mineralogy and association of the PGMs especially in the case of the Great Dyke oxidized ores (including pervasively oxidized ones). This will help in formulating strategies to recover these PGEs that make up a large portion of the Great Dyke. Test work similar to that conducted in this current study can also be performed on pervasively oxidized Great Dyke PGE ores to gain even greater insight in how to process them effectively. Additionally, tests should be conducted to distinguish between the Ni in the silicates and sulfides could help clarify reasons for differences in Ni recovery for certain ores despite having similar Ni content in the feed.

On the whole, even a seemingly small difference in the mineralogy of the ores resulted in a marked change in their flotation responses. Continual assessment of an ore's mineralogy (including the PGMs), an understanding of the repercussions and application of the appropriate response or measures is therefore paramount to ensure consistent grades and recoveries in mining operations. Such measures could include, but are not limited to, ore blending strategies, use of different reagent suites, optimized mass pull and even the design of the reagents that target the more oxidized valuable minerals.

Chapter 6 - References

Ackerman, P.K., Harris, G.H., Klimpel, R.R. and Aplan, F.F., 1987. Evaluation of flotation collectors for copper sulfides and pyrite, I. Common sulphydryl collectors. *International Journal of Mineral Processing*, 21, pp.105–127.

Aktas, Z., Cilliers, J.J. and Banford, A.W. 2008. Dynamic froth stability: Particle size, airflow rate and conditioning time effects. *International Journal of Mineral Processing*, 87(1–2), pp.65-71.

Arnold, B.J. and Aplan, F.F., 1986. The effect of clay slimes on coal flotation, part 2: the role of water quality. *International Journal of Mineral Processing*, 17, pp.243–260.

Bakker, C.W., Meyer, C.J. and Deglon, D.A., 2010. The development of a cavern model for mechanical flotation cells. *Minerals Engineering*, 23(11), pp.968-972.

Barbian, N., Hadler, K., Ventura-Medina, E. and Cilliers, J. J., 2005. The froth stability column: linking froth stability and floatation performance. *Minerals Engineering*, 18(3), pp.317-324.

Barbian, N., Ventura-Medina, E. and Cilliers, J.J., 2003. Dynamic froth stability in froth flotation. *Minerals Engineering*, 16(11), pp.1111-1116.

Barnes, H.A., Hutton, J.F. and Walters, K., 1989. An Introduction to Rheology. Elsevier Science Publishers, Amsterdam. pp.119-130.

Baum, W., 2014. Ore characterization, process mineralogy and lab automation a roadmap for future mining. *Minerals Engineering*, 60, pp.69-73.

Beattie, D.A., Huynh, L., Kaggwa, G.B. and Ralston, J., 2006. Influence of adsorbed polysaccharides and polyacrylamides on talc flotation. *International Journal of Mineral Processing*, 78(4), pp.238–249.

Becker, M., Broadhurst, J.L. and Bradshaw, D.J., 2017. Process mineralogy: the key to unlocking the provision of minerals and metals to a sustainable world. *MEI Process Mineralogy 17*, Cape Town.

Becker, M., Harris, P.J., Wiese, J.G. and Bradshaw, D.J., 2009. Mineralogical characterisation of naturally floatable gangue in Merensky Reef ore flotation. *International Journal of Mineral Processing*, 93(3-4), pp.246–255.

Becker, M., Wiese, J. and Ramonotsi, M., 2014. Investigation into the mineralogy and flotation performance of oxidised PGM ore. *Minerals Engineering*, 65, pp.24–32.

Becker, M., Yorath, G., Ndlovu, B., Harris, M., Deglon, D. and Franzidis, J.P., 2013. A rheological investigation of the behaviour of two Southern African platinum ores. *Minerals Engineering*, *49*, pp.92-97.

Bikerman, J., 1973. Foams. 1st ed. Springer, New York.

Board, N., 2002. Modern Technology of Synthetic Resins and Their Applications. Asia Pacific Business Press Inc. New Delhi, India. pp.556-560.

Bradshaw, D., 2014. The role of "process mineralogy" in improving the process performance of complex sulphide ores. In *Proceedings of the XXVII International Mineral Processing Congress, Santiago, Chile*. pp. 1–23.

Bradshaw, D.J., Oostendorp, B. and Harris, P.J., 2005. Development of methodologies to improve the assessment of reagent behaviour in flotation with particular reference to collectors and depressants. *Minerals Engineering*, 18(2). pp.239–246.

Brough, C., 2008. An investigation into the process mineralogy of the Merensky Reef at Northam Platinum Limited. MSc Dissertation. University of Cape Town.

Bulatovic, S., 2003. Evaluation of alternative reagent schemes for the flotation of platinum group minerals from various ores. *Minerals Engineering*, 16(10), pp.931–939.

Bulatovic, S.M., 2007. Handbook of flotation reagents: chemistry, theory and practice: Volume 1: flotation of sulfide ores. Elsevier. Amsterdam, Netherlands. pp.147-150.

Burdukova, E., Becker, M., Ndlovu, B., Mokgethi. & Deglon, D. 2008, "Relationship between slurry rheology and mineralogical content", In *XXIV International Minerals Processing Congress (IMPC), China, Beijing*. pp.2169-2178.

Burdukova, E., Bradshaw, D.J. and Laskowski, J.S., 2007. Effect of CMC and pH on the rheology of suspensions of isotropic and anisotropic minerals. *Canadian Metallurgical Quarterly*, 46(3), pp.273-278.

Burdukova, E., Laskowski, J.S. and Bradshaw, D.J., 2006. Surface properties of talc and their effect on the behaviour of talc suspensions. In *Proceedings of the XXIII International Mineral Processing Congress, Istanbul, Turkey*. pp.904-910.

Cawthorn, R.G., 2010. The platinum group element deposits of the Bushveld Complex in South Africa. *Platinum Metals Review*, 54, pp.205–215.

Chanturiya, V., Makarov, V., Forsling, W., Makarov, D., Vasil'eva, T.Y., Trofimenko, T.Y. and Kuznetsov, V., 2004. The effect of crystallochemical peculiarities of nickel sulphide minerals on flotation of copper–nickel ore. *International Journal of Mineral Processing*, *74*(1), pp.289-301.

Chehreh Chelgani, S. and Hart, B., 2014. TOF-SIMS studies of surface chemistry of minerals subjected to flotation separation - A review. *Minerals Engineering*, 57, pp.1–11.

Chen, H.T., Ravishankar, S. A. and Farinato, R.S., 2003. Rational polymer design for solid-liquid separations in mineral processing applications. *International Journal of Mineral Processing*, 72(1-4), pp.75–86.

Chetty, D., Gryffenberg, L., Lekgetho, T.B. and Molebale, I.J., 2009. Automated SEM study of PGM distribution across a UG2 flotation concentrate bank: Implications for understanding PGM floatability. *Journal of the Southern African Institute of Mining and Metallurgy*, 109(10), pp.587–593.

Coghill, B.M. and Wilson, A.H., 1993. Platinum-group minerals in the Selukwe Subchamber, Great Dyke, Zimbabwe: implications for PGE collection mechanisms and post-formational redistribution. *Mineralogical Magazine*, 57(389), pp.613-634.

Connelly, D., 2011. High clay ores — a mineral processing nightmare. *Australian Journal of Mining, July/August Edition: Mineral Processing—Flotation and Separation.* pp.28–29.

Cruz, N., Peng, Y., Farrokhpay, S. and Bradshaw, D., 2013. Interactions of clay minerals in copper-gold flotation: Part 1 - Rheological properties of clay mineral suspensions in the presence of flotation reagents. *Minerals Engineering*, 50-51, pp.30–37.

de Jager, G., Hartfield, D. P., Bradshaw, D. J., Francis, J. J., and Morar, S. H., 2004. A method and a control system for extracting valuable minerals from mined ore. "Smartfroth", Adams and Adams Patent Attorneys, Pretoria, AandA REF: v16148 (1-9), Provisional Patent lodged 24 Feb 2004.

Dimou, A., 1986. The Flotation of Pyrite using Xanthate Collectors. MSc Dissertation. University of Cape Town.

Dippenaar, A., 1982. The destabilization of froth by solids. I. The mechanism of film rupture. *International Journal of Mineral Processing*, 9, pp.1–14.

Eksteen, J. J., Oraby, E.A, and Tanda B.C., 2016. Developing Robust Hydrometallurgical Processes to Recover Metals from Deposits with Large Geometallurgical Variation. In *GeoMet 2016: The Third AusIMM International Geometallurgy Conference*, *Perth, Australia*. pp.15-20.

Engelbrecht, J.A. and Woodburn, E.T., 1975. The effects of froth height, aeration rate and gas precipitation of flotation. *Journal of South African Institute of Mining and Metallurgy,* pp.125 – 132.

Evans, D.M., 2002. Potential for bulk mining of oxidized platinum-group element deposits. *Applied Earth Science*, 111(1), pp.81–86.

Evans, D.M., Buchanan, D.L. and Hall, G.E.M., 1994. Dispersion of platinum, palladium and gold from the Main Sulphide Zone, Great Dyke, Zimbabwe. *Transactions of the Institution of Mining and Metallurgy-Section B-Applied Earth Science*, 103, p.B57-67.

Farrokhpay, S. and Ndlovu, B., 2013. Effect of Phyllosilicate Minerals on the Rheology, Colloidal and Flotation Behaviour of Chalcopyrite Mineral. *Chemeca 2013: Australasian Conference on Chemical Engineering*, *Perth, Australia, 28 September – 1 October 2013*. pp.1–7.

Farrokhpay, S. and Zanin, M., 2012. Effect of water quality on froth stability in flotation. *Advanced Powder Technology,* 23, pp.493-497.

Farrokhpay, S., 2012. The importance of rheology in mineral flotation: A review. *Minerals Engineering*, 36-38, pp.272–278.

Farrokhpay, S., Ametov, I. and Grano, S., 2011. Improving the recovery of low grade coarse composite particles in porphyry copper ores. *Advanced Powder Technology*, 22(4), pp.464–470.

Feng, B., Lu, Y., Feng, Q., Zhang, M. and Gu, Y., 2012. Talc-serpentine interactions and implications for talc depression. *Minerals Engineering*, 32, pp.68–73.

Forbes, E., Davey, K.J. and Smith, L., 2014. Decoupling rheology and slime coatings effect on the natural floatability of chalcopyrite in a clay-rich flotation pulp. *Minerals Engineering*, 56, pp.136–144.

Glaister, B.J. and Mudd, G.M., 2010. The environmental costs of platinum-PGM mining and sustainability: Is the glass half-full or half-empty? *Minerals Engineering*, 23(5), pp.438–450.

Grobler, W.A., Sondashi, S. and Chidley, F.J., 2005. Recent developments in flotation reagents to improve base metal recovery. In *3rd Southern African Base Metals Conference, Kitwe, Zambia*. pp.185-190.

Guilbert, J.M. and Park Jr, C.F., 2007. The geology of ore deposits. Waveland Press. Long Grove, Illinois. pp. 774-814.

Gupta, V., Hampton, M.A., Stokes, J.R., Nguyen, A.V. and Miller, J.D., 2011. Particle interactions in kaolinite suspensions and corresponding aggregate structures. *Journal of Colloid and Interface Science*, 359(1), pp.95-103.

Gy, P.M., 1979. Sampling of particulate materials – theory and practice. Elsevier, Amsterdam, Netherlands.

Hay, M.P. and Rule, C.M., 2003. SUPASIM: A flotation plant design and analysis methodology. *Minerals Engineering*, 16(11), pp.1103–1109.

Hendricks, S.B., 1942. Lattice structure of clay minerals and some properties of clays. *The Journal of Geology*, 50(3), pp.276-290.

Hey, P.V., 1999. The effects of weathering on the UG2 Chromitite reef of the Bushveld Complex, with special reference to the platinum-group minerals. *South African Journal of Geology*, 102(3). pp.251-260.

Horie, M. and Pinder, K.L., 1979. Time-dependent shear flow of artificial slurries in coaxial cylinder viscometer with a wide gap. *The Canadian Journal of Chemical Engineering*, 57(2), pp.125-134.

Hunter, T.N., Pugh, R.J., Franks, G. V. and Jameson, G.J., 2008. The role of particles in stabilising foams and emulsions. *Advances in Colloid and Interface Science*, 137(2), pp.57–81.

Implats, 2016. Mineral Resource and Mineral Reserve Statement 2016, Impala Platinum Holdings Limited. Available at: http://bastiongraphics.co.za/bastion-ir/2016/Implats-2016/Implats-MRR-2016/downloads/Implats%20MR%202016.pdf

Jasieniak, M. and Smart, R.S.C., 2009. Collectorless flotation of pyroxene in Merensky ore: Residual layer identification using statistical ToF-SIMS analysis. *International Journal of Mineral Processing*, 92(3-4), pp.169–176.

Jasieniak, M. and Smart, R.S.C., 2010. Surface chemical mechanisms of inadvertent recovery of chromite in UG2 ore flotation: Residual layer identification using statistical ToF-SIMS analysis. *International Journal of Mineral Processing*, 94(1-2), pp.72–82.

Johnson Matthey, 2016. Platinum 2016. Available at: http://www.platinum.matthey.com/documents/new-item/pgm%20market%20reports/pgm-market-report-may-2016.pdf

Johnson, S.B., Franks, G.V., Scales, P.J., Boger, D.V. and Healy, T.W., 2000. Surface chemistry-rheology relationships in concentrated mineral suspensions. *International Journal of Mineral Processing*, 58(1-4), pp.267–304.

Johnson, S.B., Russell, A.S. and Scales, P.J., 1998. Volume fraction effects in shear rheology and electroacoustic studies of concentrated alumina and kaolin suspensions. *Colloids and Surfaces A: Physicochemical and Engineering Aspects*, *141*(1), pp.119-130.

Jones, R.T., 2005. An overview of Southern African PGM smelting. *Nickel and Cobalt 2005: Challenges in Extraction and Production*, pp.147-178.

Jorjani, E., Barkhordar, H.R., Tayebi Khormani, M., Fazeli, A., 2011. Effects of aluminosilicate minerals on copper–molybdenum flotation from Sarcheshmeh porphyry ores. *Minerals Engineering*. 24, 754–759.

Kästner, U., Hoffmann, H., Dönges, R. and Hilbig, J., 1997. Structure and solution properties of sodium carboxymethyl cellulose carboxymethyl. *Colloids and surfaces. A, Physicochemical and engineering aspects*, *123*, pp.307-328.

Kawatra, S.K., 2002. Froth Flotation-Fundamental Principles. Research, Michigan Technical University, pp.1–30.

Khraisheh, M., Holland, C., Creany, C., Harris, P. and Parolis, L., 2005. Effect of molecular weight and concentration on the adsorption of CMC onto talc at different ionic strengths. *International Journal of Mineral Processing*, 75(3-4), pp.197–206.

Klimpel, R.R., 1980. Selection of chemical reagents for flotation. *Mineral processing plant design*, 2, pp.907-934.

Kraemer, D., Junge, M., Oberthür, T. and Bau, M., 2015. Improving recoveries of platinum and palladium from oxidized Platinum-Group Element ores of the Great Dyke, Zimbabwe, using the biogenic siderophore Desferrioxamine B. *Hydrometallurgy*, 152, pp.169-177.

Laskowski, J.S., Liu, Q. and O'Connor, C.T., 2007. Current understanding of the mechanism of polysaccharide adsorption at the mineral/aqueous solution interface. *International Journal of Mineral Processing*, 84(1-4), pp.59–68.

Lee, K., Archibald, D., McLean, J. and Reuter, M.A., 2009. Flotation of mixed copper oxide and sulphide minerals with xanthate and hydroxamate collectors. *Minerals Engineering*, 22(4), pp.395-401.

Li, C., Farrokhpay, S., Shi, F. and Runge, K., 2015. A novel approach to measure froth rheology in flotation. *Minerals Engineering*, 71, pp.89–96.

Li, C., Ripley, E.M., Oberthür, T., Miller, J.D. JR., and Joslin, G.D. 2008. Textural, mineralogical and stable isotope studies of hydrothermal alteration in the Main Sulfide Zone of the Great Dyke, Zimbabwe and the Precious Metals Zone of the Sonju Lake Intrusion, Minnesota, USA. *Mineralium Deposita*, 43, pp. 97–110.

Liu, G., Feng, Q., Ou, L., Lu, Y. and Zhang, G., 2006. Adsorption of polysaccharide onto talc. *Minerals Engineering*, 19(2), pp.147–153.

Liu, Q., Zhang, Y. and Laskowski, J.S., 2000. The adsorption of polysaccharides onto mineral surfaces: An acid/base interaction. *International Journal of Mineral Processing*, 60(3-4), pp.229–245.

Locmelis, M., Melcher, F. and Oberthür, T., 2010. Platinum-group element distribution in the oxidized main sulfide zone, Great Dyke, Zimbabwe. *Mineralium Deposita*, 45, pp.93–109.

Lotter, N.O. and Fragomeni, D., 2010. High-confidence flotation testing at Xstrata Process Support. *Minerals & Metallurgical Processing*, 27(1), p.47.

Lotter, N.O., Bradshaw, D.J., Becker, M., Parolis, L.A.S. and Kormos, L.J., 2008. A discussion of the occurrence and undesirable flotation behaviour of orthopyroxene and talc in the processing of mafic deposits. *Minerals Engineering*, 21(12), pp.905-912.

Lotter, N.O., Kormos, L.J., Oliveira, J., Fragomeni, D. and Whiteman, E., 2011. Modern process mineralogy: two case studies. *Minerals Engineering*, 24(7), pp.638-650.

Maier, W.D., 2005. Platinum-group element (PGE) deposits and occurrences: mineralization styles, genetic concepts, and exploration criteria. *Journal of African Earth Sciences*, 41(3), pp.165-191.

Martinovic, J., Bradshaw, D.J. and Harris, P.J., 2005. Investigation of surface properties of gangue minerals in platinum bearing ores. *The Journal of The South African Institute of Mining and Metallurgy*, 105, pp.349–356.

McFadzean, B., Dicks, P., Groenmeyer, G., Harris, P. and O'Connor, C., 2011. The effect of molecular weight on the adsorption and efficacy of polysaccharide depressants. *Minerals Engineering*, 24(5), pp.463–469.

Melton, I.E. and Rand, B., 1977. Particle interactions in aqueous kaolinite suspensions. *Journal of Colloid and Interface Science*, 60(2), pp.331–336.

Merve Genc, A., Kilickaplan, I. and Laskowski, J.S., 2012. Effect of pulp rheology on flotation of nickel sulphide ore with fibrous gangue particles. *Canadian Metallurgical Quarterly*, 51(4), pp.368-375.

Mierczynska-Vasilev, A. and Beattie, D.A., 2010. Adsorption of tailored carboxymethyl cellulose polymers on talc and chalcopyrite: Correlation between coverage, wettability, and flotation. *Minerals Engineering*, 23(11-13), pp.985–993.

Mishra, G., Viljoen, K.S. and Mouri, H., 2013. Influence of mineralogy and ore texture on pentlandite flotation at the Nkomati Nickel Mine, South Africa. *Minerals Engineering*, 54, pp.63–78.

Morar, S. H., Hatfield, D. P., Barbian, N., Bradshaw, D. J., Cilliers, J. J. and Triffett, B., 2006. A review and comparison of flotation froth stability measurements. In *Proceedings of the XXIII International Mineral Processing Congress, Istanbul, Turkey*. pp.739-744.

Morris, G.E., Fornasiero, D. and Ralston, J., 2002. Polymer depressants at the talc-water interface: Adsorption isotherm, microflotation and electrokinetic studies. *International Journal of Mineral Processing*, 67(1-4), pp.211–227.

Mudd, G.M., 2010. Platinum group metals: a unique case study in the sustainability of mineral resources. In *The 4th International Platinum Conference, Platinum in Transition 'Boom or Bust', Sun City, South Africa.* pp.113–120.

Mudd, G.M., 2012. Key trends in the resource sustainability of platinum group elements. *Ore Geology Reviews*, 46, pp.106–117.

Nagaraj, D.R. and Brinen, J., 1995. SIMS study of metal ion activation in gangue flotation. *Preprints-Society of Mining Engineers of AIME*.

Nagaraj, D.R. and Brinen, J.S., 1996. SIMS and XPS study of the adsorption of sulfide collectors on pyroxene: a case for inadvert metal in activation. *Colloids and Surfaces A: Physicochemical and Engineering Aspects*, *116*(3), pp.241-249.

Napier-Munn, T.J., 1998. Analysing plant trials by comparing recovery-grade regression lines. *Minerals Engineering*, 11(10), pp.949-958.

Napper, D.H., 1977. Steric stabilization. *Journal of Colloid and Interface Science*, 58(2), pp.390-407.

Nashwa, V.M., 2007. The flotation of high talc-containing ore from the Great Dyke of Zimbabwe. MSc Thesis. University of Pretoria.

Ndlovu, B., 2013. *The effect of phyllosilicate mineralogy and surface charge on the rheology of mineral slurries*. PhD Thesis. University of Cape Town.

Ndlovu, B., Becker, M., Forbes, E., Deglon, D. and Franzidis, J.P., 2011b. The influence of phyllosilicate mineralogy on the rheology of mineral slurries. *Minerals Engineering*, 24(12), pp.1314-1322.

Ndlovu, B., Farrokhpay, S. and Bradshaw, D., 2013. The effect of phyllosilicate minerals on mineral processing industry. *International Journal of Mineral Processing*, 125, pp.149–156.

Ndlovu, B., Forbes, E., Farrokhpay, S., Becker, M., Bradshaw, D. and Deglon, D., 2014. A preliminary rheological classification of phyllosilicate group minerals. *Minerals Engineering*, 55, pp.190-200.

Ndlovu, B.N., Forbes, E., Becker, M., Deglon, D.A., Franzidis, J.P. and Laskowski, J.S., 2011a. The effects of chrysotile mineralogical properties on the rheology of chrysotile suspensions. *Minerals Engineering*, 24(9), pp.1004–1009.

Neethling, S.J. and Cilliers, J.J., 2002a. Solids motion in flowing froths. *Chemical Engineering Science*, 57(4), pp.607-615.

Neethling, S.J. and Cilliers, J.J., 2002b. The entrainment of gangue into a flotation froth. *International Journal of Mineral Processing*, 64(2-3), pp.123–134.

Newell, A.J.H. and Bradshaw, D.J., 2007. The development of a sulfidisation technique to restore the flotation of oxidised pentlandite. *Minerals Engineering*, *20*(10), pp.1039-1046.

Newell, A.J.H., Bradshaw, D.J. and Harris, P.J., 2006. The effect of heavy oxidation upon flotation and potential remedies for Merensky type sulfides. *Minerals Engineering,* 19(6), pp.675-686.

Nordstrom, D.K., 2011. Sulfide Mineral Oxidation. In Encyclopedia of Geobiology. Springer. Dordrecht, Netherlands. pp.856-858.

Oberthür, T., 2002. Platinum-group element mineralization of the Great Dyke, Zimbabwe. In: *Cabri LJ (ed) The geology, geochemistry, mineralogy and mineral beneficiation of platinum-group elements, Canadian Institute of Mining, Metallurgy and Petroleum*, Special Volume 54, pp.483–506.

Oberthür, T., 2011. Platinum-group element mineralization of the main sulfide zone, Great Dyke, Zimbabwe. *Reviews in Economic Geology,* 17(12), pp.329-349.

Oberthür, T., Cabri L.J., Weiser, T.W., McMahon, G. and Muller, P., 1997. Pt, Pd and other trace elements in sulfides of the Main Sulfide Zone, Great Dyke, Zimbabwe: A reconnaissance study. *Canadian Mineralogist*, 35(3), pp.597–609.

Oberthür, T., Melcher, F., Buchholz, P. and Locmelis, M., 2013. The oxidized ores of the Main Sulphide Zone, Great Dyke, Zimbabwe: Turning resources into minable reserves-mineralogy is the key. *Journal of the Southern African Institute of Mining and Metallurgy*, 113(3), pp.191–201.

Oberthür, T., Weiser, T.W., Gast, L. and Kojonen, K., 2003a. Geochemistry and mineralogy of platinum-group elements at Hartley Platinum Mine, Zimbabwe. *Mineralium Deposita*, 38(3), pp.327–343.

Oberthür, T., Weiser, T.W., Gast, L., Kojonen, K., 2003b. Geochemistry and mineralogy of platinum-group elements at Hartley Platinum Mine, Zimbabwe. *Mineralium Deposita*, 38(3), pp.344–355.

Oberthür, T., Weiser, T.W., Gast, L., Wittich, C. and Kojonen, K., 2000. Mineralogy applied to the evaluation and processing of platinum ores of the Main Sulfide Zone, Great Dyke, Zimbabwe. *Applied Mineralogy. Balkema, Rotterdam*, pp.379-382.

Okuda, S., Inoue, K., Williamson, W.O., 1969. Negative surface charges of pyrophillite and talc. In: *International Clay Conference*. Tokyo, pp. 31–41.

Parolis, L.A., van der Merwe, R., Groenmeyer, G.V. and Harris, P.J., 2008. The influence of metal cations on the behaviour of carboxymethyl celluloses as talc depressants. *Colloids and Surfaces A: Physicochemical and Engineering Aspects*, 317(1-3), pp.109–115.

Patra, P., Nagaraj, D.R. and Somasundaran, P., 2010. In *Proceedings of The XI International Seminar on Mineral Processing Technology (MPT-2010), Jamshedpur, India*. pp.1223-1230.

Pawlik, M., 2005. Polymeric dispersants for coal-water slurries. *Colloids and Surfaces A: Physicochemical and Engineering Aspects*, 266(1-3), pp.82–90.

Pawlik, M., Laskowski, J.S. and Liu, H., 1997. Effect of humic acids and coal surface properties on rheology of coal-water slurries. *Coal Preparation*, 18(3-4), pp.129-149.

Powell, M.S., 2013. Utilising orebody knowledge to improve comminution circuit design and energy utilisation. In *GeoMet 2013: The Second AusIMM International Geometallurgy Conference, Brisbane, Australia*. pp.27-35.

Prendergast, M.D. and Wilson, A.H., 1989. The Great Dyke of Zimbabwe - II: Mineralisation and mineral deposits. In: Prendergast, M.D. and Jones, M.J. Eds. *Magmatic Sulphides-the Zimbabwe Volume: 5th Magmatic Sulphide Field Conference*. Institution of Mining and Metallurgy, pp.21-42.

Prendergast, M.D. 1990. Platinum-group minerals and hydrosilicate 'alteration' in the Wedza-Mimosa Platinum Deposit, Great Dyke, Zimbabwe - genetic and metallurgical implications. *Transactions of the Institution for Mining and Metallurgy*, 99. pp.B91–B105.

Pugh, R.J., 2005. Experimental techniques for studying the structure of foams and froths. *Advances in Colloid and Interface Science*, 114-115, pp.239–251.

Savassi, O.N., 1998. *Direct estimation of the degree of entrainment and the froth recovery of attached particles in industrial flotation cells*. PhD Thesis. University of Queensland.

Schouwstra, R.P., Kinloch, E.D. and Lee, C.A., 2000. A Short Geological Review of the Bushveld Complex. *Platinum Metals Review*, 44(1), pp.33–39.

Schubert, H., 2008. On the optimization of hydrodynamics in fine particle flotation. *Minerals Engineering*, 21(12-14), pp.930–936.

Schuhmann Jr, R., 1942. Flotation Kinetics. I. Methods for steady-state study of flotation problems. *The Journal of Physical Chemistry*, 46(8), pp.891-902.

Shabalala, N.Z.P., Harris, M., Leal Filho, L.S. and Deglon, D.A., 2011. Effect of slurry rheology on gas dispersion in a pilot-scale mechanical flotation cell. *Minerals Engineering*, 24(13), pp.1448-1453.

Shaw, W.J., Khosrowshahi S. and Weeks, A., 2013. Modelling Geometallurgical Variability – A Case Study of Managing Risk. In *GeoMet 2013: The Second AusIMM International Geometallurgy Conference, Brisbane, Australia.* pp. 247-252.

Shi, F.N. and Zheng, X.F., 2003. The rheology of flotation froths. *International Journal of Mineral Processing*, 69(1-4), pp.115–128.

Shortridge, P.G., Harris, P.J., Bradshaw, D.J. and Koopal, L.K., 2000. The effect of chemical composition and molecular weight of polysaccharide depressants on the flotation of talc. *International Journal of Mineral Processing*, 59(3), pp.215–224.

Skinner, B., 1976. A Second Iron Age Ahead? The distribution of chemical elements in the earth's crust sets natural limits to man's supply of metals that are much more important to the future of society than limits on energy. *American Scientist*. 64, 258–269.

Smith, L.K., Senior, G.D., Bruckard, W.J. and Davey, K.J., 2011. The flotation of millerite—A single mineral study. *International Journal of Mineral Processing*, *99*(1), pp.27-31.

Sposito, G., Skipper, N.T., Sutton, R., Park, S.H., Soper, A.K. and Greathouse, J.A., 1999. Surface geochemistry of the clay minerals. *Proceedings of the National Academy of Sciences*, 96(7), pp.3358-3364.

Stribrny, B., Wellmer, F.W., Burgath, K.P., Oberthür, T., Tarkian, M. and Pfeiffer, T., 2001. Unconventional PGE occurrences and PGE mineralization in the Great Dyke: metallogenic and economic aspects - a reply. *Mineralium Deposita*, 36, pp.103–104.

Taggart, A.F., 1945. Handbook of Mineral Dressing. Wiley, New York.

Tao, D., Dopico, P.G., Hines, J. and Kennedy, D., 2010. An experimental study of clay binders in fine coal froth flotation. In *Proceedings of the International Coal Preparation Congress. Lexington, USA*. pp. 478–487.

Tombácz, E. and Szekeres, M., 2006. Surface charge heterogeneity of kaolinite in aqueous suspension in comparison with montmorillonite. A*pplied Clay Science*, 34, 105–124.

Van Olphen, H., 1951. Rheological phenomena of clay sols in connection with the charge distribution on the micelles. *Discussions of the Faraday Society*, 11, pp.82-84.

Van Tonder, E., Deglon, D.A. and Napier-Munn, T.J., 2010. The effect of ore blends on the mineral processing of platinum ores. *Minerals Engineering,* 23(8), pp.621-626.

Ventura-Medina, E. and Cilliers, J.J. 2002. A model to describe flotation performance based on physics of foams and froth image analysis. *International Journal of Mineral Processing*, 67(1-4), pp.79-99.

Vermaak, M.K.G., 2005. *Fundamentals of the flotation behaviour of palladium bismuth tellurides*. Doctoral Dissertation. University of Pretoria.

Vinnett, L., Alvarez-Silva, M., Jaques, A., Hinojosa, F. and Yianatos, J., 2015. Batch flotation kinetics: Fractional calculus approach. *Minerals Engineering*, 77, pp.167-171.

Voyi, O. and Wilson, S., 2015. Is chlorite to blame for nasty flotation froths. Honours Project. University of Cape Town.

Wang, J. and Somasundaran, P., 2005. Adsorption and conformation of carboxymethyl cellulose at solid-liquid interfaces using spectroscopic, AFM and allied techniques. *Journal of Colloid and Interface Science*, 291(1), pp.75–83.

Wesseldijk, Q.I., Reuter, M.A., Bradshaw, D.J. and Harris, P.J., 1999. Flotation behaviour of chromite with respect to the beneficiation of UG2 ore. *Minerals Engineering*, 12(10), pp.1177–1184.

Weiser, T.W., Oberthür, T., Kojonen, K. and Johanson, B., 1998. Distribution of trace PGE in pentlandite and of PGM in the Main Sulfide Zone (MSZ) at Mimosa Mine, Great Dyke, Zimbabwe. In *8th International Platinum Symposium,* Johannesburg, South Africa. pp. 443-445.

Wiese, J., 2009. Investigating Depressant Behaviour on the Flotation of Selected Merensky Ores. MSc Dissertation. University of Cape Town.

Wiese, J., Harris, P. and Bradshaw, D., 2011. The effect of the reagent suite on froth stability in laboratory scale batch flotation tests. *Minerals Engineering*, 24(9), pp.995–1003.

Wiese, J.G., Harris, P.J., Bradshaw, D.J., 2005. The influence of the reagent suite on the flotation of ores from the Merensky Reef. *Minerals Engineering* 18, 189–198.

Wilson, A.H., 1996. The Great Dyke of Zimbabwe. *Developments in Petrology*, *15*, pp.365-402.

Wilson, A.H., 2001. Compositional and lithological controls on the PGE-bearing sulphide zones in the Selukwe Subchamber, Great Dyke: a combined equilibrium–Rayleigh fractionation model. *Journal of Petrology*, *42*(10), pp.1845-1867.

Wilson, A. H. and du Toit, A. J., 2010. Great Dyke Platinum in the Region of Ngezi Mine, Zimbabwe: Characteristics of the Main Sulphide Zone and Variations that Affect Mining. In *11th International Platinum Symposium*, *Sudbury, Ontario, Canada*, *21–24 June 2010*.

Wilson, A.H. and Prendergast, M.D., 2001. Platinum-group element mineralisation in the Great Dyke, Zimbabwe, and its relationship to magma evolution and magma chamber structure. *South African Journal of Geology*, 104(4), pp.319-342.

Wilson, A.H. and Tredoux, M., 1990. Lateral and vertical distribution of platinum-group elements and petrogenetic controls on the sulfide mineralization in the P1 pyroxenite layer of the Darwendale subchamber of the Great Dyke, Zimbabwe. *Economic Geology*, 85(3), pp.556–584.

Wilson, A.H., Murahwi, C.Z. and Coghill, B., 2000. Stratigraphy, geochemistry and platinum group element mineralisation of the central zone of the Selukwe Subchamber of the Great Dyke, Zimbabwe. *Journal of African Earth Sciences*, 30(4), pp.833-853.

World Platinum Investment Council (WPIC), 2016. Platinum Quarterly Q3 2016. Available at: https://www.platinuminvestment.com/files/736253/WPIC_Platinum_Quarterly_Q3_2016.pdf

Xu, M., 1998. Modified flotation rate constant and selectivity index. *Minerals Engineering*, 11(3), pp.271-278.

Zanin, M., Wightman, E., Grano, S.R. and Franzidis, J.P., 2009. Quantifying contributions to froth stability in porphyry copper plants. *International Journal of Mineral Processing*, 91(1), pp.19–27.

Zbik, M. and Smart, R.S.C., 2002. Dispersion of kaolinite and talc in aqueous solution: Nano-morphology and nano-bubble entrapment. *Minerals Engineering*, 15(4), pp.277–286.

Zhang, M. and Peng, Y., 2014. Effect of electrolytes on the flotation of copper minerals in the presence of clay minerals. *Minerals Engineering*, 66, pp.152–156.

Zhang, M. and Peng, Y., 2015. Effect of clay minerals on pulp rheology and the flotation of copper and gold minerals. *Minerals Engineering*, 70, pp.8-13.

Zhao, K., Gu, G., Wang, C., Rao, X., Wang, X. and Xiong, X., 2015. The effect of a new polysaccharide on the depression of talc and the flotation of a nickel-copper sulfide ore. *Minerals Engineering*, 77, pp.100–106.

Zhou, Z. and Gunter, W.D., 1992. The nature of the surface charge of kaolinite. *Clays and Clay minerals*, 40(3), pp.365-368.

Chapter 7 - Appendix

7.1 Feed and Concentrate Characterization

7.1.1 XRD Results

Table 7.1: Percentage of minerals present in the MIM-S ore sample as determined by XRD

Phase 1 : Quartz	0.591
Phase 2 : Chromite	0.040
Phase 3 : Diopside	10.40
Phase 4 : "Hornblende magnesian iron"	6.09
Phase 5 : "Chlorite IIb"	1.28
Phase 6 : "Forsterite iron"	0.00
Phase 7 : Anorthite	16.23
Phase 8 : Bronzite	51.85
Phase 9 : Pentlandite	0.366
Phase 10 : Dolomite	0.245
Phase 11 : Antigorite	0.97
Phase 12 : Grossularia	0.060
Phase 13 : Talc	11.89

Table 7.2: Percentage of minerals present in the ZP-S ore sample as determined by XRD

Phase 1 : Quartz	0.253
Phase 2 : Diopside	7.00
Phase 3 : "Hornblende magnesian iron"	0.90
Phase 4 : "Chlorite IIb"	1.31
Phase 5 : Anorthite	9.10
Phase 6 : Bronzite	68.35
Phase 7 : Antigorite	0.00
Phase 8 : Chrysotile	2.10
Phase 9 : Talc	10.99

Table 7.3: Percentage of minerals present in the ZP-O ore sample as determined by XRD

Phase 1 : Quartz	0.693
Phase 2 : Diopside	7.81
Phase 3 : "Hornblende magnesian iron"	0.03
Phase 4 : "Chlorite IIb"	1.96
Phase 5 : Anorthite	12.20
Phase 6 : Bronzite	73.17
Phase 7 : Talc	4.14

7.1.2 XRF Results

Table 7.4: Whole rock analyses of the 3 ore samples in oxide percent as determined by XRF. (LOI stands for loss on ignition. LOI is the sum of the moisture content (H_2O^-) and bound water in a sample. The bound water is representative of the percentage of the sample that is made up of water molecules present in the structure of hydrous silicates e.g. phyllosilicates. 'b.d.' implies a measurement that is below detection limit which is any percent less than 0.01 in this case.)

Sample Name	MIM-S				ZP-S				ZP-O			
Size Fraction	**-300/75**	**-75/53**	**-53/25**	**-25**	**-300/75**	**-75/53**	**-53/25**	**-25**	**-300/75**	**-75/53**	**-53/25**	**-25**
SiO_2	51.8	50.9	51.3	50.1	53.2	53.2	52.5	50.5	51.8	52.2	51.7	51.0
TiO_2	0.2	0.2	0.2	0.2	0.1	0.1	0.1	0.1	0.2	0.2	0.2	0.2
Al_2O_3	3.3	4.1	4.7	4.8	2.1	2.3	2.5	3.1	2.4	2.8	3.2	3.6
Fe_2O_3	12	11.8	12	12.6	12.2	12.4	12.5	13.3	12.6	12.6	12.9	13.7
MnO	0.2	0.2	0.2	0.2	0.2	0.2	0.2	0.2	0.2	0.2	0.2	0.2
MgO	25.9	24.4	23.3	22.6	27.4	26.9	26.3	25.4	27.7	26.9	26.2	24.8
CaO	4.3	4.5	5	4.8	2.5	2.7	2.8	3	2.6	2.9	3	3.2
Na_2O	0.6	0.7	0.8	0.7	0.1	0.2	0.2	0.5	0.5	0.5	0.6	0.6
K_2O	0.1	0.2	0.2	0.2	0.1	0.1	0.1	0.1	b.d.	0.1	0.1	0.1
P_2O_5	b.d.	b.d.	b.d.	b.d.	b.d.	b.d.	b.d.	b.d.	b.d.	b.d.	b.d.	b.d.
SO_3	0.1	0.2	0.2	0.7	0.1	0.1	0.2	0.4	0	0	0.1	0.1
Cr_2O_3	0.4	0.4	0.5	0.6	0.5	0.5	0.5	0.7	0.4	0.4	0.5	0.7
NiO	0.1	0.2	0.3	0.5	0.1	0.1	0.2	0.3	0.1	0.1	0.2	0.3
H_2O^-	b.d.	1.2	0.1	0.2	0.1	0	0.1	0.1	0.3	0.1	0.1	0.2
LOI	0.4	0.5	0.7	1.2	0.4	0.5	0.6	0.6	0.1	0.1	0.1	0.3
Sum	**99.5**	**99.4**	**99.4**	**99.3**	**99.1**	**99.3**	**98.9**	**98.4**	**99.1**	**99.2**	**99.0**	**99.0**

7.1.3 QEMSCAN and PSD results

Table 7.5: Percentage of sample present in each size fraction (particle size distribution), elemental composition of the samples as determined by QEMSCAN and XRF for validation (Noted by Chemical next to the element) as well as the mineral composition in each size class of the 3 feed ore samples.

	Sample Name	MIM-S					ZP-S					ZP-O				
	Fraction	**Combined**	**-300/+75**	**-75/+53**	**-53/+25**	**-25**	**Combined**	**-300/+75**	**-75/+53**	**-53/+25**	**-25**	**Combined**	**-300/+75**	**-75/+53**	**-53/+25**	**-25**
	Percent in fraction	**100.0**	33.8	17.1	15.8	33.3	**100.0**	35.0	17.9	17.5	29.6	**100.0**	33.0	20.7	20.1	26.2
Elemental Mass (%)	Al (QEMSCAN)	**2.0**	1.1	1.8	2.5	2.9	**0.8**	0.4	0.7	0.9	1.2	**0.9**	0.4	0.8	1.0	1.4
	Al (Chemical)	**2.2**	1.8	2.2	2.5	2.5	**1.3**	1.1	1.2	1.3	1.7	**1.6**	1.3	1.5	1.7	1.9
	Ca (QEMSCAN)	**2.6**	1.9	2.4	3.0	3.4	**1.0**	0.6	0.9	1.2	1.4	**1.1**	0.7	1.0	1.2	1.5
	Ca (Chemical)	**3.3**	3.1	3.3	3.6	3.4	**1.9**	1.8	1.9	2.0	2.1	**2.1**	1.9	2.1	2.1	2.3
	Cr (QEMSCAN)	**0.1**	0.0	0.1	0.1	0.2	**0.2**	0.1	0.1	0.3	0.2	**0.1**	0.0	0.1	0.1	0.2
	Cr (Chemical)	**0.3**	0.3	0.3	0.3	0.4	**0.4**	0.3	0.3	0.4	0.5	**0.3**	0.3	0.3	0.3	0.5
	Cu (QEMSCAN)	**0.1**	0.1	0.1	0.1	0.3	**0.1**	0.0	0.1	0.1	0.2	**0.1**	0.0	0.1	0.1	0.3
	Fe (QEMSCAN)	**7.6**	7.8	7.7	7.6	7.4	**8.0**	8.0	7.8	7.9	8.1	**8.6**	8.4	8.5	8.4	9.0
	Fe (Chemical)	**8.6**	8.5	8.4	8.5	8.8	**8.8**	8.6	8.7	8.8	9.3	**9.1**	8.8	8.8	9.0	9.6
	K (QEMSCAN)	**0.1**	0.0	0.1	0.1	0.1	**0.1**	0.0	0.0	0.1	0.1	**0.0**	0.0	0.0	0.0	0.1
	K (Chemical)	**0.2**	0.1	0.2	0.2	0.2	**0.1**	0.0	0.0	0.1	0.1	**0.0**	0.0	0.0	0.1	0.1
	Mg (QEMSCAN)	**14.9**	16.1	15.3	14.4	13.8	**16.4**	17.0	16.7	16.2	15.7	**16.2**	16.9	16.4	16.2	15.3
	Mg (Chemical)	**14.7**	15.7	15.0	14.2	13.6	**16.0**	16.5	16.2	15.8	15.3	**16.0**	16.7	16.2	15.8	15.0
	Na (QEMSCAN)	**0.1**	0.1	0.1	0.1	0.2	**0.1**	0.0	0.0	0.1	0.1	**0.1**	0.0	0.1	0.1	0.1
	Na (Chemical)	**0.5**	0.4	0.5	0.6	0.5	**0.2**	0.1	0.1	0.2	0.4	**0.4**	0.3	0.4	0.4	0.5
	Ni (QEMSCAN)	**0.2**	0.0	0.1	0.2	0.3	**0.1**	0.0	0.1	0.1	0.2	**0.1**	0.0	0.1	0.1	0.2
	Ni (Chemical)	**0.2**	0.1	0.2	0.3	0.4	**0.1**	0.1	0.1	0.1	0.2	**0.1**	0.1	0.1	0.1	0.2
	S (QEMSCAN)	**0.6**	0.2	0.5	0.7	0.9	**0.3**	0.2	0.2	0.4	0.6	**0.4**	0.2	0.4	0.4	0.6
	S (Chemical)	**0.3**	0.7	0.0	0.0	0.0	**0.1**	0.0	0.1	0.1	0.2	**0.0**	0.0	0.0	0.0	0.1
	Si (QEMSCAN)	**24.5**	25.0	24.6	24.3	24.1	**25.1**	25.4	25.4	25.0	24.8	**24.9**	25.3	25.0	24.9	24.4
	Si (Chemical)	**24.0**	24.4	24.3	24.3	23.4	**24.4**	24.9	24.8	24.5	23.6	**24.2**	24.2	24.4	24.2	23.9
	Ti (QEMSCAN)	**0.2**	0.2	0.2	0.2	0.2	**0.1**	0.3	0.1	0.1	0.1	**0.1**	0.1	0.1	0.1	0.1
	Ti (Chemical)	**0.1**	0.1	0.1	0.1	0.1	**0.1**	0.1	0.1	0.1	0.1	**0.1**	0.1	0.1	0.1	0.1
Mineral Mass(%)	Pentlandite	**0.5**	0.1	0.4	0.7	0.9	**0.3**	0.1	0.2	0.3	0.7	**0.2**	0.1	0.2	0.3	0.5
	Chalcopyrite	**0.4**	0.2	0.3	0.4	0.8	**0.3**	0.1	0.2	0.2	0.5	**0.3**	0.1	0.2	0.3	0.7
	Pyrrhotite	**0.5**	0.3	0.5	0.7	0.7	**0.2**	0.1	0.2	0.3	0.3	**0.1**	0.1	0.2	0.1	0.1
	Pyrite	**0.1**	0.1	0.1	0.1	0.1	**0.1**	0.1	0.1	0.1	0.2	**0.3**	0.2	0.3	0.3	0.4
	Other sulfides	**0.0**	0.0	0.0	0.0	0.0	**0.0**	0.0	0.0	0.0	0.0	**0.0**	0.0	0.0	0.0	0.0
	Olivine	**1.8**	2.1	2.4	2.5	0.9	**1.4**	1.0	1.4	1.7	1.6	**1.3**	1.2	1.4	1.8	1.0
	Orthopyroxene	**64.9**	75.3	68.2	59.8	55.0	**78.2**	87.2	81.3	75.6	67.0	**81.9**	89.6	84.5	80.3	71.3
	Clinopyroxene	**8.5**	8.4	7.8	8.3	9.0	**2.7**	2.1	2.8	3.2	3.1	**3.3**	2.8	3.6	3.6	3.6
	Serpentine	**0.1**	0.0	0.0	0.1	0.1	**0.2**	0.1	0.2	0.2	0.3	**0.1**	0.0	0.3	0.0	0.0
	Talc	**8.4**	5.8	7.5	9.0	11.2	**9.1**	5.3	7.7	9.4	14.2	**4.9**	2.4	3.3	5.1	9.2
	Chlorite	**1.3**	0.6	0.8	1.2	2.1	**0.6**	0.3	0.4	0.6	1.0	**0.3**	0.2	0.3	0.3	0.6
	Hornblende	**3.8**	2.6	3.2	4.5	4.9	**1.8**	1.0	1.5	2.1	2.7	**1.5**	1.0	1.2	1.6	2.3
	Plagioclase	**7.1**	2.8	6.1	9.4	10.8	**2.7**	1.0	2.3	3.4	4.7	**3.2**	1.2	2.7	3.9	5.6
	Biotite/Phlogopite	**0.5**	0.4	0.5	0.6	0.5	**0.2**	0.1	0.2	0.3	0.4	**0.1**	0.1	0.1	0.1	0.2
	Calcite	**0.2**	0.1	0.1	0.2	0.4	**0.3**	0.1	0.2	0.4	0.5	**0.0**	0.0	0.0	0.0	0.1
	Chromite	**0.2**	0.1	0.2	0.3	0.4	**0.3**	0.2	0.2	0.6	0.4	**0.2**	0.0	0.2	0.2	0.3
	Fe oxides / hydroxides	**0.9**	0.7	0.9	1.2	1.0	**0.9**	0.5	0.6	0.9	1.5	**1.6**	0.9	1.2	1.5	3.0
	Other	**0.9**	0.5	0.7	1.1	1.3	**0.8**	0.6	0.6	0.8	1.0	**0.5**	0.2	0.3	0.5	1.0
	Total	**100.0**	**100.0**	**100.0**	**100.0**	**100.0**	**100.0**	**100.0**	**100.0**	**100.0**	**100.0**	**100.0**	**100.0**	**100.0**	**100.0**	**100.0**

Table 7.6: Base Metal Sulphide liberation and associations in the 3 ore samples. Liberated BMS: Area % BMS > 90.

	MIM-S	ZP-S	ZP-O
Liberated BMS	90.0	90.0	85.5
Pyroxene	5.1	4.4	3.7
Alteration minerals	1.9	2.1	1.7
Plagioclase	0.7	0.6	0.8
Mica	0.1	0.2	0.0
Oxides	1.9	2.3	7.0
Other	0.3	0.5	1.1

Table 7.7: Cu deportment in the feed and the -75/+38 µm fraction of the batch flotation concentrates of the 3 ore samples

	Feed			Concentrate		
Mineral	MIM-S	ZP-S	ZP-O	MIM-S	ZP-S	ZP-O
Chalcopyrite	99.9	97.3	88.4	99.8	99.5	91.2
Pyrite	0.1	0.2	0.6	0.2	0.4	0.5
Covellite	0.0	0.0	7.8	0.0	0.0	6.6
Chalcocite	0.0	1.1	1.9	0.0	0.0	0.6
Bornite	0.0	1.3	0.4	0.0	0.0	0.9
Cuprite	0.0	0.0	0.0	0.0	0.0	0.0
Malachite	0.0	0.0	0.0	0.0	0.0	0.0
Chrysocolla	0.0	0.0	0.4	0.0	0.0	0.0
Chlorite	0.0	0.0	0.0	0.0	0.0	0.0
Plagioclase	0.0	0.0	0.1	0.0	0.0	0.1
Biotite/Phlogopite	0.0	0.0	0.1	0.0	0.0	0.0
Fe-Oxides/Hydroxides	0.0	0.0	0.1	0.0	0.0	0.0
Other	0.0	0.0	0.1	0.0	0.0	0.1

Table 7.8: Ni deportment in the feed and the -75/+38 µm fraction of the batch flotation concentrates of the 3 ore samples

	Feed			Concentrate		
Mineral	MIM-S	ZP-S	ZP-O	MIM-S	ZP-S	ZP-O
Pentlandite	98.1	98.3	90.6	98.0	97.5	87.7
Pyrrhotite	1.5	1.0	0.7	1.7	1.8	1.2
Violarite	0.4	0.7	8.6	0.3	0.6	8.0
Millerite	0.0	0.0	0.1	0.0	0.0	3.1

7.2 Naturally Floating Gangue

7.2.1 Composition of Naturally Floating Gangue

Table 7.9: Bulk mineralogy of the -75/+38 μm fraction of the batch flotation concentrate samples from QEMSCAN (wt.%). 'Other sulfides' are mainly made up of galena while a major constituent of 'Other' is quartz.

	MIM-S	ZP-S	ZP-O
Ni-sulfides	1.1	1.5	2.1
Cu-sulfides	1.1	0.9	2.1
Pyrrhotite	1.2	2.0	1.8
Pyrite	0.2	0.3	3.8
Other sulfides	< 0.1	< 0.1	< 0.1
Olivine	1.2	1.6	1.0
Orthopyroxene	65.5	66.7	57.2
Clinopyroxene	6.1	2.0	2.2
Serpentine*	0.0	0.2	0.0
Talc*	5.3	12.4	16.3
Chlorite*	1.6	1.4	0.7
Mica*	1.9	0.6	0.3
Hornblende	2.9	3.0	2.2
Plagioclase	2.2	0.8	1.5
Calcite	< 0.1	< 0.1	< 0.1
Chromite	7.1	4.0	4.8
Fe oxides / hydroxides	1.5	1.7	3.0
Other	0.8	0.5	0.9

* Phyllosilicate minerals

Table 7.10: Mass of minerals (g) in the -75/+38 μm fraction of the batch flotation concentrates of the 3 ores.

	MIM-S	ZP-S	ZP-O
BMS	0.9	1.2	2.0
Pyroxene	18.8	18.1	12.1
Talc	1.4	3.2	3.3
Alteration Minerals	1.7	1.3	0.6
Plagioclase	0.6	0.2	0.3
Oxides	2.2	1.5	1.6
Other	0.3	0.2	0.2
Total	**25.9**	**25.7**	**20.0**

* Alteration Minerals here include Serpentine, Chlorite, Mica and Amphibole

Table 7.11: Mass of minerals (g) in the -75/+38 μm fraction of the batch flotation concentrates of the 3 ores. (Assoc is short for Associated)

	MIM-S	ZP-S	ZP-O
Liberated Pyroxene	< 0.1	< 0.1	< 0.1
Pyroxene Assoc with BMS	0.5	0.3	0.1
Pyroxene Assoc with Talc	19.6	23.0	14.8
Pyroxene Assoc with *Alteration Minerals	0.3	0.2	0.2
Pyroxene Assoc with Plagioclase	0.0	0.0	0.0
Pyroxene Assoc with Other	3.4	0.7	2.1
Remaining BMS	0.7	1.0	1.8
Remaining Talc	0.0	0.1	0.2
Remaining *Alteration Minerals	0.5	0.2	0.1
Remaining Plagioclase	0.3	0.1	0.2
Remaining Oxides	0.3	0.1	0.4
Remaining Other Minerals	0.1	0.1	0.1
Total	**25.9**	**25.7**	**20.0**

* Alteration Minerals here include Serpentine, Chlorite, Mica and Amphibole

Table 7.12: Talc liberation in the feed ore samples. Liberated: Area % Talc > 90, High Grade Middlings: 90 ≥ Area % Talc > 60, Low Grade Middlings: 60 ≥ Area % Talc > 30, Locked: Area % Talc < 30.

	MIM-S	ZP-S	ZP-O
Liberated	4.9	1.8	2.2
High Grade Middlings	18.4	23.2	31.2
Low Grade Middlings	23.8	32.0	30.2
Locked	52.9	43.1	36.5

Table 7.13: Talc liberation in the -75/+38 μm fraction of the batch flotation concentrates of the 3 ores. Liberated: Area % Talc > 90, High Grade Middlings: 90 ≥ Area % Talc > 60, Low Grade Middlings: 60 ≥ Area % Talc > 30, Locked: Area % Talc < 30.

	MIM-S	ZP-S	ZP-O
Liberated	0.7	16.3	27.7
High Grade Middlings	8.1	20.5	30.0
Low Grade Middlings	20.0	22.7	21.2
Locked	71.1	40.5	21.1

7.2.2 Quantifying the Naturally Floating Gangue

The total amount of gangue was calculated as follows

$$Total\ Gangue = Total\ Mass\ of\ Solids\ Recovered - Mass\ of\ Sulfide\ Minerals\ in\ Concentrate \quad \text{(Equation 7.1)}$$

The entrainability factor which is the slope of the graph of total gangue versus water recovered (shown in Figure 7.1) was then determined and in the example shown is 0.0388.

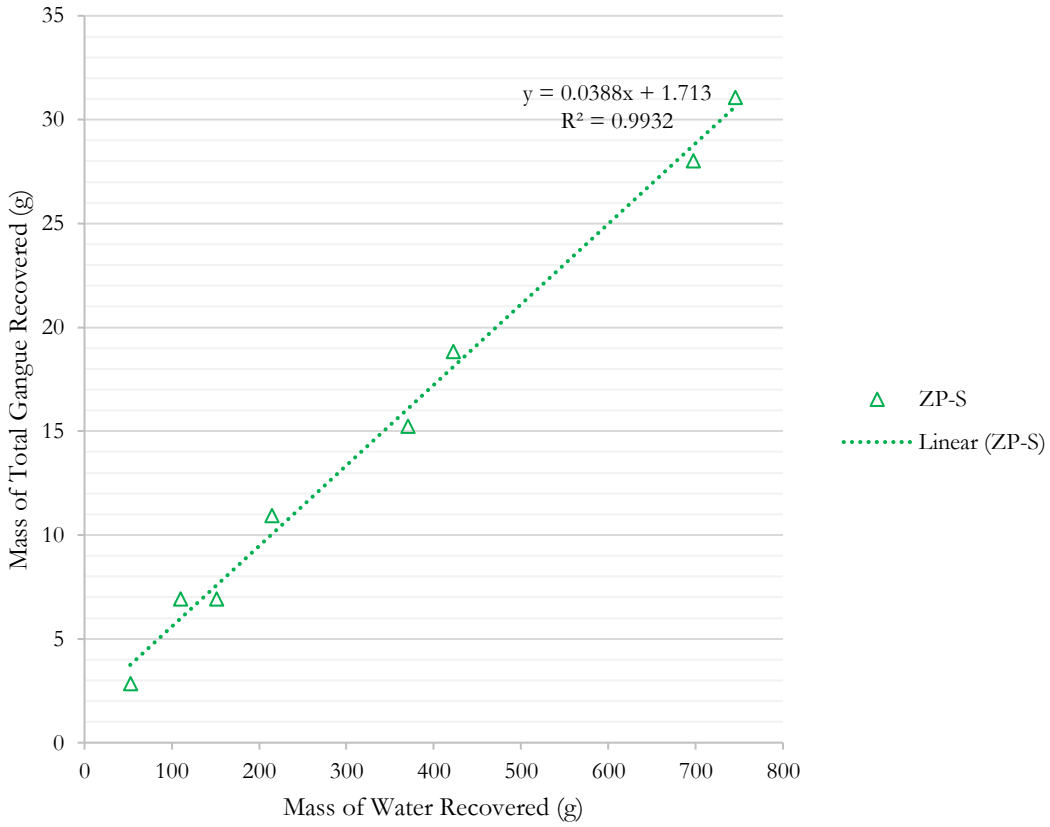

Figure 7.1: Mass of total gangue recovered versus mass of water recovered used to obtain entrainability factor.

The product of this and the total mass of water recovered is the amount of entrained gangue:

$$Mass\ of\ Entrained\ Gangue = Mass\ of\ Total\ Water\ Recovered \times Entrainability\ factor \quad \text{(Equation 4.1)}$$

And finally, the difference between the Mass of Total Gangue Recovered and the Mass of Entrained Gangue gives the Mass of Floating Gangue

$$Mass\ of\ Floating\ Gangue = Mass\ of\ Total\ Gangue - Mass\ of\ Entrained\ Gangue \quad \text{(Equation 4.2)}$$

Figure 7.2 shows the mass of naturally floating gangue recovered with the 3 ores using the 3 depressants.

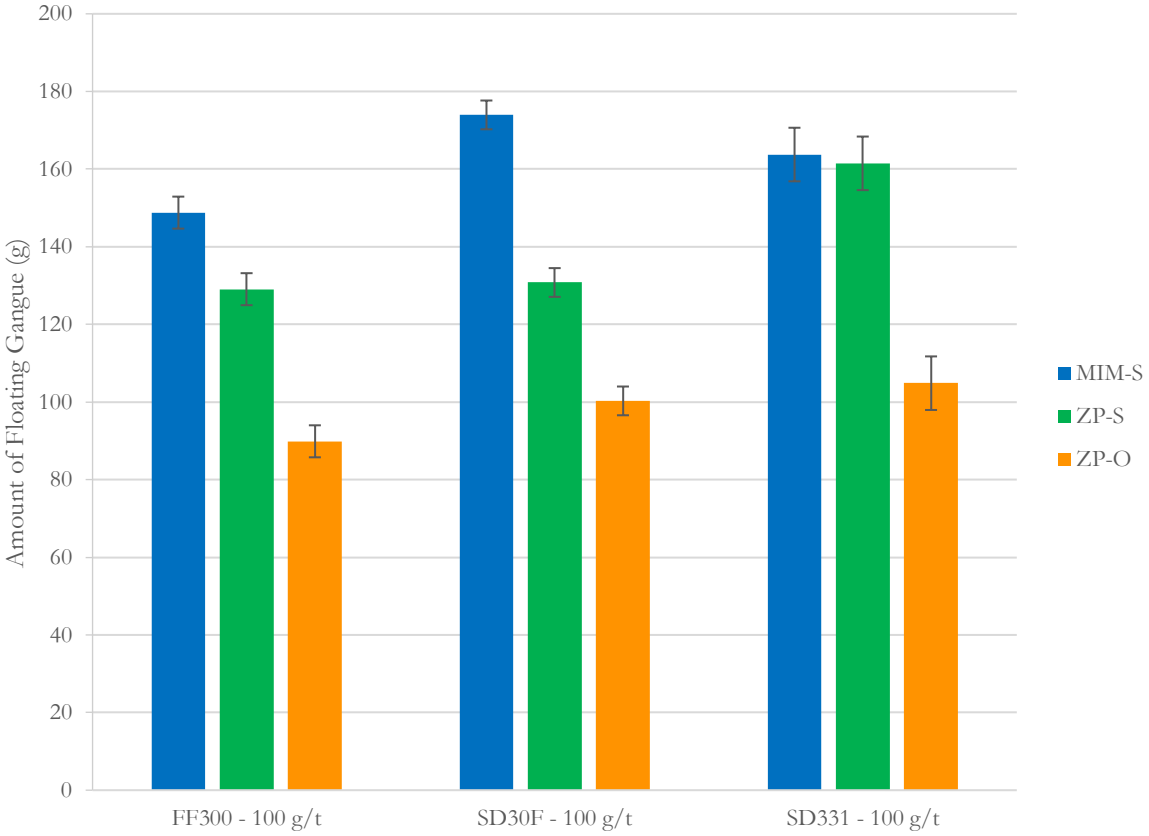

Figure 7.2: Amount of floating gangue recovered for each of the 3 ores while varying depressant type.

7.3 Froth Stability Tests

7.3.1 Froth Stability Tests Raw Data

Table 7.14: Change of froth height with time for the 3 ore samples

Time (s)	Froth Height (mm)					
	MIM-S A	**MIM-S B**	**ZP-S A**	**ZP-S B**	**ZP-O A**	**ZP-O B**
0	0	0	0	0	0	0
5	77	93	62	52	46	51
10	124	128	95	79	73	66
15	151	163	112	102	119	103
20	186	203	140	129	148	120
25	228	243	148	138	170	136
30	265	289	153	149	181	148
35	300	319	165	168	188	172
40	329	339	172	173	203	182
45	336	358	177	180	215	193
50	354	382	186	186	225	195
55	368	403	196	193	234	201
60	387	415	204	200	237	221
65	394	415	209	208	237	224
70	394	415	209	208	235	224

7.3.2 Froth Stability Tests – Model Fitting

1. The stability coefficient and characteristic bubble lifetime (τ) were determined through the fitting of experimental data to the Equation 2.7 and minimizing the sum of least squares:

$$H(t) = H_{max}\left(1 - e^{-\frac{t}{\tau}}\right) \quad \text{(Equation 2.7)}$$

2. The "Solver" function present in MS Excel 2016 was then used to minimize the sum of the square of the difference between the experimental data and that determined by the model.

$$Residual = \sum_{i=0}^{n}(H_{calculated} - H_{observed})^2 \quad \text{(Equation 7.2)}$$

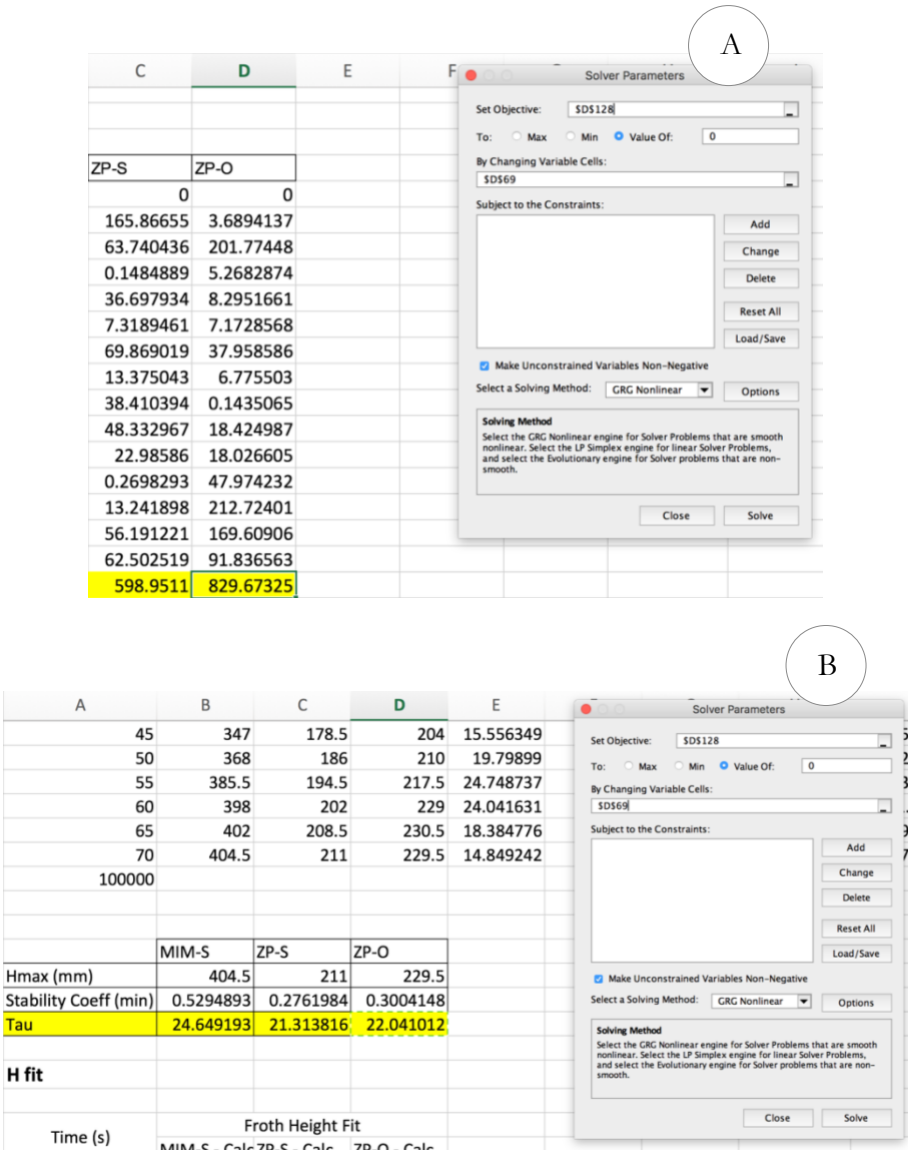

Figure 7.3: Screen shots showing steps A and B for using the solver function in MS Excel 2016

7.4 Kinetic Tests – Model Fitting

The Klimpel Model was applied as follows:

1. The method of least squares (as described for the model fitting for the froth stability tests) was used for the determination of the kinetic rate constant through fitting of the Klimpel Model (Equation 4.3) to the experimental results.

$$R(t) = R_{max}\left[1 - \frac{1}{kt}(1 - e^{-kt})\right] \quad \text{(Equation 4.3)}$$

2. The "Solver" function present in MS Excel 2016 was then used to minimize the sum of the square of the difference between the experimental data and that determined by the model.

$$Residual = \sum_{i=0}^{n}(k_{calculated} - k_{observed})^2 \quad \text{(Equation 7.3)}$$

7.5 Rheology

7.5.1 Sample Mass Calculation

The mass of ore sample as well as water used in the rheology tests is given in the tables reported in this section.

Table 7.15: Density of samples used in this study, determined by a Micromeritics Helium Pycnometer AccuPyc 1330.

	Density (kg/m^3)
MIM-S	3243
ZP-S	3329
ZP-O	3319
Talc	2871

Based on the densites shown in Table 7.15 the mass of Ore Sample required for the rheology tests was calculated using the formulae below:

$$Rheometer\ pot\ volume = 60\ mm \quad \text{(Equation 7.4)}$$

$$Volume\ of\ Sample = vol\ \% \times Rheometer\ pot\ volume \quad \text{(Equation 7.5)}$$

$$Mass\ of\ Solids = Volume\ of\ Sample \times Density\ of\ Sample \quad \text{(Equation 7.6)}$$

Table 7.16: Mass of MIM-S samples, volume of water and volume of depressant used in the rheological characterization part of this study. The depressant was in a 1% solution

% Solids by volume	Volume of Ore Sample (mm)	Volume of water without Depressant (mm	**Mass of sample (g)**	Mass of Depressant (g)	Volume of Depressant (mm)	Volume of water in tests with Depressant (mm)
5	3	57	**9.7**	0.0049	0.49	56.51
10	6	54	**19.5**	0.0097	0.97	53.03
15	9	51	**29.2**	0.0146	1.46	49.54
20	12	48	**38.9**	0.0195	1.95	46.05
25	15	45	**48.6**	0.0243	2.43	42.57
30	18	42	**58.4**	0.0292	2.92	39.08
35	21	39	**68.1**	0.0341	3.41	35.59
40	24	36	**77.8**	0.0389	3.89	32.11
45	27	33	**87.6**	0.0438	4.38	28.62

Table 7.17: Mass of ZP-S samples, volume of water and volume of depressant used in the rheological characterization part of this study. The depressant was in a 1% solution

% Solids by volume	Volume of Ore Sample (mm)	Volume of water without Depressant (mm)	**Mass of sample (g)**	Mass of Depressant (g)	Volume of Depressant (mm)	Volume of water in tests with Depressant (mm)
5	3	57	**10.0**	0.0050	0.50	56.50
10	6	54	**20.0**	0.0100	1.00	53.00
15	9	51	**30.0**	0.0150	1.50	49.50
20	12	48	**39.9**	0.0200	2.00	46.00
25	15	45	**49.9**	0.0250	2.50	42.50
30	18	42	**59.9**	0.0300	3.00	39.00
35	21	39	**69.9**	0.0350	3.50	35.50
40	24	36	**79.9**	0.0399	3.99	32.01
45	27	33	**89.9**	0.0449	4.49	28.51

Table 7.18: Mass of ZP-O samples, volume of water and volume of depressant used in the rheological characterization part of this study. The depressant was in a 1% solution

% Solids by volume	Volume of Ore Sample (mm)	Volume of water (mm)	**Mass of sample (g)**	Mass of Depressant (g)	Volume of Depressant (mm)	Volume of water in tests with Depressant (mm)
5	3	57	**10.0**	0.0050	0.50	56.50
10	6	54	**19.9**	0.0100	1.00	53.00
15	9	51	**29.9**	0.0149	1.49	49.51
20	12	48	**39.8**	0.0199	1.99	46.01
25	15	45	**49.8**	0.0249	2.49	42.51
30	18	42	**59.7**	0.0299	2.99	39.01
35	21	39	**69.7**	0.0349	3.49	35.51
40	24	36	**79.7**	0.0398	3.98	32.02
45	27	33	**89.6**	0.0448	4.48	28.52

Table 7.19: Mass of Talc samples, volume of water and volume of depressant used in the rheological characterization part of this study. No depressant was used here

% Solids by volume	Volume of Ore Sample (mm)	Volume of water (mm)	**Mass of sample (g)**
5	3	57	**8.6**
10	6	54	**17.2**
15	9	51	**25.8**
20	12	48	**34.5**
25	15	45	**43.1**
30	18	42	**51.7**
35	21	39	**60.3**
40	24	36	**68.9**
45	27	33	**77.5**

7.5.2 Bingham yield stress calculation

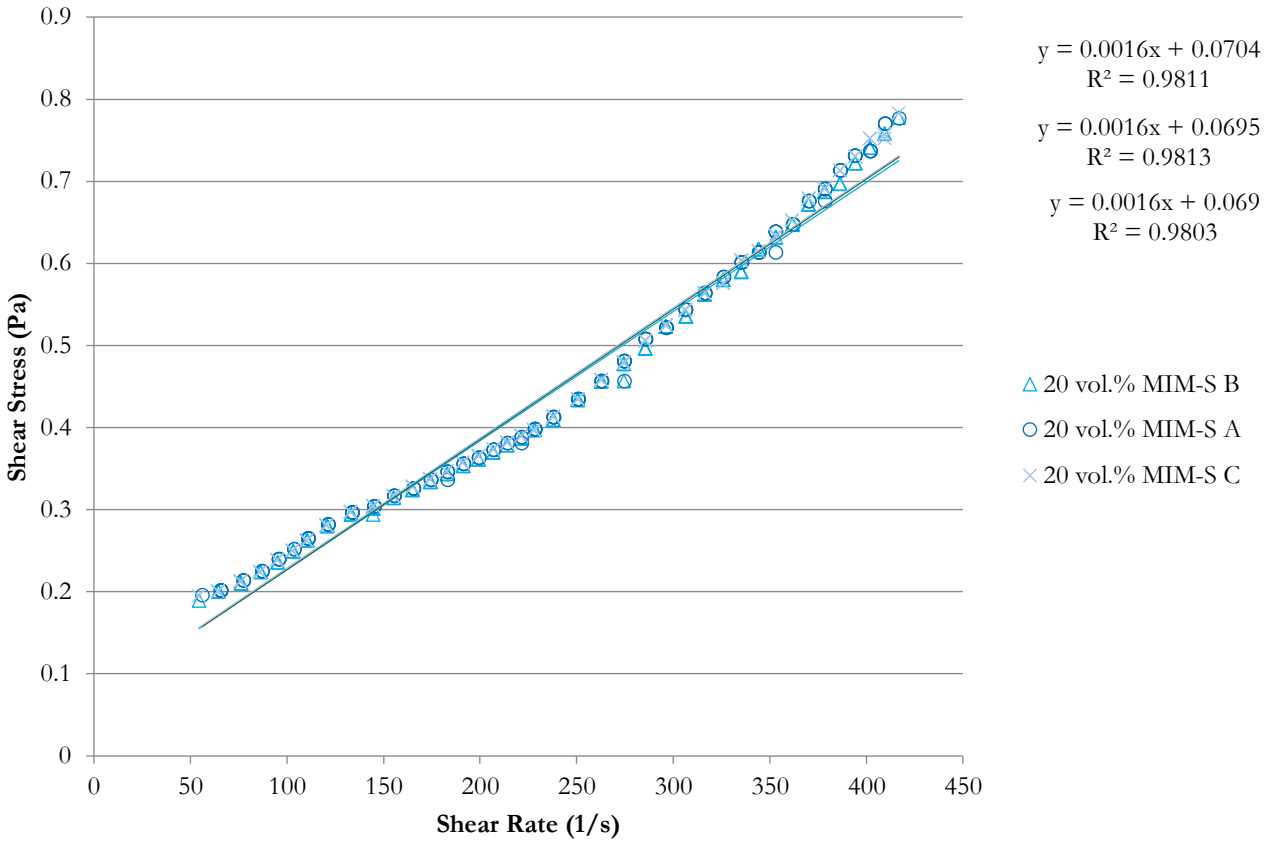

Figure 7.4: Rheogram showing linear trendlines that were used in the calculation of yield stress.

The points of intersection of the linear trendlines with the y-axis on the graphs were averaged so as to calculate the yield stress.

For the example above the yield stress was calculated as follows:

$$Yield\ Stress = Average(0.0704; 0.0695; 0.069) = 0.0696\ Pa \quad \text{(Equation 7.7)}$$

7.5.3 Rheograms for tests at different solids concentrations

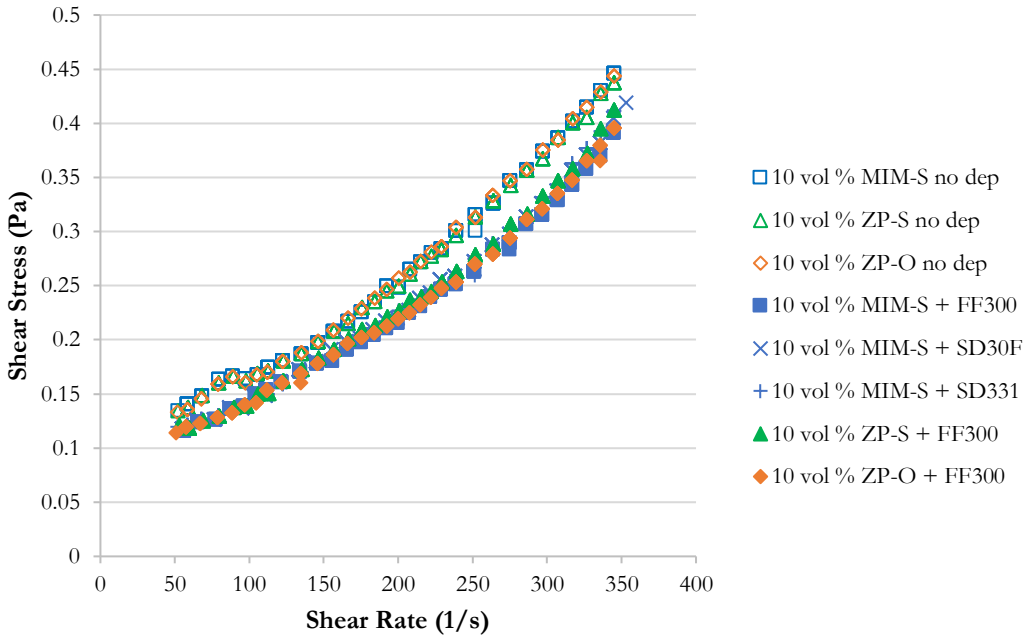

Figure 7.5: Rheograms for tests conducted at 10 vol.% solids.

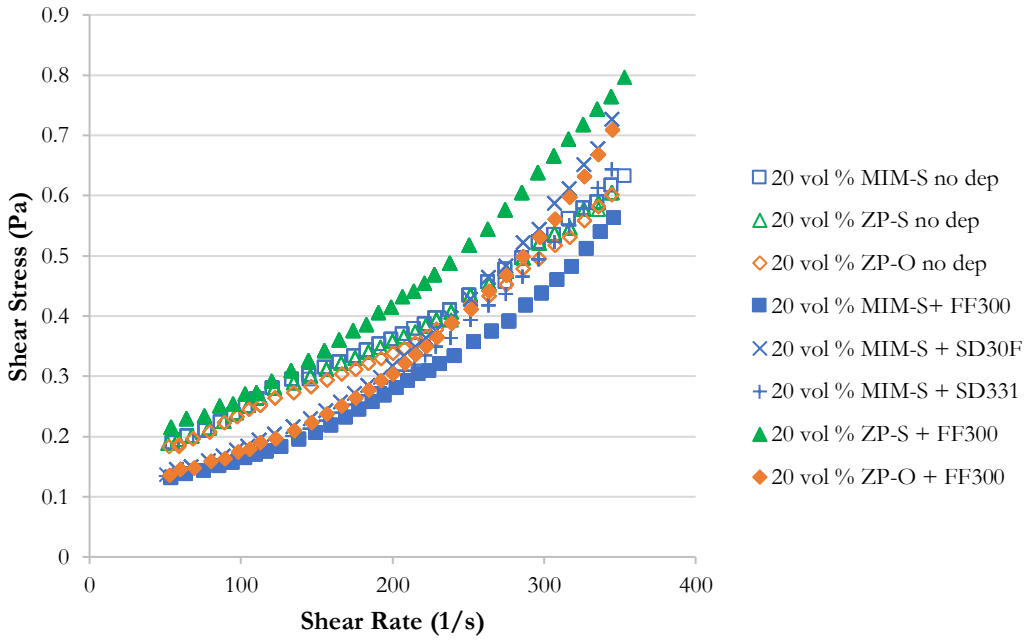

Figure 7.6: Rheograms for tests conducted at 20 vol.% solids.

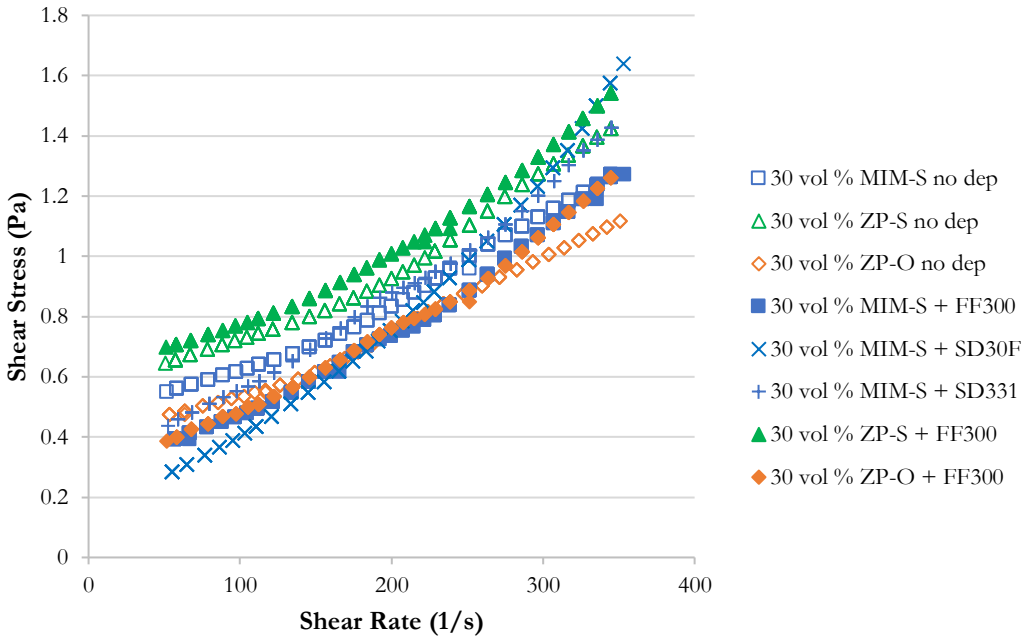

Figure 7.7: Rheograms for tests conducted at 30 vol.% solids.

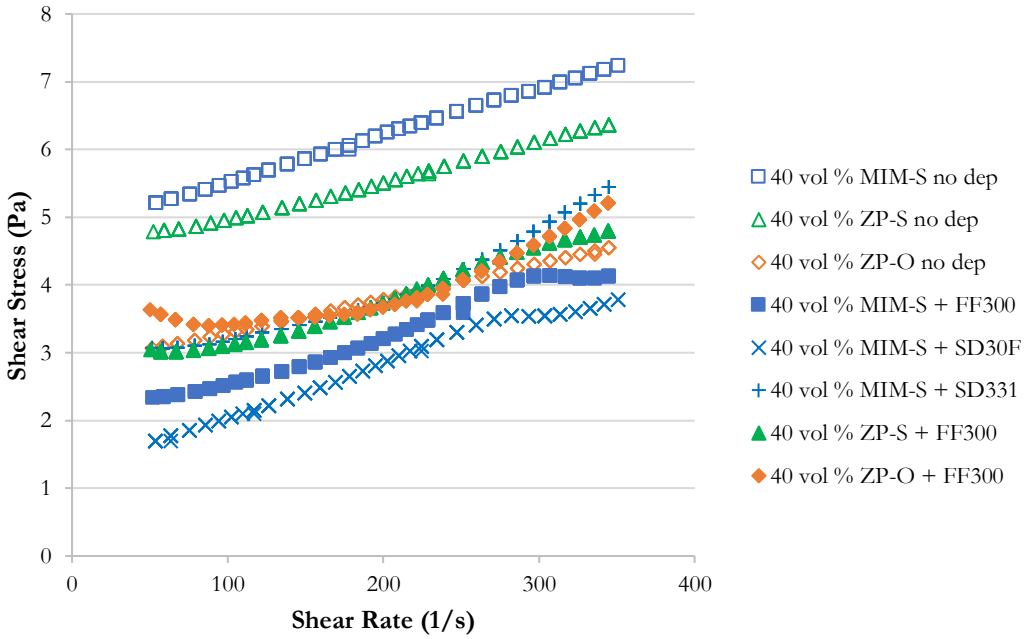

Figure 7.8: Rheograms for tests conducted at 40 vol.% solids.

Table 7.20: Apparent viscosity and yield stress at varying solids concentrations for the Texas Talc Sample.

Solids Concentration (vol.%)	5	10	15	16.5	18.5	20	22.5
Apparent Viscosity (mPa.s)	1.29	1.50	3.88	6.94	13.3	22.1	40.1
Yield Stress (Pa)	0.0441	0.0420	0.117	0.413	1.03	2.32	4.73

Table 7.21: Apparent viscosity and yield stress at varying solids concentrations for the 3 ore samples with and without a depressant.

Solids Concentration (vol.%)		10	20	30	35	40
Apparent Viscosity (mPa.s)	**MIM-S no dep**	1.56	2.01	4.52	9.35	36.8
	ZP-S no dep	1.31	1.96	5.17	10.1	32.7
	ZP-O no dep	1.33	1.68	3.96	8.34	22.4
	MIM-S + FF300	1.16	1.37	3.90	8.62	17.9
	MIM-S + SD30F	1.22	1.57	3.77	6.77	15.4
	MIM-S + SD331	1.19	1.44	4.61	8.41	21.8
	ZP-S + FF300	1.22	2.20	5.51	9.67	21.1
	ZP-O + FF300	1.20	1.51	3.99	8.83	22.0
Yield Stress (Pa)	**MIM-S no dep**	0.0720	0.0988	0.358	1.012	4.83
	ZP-S no dep	0.0584	0.0990	0.433	1.094	4.40
	ZP-O no dep	0.0562	0.0779	0.303	0.846	2.78
	MIM-S + FF300	0.0100	0.0114	0.165	0.708	1.82
	MIM-S + SD30F	0.00740	0.0566	0.149	0.454	1.36
	MIM-S + SD331	0.0116	0.0739	0.176	0.599	2.26
	ZP-S + FF300	0.0442	0.0696	0.206	0.539	2.40
	ZP-O + FF300	0.0476	0.0500	0.186	0.764	2.64

7.6 Preliminary Batch Flotation Test Results for determination of 'low' and 'high' depressant dosages

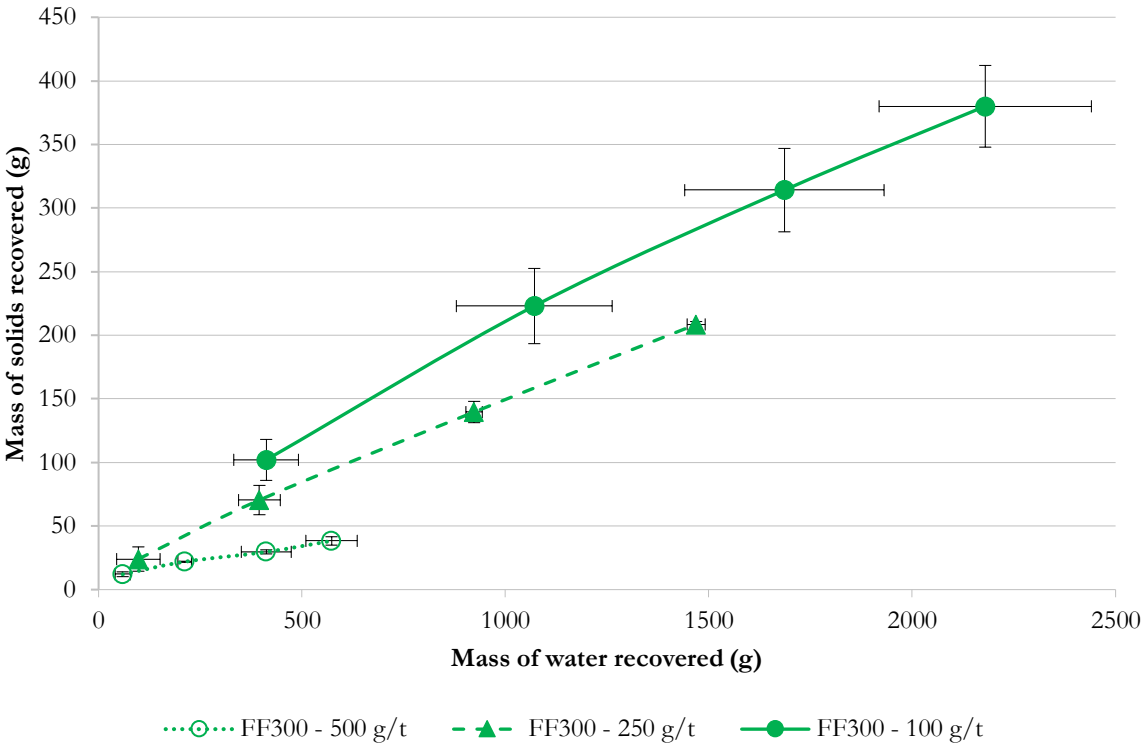

Figure 7.9: Preliminary batch flotation mass of solids and water recovered results for ZP-S in an 8 L Leeds Batch Flotation Cell for the determination of the 'High' and 'Low' depressant dosages. Beyond 500 g/t the froth was too unstable to flow over the lip of the flotation cell. The error bars in the graph represent standard error.

7.7 Batch Flotation Test Results

Table 7.22: Summary of Batch flotation test results including standard error

Ore	Depressant Type	Depressant Dosage (g/t)	Mass of Solids Recovered (g)		Mass of Water Recovered (g)		Copper				Nickel				Platinum				Palladium			
							Recovery (%)		Grade (%)		Recovery (%)		Grade (%)		Recovery (%)		Grade (g/t)		Recovery (%)		Grade (g/t)	
			Average	Standard Error	Average	Standard Error	Average	Standard Error	Average	Standard Error	Average	Standard Error	Average	Standard Error	Average	Standard Error	Average	Standard Error	Average	Standard Error	Average	Standard Error
MIM-S	FF300	100	210.51	1.68	1360.92	24.44	87.36	0.30	0.63	0.00	67.02	0.15	0.89	0.01	86.69	0.69	6.01	0.05	84.36	0.67	4.38	0.03
		500	34.70	1.91	721.21	34.21	73.25	0.87	3.64	0.06	52.22	0.32	5.42	0.01	72.62	0.58	46.00	0.37	70.48	0.56	36.00	0.29
	SD30F	100	235.40	2.93	1376.24	23.66	88.34	0.03	0.58	0.00	65.24	0.59	0.68	0.01	89.86	0.72	6.23	0.05	88.46	0.70	4.90	0.04
		500	36.70	0.75	603.10	23.78	75.27	1.22	2.74	0.04	53.55	0.64	3.86	0.04	80.26	0.64	39.00	0.31	79.90	0.64	34.00	0.27
	SD331	100	231.78	6.58	1415.42	17.58	88.29	0.07	0.58	0.01	69.52	0.06	0.85	0.01	88.39	0.70	6.43	0.05	86.81	0.69	4.92	0.04
		500	29.23	0.63	455.65	19.19	74.51	0.43	3.20	0.02	53.25	0.12	4.72	0.02	75.44	0.60	43.00	0.34	70.10	0.56	29.00	0.23
ZP-S	FF300	100	198.23	3.72	1610.11	35.24	82.91	1.72	0.37	0.04	54.15	0.85	0.53	0.00	85.87	0.68	6.84	0.05	85.71	0.68	5.00	0.04
		500	34.70	1.91	721.21	34.21	74.43	0.05	1.81	0.05	47.12	0.66	2.86	0.16	75.45	0.60	33.00	0.26	79.72	0.63	30.00	0.24
	SD30F	100	196.61	5.53	1623.48	43.90	82.79	0.53	0.37	0.03	54.71	0.84	0.59	0.07	86.65	0.69	6.61	0.05	87.01	0.69	5.46	0.04
		500	34.48	0.18	727.10	6.09	72.94	1.59	1.75	0.06	44.75	2.64	2.59	0.09	75.08	0.60	31.00	0.25	78.24	0.62	27.00	0.21
	SD331	100	150.65	0.41	1558.21	20.62	79.50	3.28	0.26	0.05	52.14	2.17	0.46	0.04	86.90	0.69	6.11	0.05	88.30	0.70	5.28	0.04
		500	36.50	2.11	919.02	22.37	72.64	0.79	1.64	0.05	44.89	2.38	2.62	0.00	74.56	0.59	28.00	0.22	74.92	0.60	23.00	0.18
ZP-O	FF300	100	139.84	0.42	1604.73	0.63	68.66	1.32	0.72	0.01	46.17	0.52	0.95	0.03	77.26	0.61	11.10	0.09	62.06	0.49	3.63	0.03
		500	36.79	2.04	996.97	12.16	59.01	2.14	2.24	0.04	35.64	2.25	2.76	0.05	68.28	0.54	39.00	0.31	56.35	0.45	13.70	0.11
	SD30F	100	196.61	5.53	1623.48	43.90	73.08	0.01	0.69	0.00	52.60	0.23	0.98	0.01	78.88	0.63	10.90	0.09	66.16	0.53	3.84	0.03
		500	32.81	0.56	939.64	1.94	57.43	2.45	2.30	0.02	32.67	1.81	2.61	0.02	65.13	0.52	42.00	0.33	53.04	0.42	15.50	0.12
	SD331	100	157.38	3.05	1645.31	11.09	70.43	0.78	0.64	0.02	49.15	0.29	0.89	0.02	74.23	0.59	10.00	0.08	56.36	0.45	3.38	0.03
		500	33.16	0.56	917.39	5.53	57.55	0.02	2.21	0.05	32.42	0.25	2.53	0.03	64.04	0.51	42.00	0.33	50.58	0.40	15.60	0.12

Table 7.23: MIM-S batch flotation test results

Run no.	Reagents	Sample	Time (min)	Mass Pull (g)	Water Rec (g)	Cum Mass (g)	Cum Water (g)	Copper Grade (%)	Copper Rec %	Nickel Grade (%)	Nickel Rec (%)	Sulfur Grade (%)	Sulfur Rec (%)
1	FF300 - 500 g/t	C1	2	10.49	84.75	10.49	84.75	6.22	53.88	7.59	31.18	14.70	37.04
	SIBX - 300 g/t	C2	6	4.23	65.89	14.72	150.64	5.28	64.26	7.32	42.21	14.38	50.86
	Sasfroth200 - 75 g/t	C3	12	3.11	65.13	17.83	215.77	4.67	68.78	6.70	46.84	13.64	58.40
		C4	20	6.61	165.17	24.44	380.94	3.59	72.38	5.42	51.90	11.07	64.96
		F		997.82									
		T		956.63									
2	FF300 - 500 g/t	C1	2	12.68	105.13	12.68	105.13	5.71	55.08	6.89	32.13	11.10	38.26
	SIBX - 300 g/t	C2	6	4.40	70.44	17.08	175.57	5.10	66.30	6.95	43.64	11.49	53.33
	Sasfroth200 - 75 g/t	C3	12	3.63	73.22	20.71	248.79	4.51	71.10	6.35	48.35	10.90	61.35
		C4	20	5.59	142.39	26.30	391.18	3.70	74.12	5.43	52.54	9.59	68.55
		F		1001.26									
		T		956.17									
3	FF300 - 100 g/t	C1	2	61.33	279.11	61.33	279.11	1.83	74.12	2.17	47.75	5.66	69.80
	SIBX - 300 g/t	C2	6	68.08	420.28	129.41	699.39	0.97	82.54	1.28	59.54	3.19	83.05
	Sasfroth200 - 75 g/t	C3	12	53.01	425.62	182.42	1125.01	0.72	86.05	0.99	64.89	2.44	89.32
		C4	20	26.41	260.35	208.83	1385.36	0.64	87.65	0.90	67.18	2.18	91.48
		F		992.99									
		T		767.87									
4	FF300 - 100 g/t	C1	2	48.83	199.90	48.83	199.90	2.27	72.11	2.55	44.20	4.86	62.17
	SIBX - 300 g/t	C2	6	71.79	413.78	120.62	613.68	1.04	81.23	1.36	58.25	2.45	77.34
	Sasfroth200 - 75 g/t	C3	12	57.80	414.63	178.42	1028.31	0.74	85.21	1.01	64.21	1.85	86.24
		C4	20	33.76	308.17	212.18	1336.48	0.63	87.06	0.89	66.87	1.62	89.85
		F		1006.57									
		T		785.73									
5	SD30F - 500 g/t	C1	2	16.74	143.57	16.74	143.57	4.67	60.00	5.32	34.31	11.60	51.59
	SIBX - 300 g/t	C2	6	4.95	86.92	21.69	230.49	4.17	69.43	5.14	43.00	11.33	65.26
	Sasfroth200 - 75 g/t	C3	12	6.58	147.95	28.27	378.44	3.40	73.73	4.49	48.86	9.85	74.00
		C4	20	7.68	200.88	35.95	579.32	2.77	76.49	3.82	52.91	8.38	80.02
		F		1007.12									
		T		951.81									
6	SD30F - 500 g/t	C1	2	14.35	124.54	14.35	124.54	5.17	54.33	6.10	32.57	13.00	44.09
	SIBX - 300 g/t	C2	6	5.80	96.07	20.15	220.61	4.44	65.58	5.70	42.72	12.34	58.75
	Sasfroth200 - 75 g/t	C3	12	8.57	184.74	28.72	405.35	3.37	70.88	4.66	49.76	10.20	69.22
		C4	20	8.73	221.53	37.45	626.88	2.70	74.06	3.89	54.20	8.61	76.18
		F		1007.45									
		T		951.03									
7	SD30F - 100 g/t	C1	2	86.54	271.01	86.54	271.01	1.36	75.01	1.15	40.09	2.76	64.15
	SIBX - 300 g/t	C2	6	79.18	419.49	165.72	690.50	0.79	83.79	0.84	56.39	1.85	82.18
	Sasfroth200 - 75 g/t	C3	12	47.64	384.96	213.36	1075.46	0.64	86.97	0.72	62.07	1.54	88.45
		C4	20	24.96	277.12	238.32	1352.58	0.58	88.31	0.67	64.66	1.44	91.94
		F		1007.63									
		T		753.51									
8	SD30F - 100 g/t	C1	2	91.43	321.51	91.43	321.51	1.27	75.55	1.17	44.07	2.60	65.77
	SIBX - 300 g/t	C2	6	73.64	432.46	165.07	753.97	0.78	83.91	0.85	58.14	1.81	82.43
	Sasfroth200 - 75 g/t	C3	12	43.45	369.74	208.52	1123.71	0.64	86.85	0.73	63.33	1.54	88.63
		C4	20	23.95	276.19	232.47	1399.90	0.58	88.37	0.68	65.83	1.44	92.36
		F		997.06									
		T		750.79									
9	SD331 - 500 g/t	C1	2	12.09	100.88	12.09	100.88	5.90	56.37	7.66	35.23	15.40	50.95
	SIBX - 300 g/t	C2	6	4.55	70.26	16.64	171.14	5.08	66.85	6.98	44.17	14.63	66.64
	Sasfroth200 - 75 g/t	C3	12	5.63	116.36	22.27	287.50	4.07	71.61	5.92	50.14	12.49	76.11
		C4	20	7.59	187.34	29.86	474.84	3.17	74.94	4.70	53.36	10.20	83.34
		F		994.02									
		T		949.11									
10	SD331 - 500 g/t	C1	2	10.08	74.34	10.08	74.34	6.51	52.79	7.76	30.62	16.70	45.84
	SIBX - 300 g/t	C2	6	5.34	75.27	15.42	149.61	5.29	65.56	7.05	42.58	15.52	65.18
	Sasfroth200 - 75 g/t	C3	12	6.24	123.67	21.66	273.28	4.07	70.88	5.88	49.92	13.17	77.71
		C4	20	6.94	163.18	28.60	436.46	3.22	74.07	4.74	53.13	10.86	84.55
		F		994.99									
		T		953.63									
11	SD331 - 100 g/t	C1	2	74.77	284.64	74.77	284.64	1.51	74.84	1.89	50.89	4.36	72.42
	SIBX - 300 g/t	C2	6	75.20	407.17	149.97	691.81	0.84	83.30	1.16	62.51	2.63	87.69
	Sasfroth200 - 75 g/t	C3	12	48.72	453.51	198.69	1145.32	0.66	86.73	0.94	67.20	2.11	92.93
		C4	20	26.51	287.68	225.20	1433.00	0.59	88.37	0.86	69.46	1.90	95.09
		F		996.09									
		T		754.84									
12	SD331 - 100 g/t	C1	2	74.77	268.09	74.77	268.09	1.51	73.86	1.93	49.80	4.44	69.27
	SIBX - 300 g/t	C2	6	78.95	438.19	153.72	706.28	0.82	82.66	1.17	61.98	2.66	85.21
	Sasfroth200 - 75 g/t	C3	12	53.70	403.09	207.42	1109.37	0.64	86.41	0.94	67.03	2.12	91.93
		C4	20	30.93	288.47	238.35	1397.84	0.57	88.22	0.85	69.58	1.91	94.96
		F		1005.95									
		T		751.52									

Table 7.24: ZP-S batch flotation test results

Run no.	Reagents	Sample	Time (min)	Mass Pull (g)	Water Rec (g)	Cum Mass (g)	Cum Water (g)	Copper Grade (%)	Copper Rec %	Nickel Grade (%)	Nickel Rec (%)	Sulfur Grade (%)	Sulfur Rec (%)
1	FF300 - 500 g/t	C1	2	5.53	52.34	5.53	52.34	7.82	51.68	8.29	21.79	17.70	45.93
	SIBX - 300 g/t	C2	6	5.19	98.67	10.72	151.01	5.08	65.02	6.81	34.68	12.86	64.68
	Sasfroth200 - 75 g/t	C3	12	9.29	219.33	20.01	370.34	2.97	70.92	4.60	43.71	8.69	81.60
		C4	20	13.34	326.68	33.35	697.02	1.87	74.38	3.02	47.78	5.82	91.11
		F		1031.84									
		T		983.75									
2	FF300 - 500 g/t	C1	2	9.68	109.57	9.68	109.57	4.74	53.89	5.17	23.83	10.40	53.09
	SIBX - 300 g/t	C2	6	5.00	104.69	14.68	214.26	3.82	65.77	4.93	34.48	9.26	71.66
	Sasfroth200 - 75 g/t	C3	12	8.66	207.58	23.34	421.84	2.59	71.08	3.82	42.45	7.02	86.41
		C4	20	12.71	323.56	36.05	745.40	1.76	74.48	2.71	46.47	5.03	95.66
		F		1029.57									
		T		956.17									
3	FF300 - 100 g/t	C1	2	56.29	327.80	56.29	327.80	0.98	65.99	1.10	30.98	3.30	68.88
	SIBX - 300 g/t	C2	6	66.72	499.63	123.01	827.43	0.51	74.96	0.73	44.80	1.83	83.68
	Sasfroth200 - 75 g/t	C3	12	51.06	487.24	174.07	1314.67	0.38	79.26	0.58	50.65	1.39	89.87
		C4	20	27.87	330.68	201.94	1645.35	0.34	81.19	0.53	53.30	1.24	92.55
		F		1039.14									
		T		822.10									
4	FF300 - 100 g/t	C1	2	46.66	255.39	46.66	255.39	1.41	69.91	1.17	29.02	3.63	66.68
	SIBX - 300 g/t	C2	6	65.02	473.61	111.68	729.00	0.66	78.64	0.76	45.06	1.88	82.84
	Sasfroth200 - 75 g/t	C3	12	53.88	510.42	165.56	1239.42	0.47	82.74	0.59	51.92	1.39	90.66
		C4	20	28.95	335.44	194.51	1574.86	0.41	84.63	0.53	55.01	1.22	93.64
		F		1042.43									
		T		830.69									
5	SD30F - 500 g/t	C1	2	8.83	100.82	8.83	100.82	4.81	54.06	5.11	24.67	12.90	52.26
	SIBX - 300 g/t	C2	6	4.15	83.15	12.98	183.97	3.90	64.47	4.83	34.32	11.08	66.00
	Sasfroth200 - 75 g/t	C3	12	8.09	190.73	21.07	374.70	2.63	70.52	3.71	42.76	8.40	81.18
		C4	20	13.59	358.49	34.66	733.19	1.69	74.53	2.50	47.39	5.62	89.41
		F		1026.58									
		T		976.07									
6	SD30F - 500 g/t	C1	2	12.23	143.27	12.23	143.27	3.88	54.74	4.55	25.52	9.67	56.18
	SIBX - 300 g/t	C2	6	4.25	88.34	16.48	231.61	3.37	63.95	4.36	32.98	9.00	70.48
	Sasfroth200 - 75 g/t	C3	12	7.40	180.72	23.88	412.33	2.48	68.35	3.55	38.93	7.26	82.36
		C4	20	10.42	308.68	34.30	721.01	1.80	71.35	2.68	42.11	5.46	89.04
		F		990.84									
		T		941.35									
7	SD30F - 100 g/t	C1	2	45.82	252.10	45.82	252.10	1.41	69.74	1.80	36.29	4.17	71.47
	SIBX - 300 g/t	C2	6	65.44	496.96	111.26	749.06	0.65	77.83	0.98	48.03	2.08	86.69
	Sasfroth200 - 75 g/t	C3	12	50.65	488.60	161.91	1237.66	0.47	81.52	0.74	52.98	1.52	92.26
		C4	20	29.17	341.92	191.08	1579.58	0.40	83.32	0.66	55.55	1.32	94.65
		F		1008.77									
		T		803.13									
8	SD30F - 100 g/t	C1	2	57.95	340.69	57.95	340.69	0.96	67.34	1.15	33.64	3.29	73.03
	SIBX - 300 g/t	C2	6	61.64	464.34	119.59	805.03	0.52	75.78	0.74	45.10	1.87	85.52
	Sasfroth200 - 75 g/t	C3	12	54.07	520.27	173.66	1325.30	0.38	80.24	0.58	51.05	1.39	92.21
		C4	20	28.47	342.07	202.13	1667.37	0.33	82.26	0.53	53.87	1.23	95.06
		F		1018.66									
		T		799.29									
9	SD331 - 500 g/t	C1	2	11.24	145.41	11.24	145.41	4.36	58.74	6.01	31.64	9.98	61.91
	SIBX - 300 g/t	C2	6	5.89	146.08	17.13	291.49	3.23	66.21	5.01	40.20	8.08	76.40
	Sasfroth200 - 75 g/t	C3	12	10.31	292.03	27.44	583.52	2.15	70.84	3.47	44.53	5.73	86.76
		C4	20	11.16	357.87	38.60	941.39	1.59	73.43	2.62	47.26	4.35	92.76
		F		1027.70									
		T		974.82									
10	SD331 - 500 g/t	C1	2	10.18	144.65	10.18	144.65	4.61	58.02	5.79	27.82	10.20	51.24
	SIBX - 300 g/t	C2	6	5.41	146.85	15.59	291.50	3.37	64.94	4.85	35.66	8.24	63.36
	Sasfroth200 - 75 g/t	C3	12	8.11	245.54	23.70	537.04	2.36	69.17	3.54	39.63	6.26	73.24
		C4	20	10.69	359.61	34.39	896.65	1.69	71.85	2.62	42.51	4.75	80.57
		F		1009.53									
		T		962.61									
11	SD331 - 100 g/t	C1	2	71.19	365.40	71.19	365.40	0.80	68.79	0.94	33.30	2.77	69.36
	SIBX - 300 g/t	C2	6	72.54	526.67	143.73	892.07	0.44	77.02	0.65	46.42	1.65	83.37
	Sasfroth200 - 75 g/t	C3	12	49.85	491.29	193.58	1383.36	0.35	80.96	0.54	51.76	1.31	89.19
		C4	20	26.10	340.61	219.68	1723.97	0.31	82.78	0.50	54.30	1.18	91.39
		F		1027.67									
		T		792.60									
12	SD331 - 100 g/t	C1	2	56.07	284.34	56.07	284.34	0.58	54.26	0.77	24.25	1.80	51.39
	SIBX - 300 g/t	C2	6	72.42	510.06	128.49	794.40	0.31	67.32	0.55	40.11	1.13	73.77
	Sasfroth200 - 75 g/t	C3	12	53.69	498.14	182.18	1292.54	0.24	73.42	0.45	46.72	0.89	82.27
		C4	20	29.56	365.26	211.74	1657.80	0.21	76.23	0.42	49.97	0.80	86.15
		F		1023.58									
		T		796.55									

Table 7.25: ZP-O batch flotation test results

Run no.	Reagents	Sample	Time (min)	Mass Pull (g)	Water Rec (g)	Cum Mass (g)	Cum Water (g)	Copper Grade (%)	Copper Rec %	Nickel Grade (%)	Nickel Rec (%)	Sulfur Grade (%)	Sulfur Rec (%)
1	FF300 - 500 g/t	C1	2	9.80	150.82	9.80	150.82	5.27	37.79	4.34	14.82	11.80	42.05
	SIBX - 300 g/t	C2	6	5.89	143.81	15.69	294.63	4.22	48.45	4.45	24.32	10.21	58.27
	Sasfroth200 - 75 g/t	C3	12	10.24	334.66	25.93	629.29	2.84	53.83	3.40	30.72	7.56	71.30
		C4	20	9.41	359.08	35.34	988.37	2.20	56.87	2.71	33.38	6.10	78.35
		F		997.64									
		T		947.08									
2	FF300 - 500 g/t	C1	2	9.45	126.16	9.45	126.16	6.10	40.33	4.94	16.46	12.10	40.10
	SIBX - 300 g/t	C2	6	8.58	183.58	18.03	309.74	4.21	53.07	4.53	28.77	9.51	60.15
	Sasfroth200 - 75 g/t	C3	12	9.58	303.16	27.61	612.90	2.99	57.84	3.57	34.79	7.59	73.49
		C4	20	10.62	392.67	38.23	1005.57	2.29	61.16	2.81	37.89	6.10	81.76
		F		1011.15									
		T		956.17									
3	FF300 - 100 g/t	C1	2	33.21	244.88	33.21	244.88	2.25	53.10	2.45	29.50	4.37	67.98
	SIBX - 300 g/t	C2	6	48.48	502.54	81.69	747.42	1.07	62.37	1.29	38.36	2.13	81.49
	Sasfroth200 - 75 g/t	C3	12	35.88	486.20	117.57	1233.62	0.80	67.26	1.02	43.57	1.57	86.65
		C4	20	21.84	370.48	139.41	1604.10	0.71	69.99	0.92	46.69	1.36	88.55
		F		1011.65									
		T		822.10									
4	FF300 - 100 g/t	C1	2	38.77	289.33	38.77	289.33	2.07	52.65	2.40	31.00	4.10	69.91
	SIBX - 300 g/t	C2	6	43.98	460.37	82.75	749.70	1.11	60.38	1.38	38.09	2.25	81.96
	Sasfroth200 - 75 g/t	C3	12	36.82	504.78	119.57	1254.48	0.83	64.92	1.08	42.91	1.65	86.67
		C4	20	20.69	350.87	140.26	1605.35	0.73	67.34	0.98	45.64	1.43	88.39
		F		1024.17									
		T		830.69									
5	SD30F - 500 g/t	C1	2	8.47	115.61	8.47	115.61	6.17	41.19	4.90	16.62	14.10	45.47
	SIBX - 300 g/t	C2	6	5.98	153.99	14.45	269.60	4.56	51.95	4.61	26.70	11.18	61.50
	Sasfroth200 - 75 g/t	C3	12	9.29	298.01	23.74	567.61	3.04	56.83	3.25	30.87	8.16	73.74
		C4	20	9.62	373.97	33.36	941.58	2.28	59.87	2.58	34.48	6.41	81.36
		F		996.89									
		T		947.94									
6	SD30F - 500 g/t	C1	2	7.71	102.48	7.71	102.48	6.51	36.89	5.27	14.79	15.90	46.00
	SIBX - 300 g/t	C2	6	5.78	155.02	13.49	257.50	4.78	47.34	4.93	24.21	12.39	62.71
	Sasfroth200 - 75 g/t	C3	12	9.40	316.56	22.89	574.06	3.09	51.96	3.38	28.17	8.73	75.02
		C4	20	9.36	363.64	32.25	937.70	2.32	54.98	2.63	30.86	6.65	80.43
		F		1015.50									
		T		967.68									
7	SD30F - 100 g/t	C1	2	46.16	313.00	46.16	313.00	1.81	58.48	2.33	38.09	5.37	74.46
	SIBX - 300 g/t	C2	6	48.83	470.64	94.99	783.64	1.00	66.48	1.36	45.67	2.91	82.91
	Sasfroth200 - 75 g/t	C3	12	35.23	460.31	130.22	1243.95	0.77	70.68	1.09	50.12	2.25	87.99
		C4	20	20.02	334.88	150.24	1578.83	0.69	73.10	0.99	52.83	2.01	90.55
		F		1020.14									
		T		854.90									
8	SD30F - 100 g/t	C1	2	43.50	280.57	43.50	280.57	1.87	57.51	2.32	36.12	7.03	82.92
	SIBX - 300 g/t	C2	6	51.05	477.46	94.55	758.03	0.99	66.51	1.33	44.90	3.52	90.32
	Sasfroth200 - 75 g/t	C3	12	36.24	458.36	130.79	1216.39	0.76	70.61	1.06	49.56	2.63	93.38
		C4	20	20.26	321.20	151.05	1537.59	0.68	73.07	0.97	52.37	2.31	94.45
		F		1001.61									
		T		835.84									
9	SD331 - 500 g/t	C1	2	8.99	124.01	8.99	124.01	5.65	39.64	4.91	16.95	14.00	52.35
	SIBX - 300 g/t	C2	6	5.48	146.77	14.47	270.78	4.37	49.39	4.56	25.38	11.62	69.95
	Sasfroth200 - 75 g/t	C3	12	8.69	281.07	23.16	551.85	3.00	54.34	3.30	29.35	8.12	78.23
		C4	20	9.44	360.01	32.60	911.86	2.26	57.53	2.57	32.18	6.02	81.69
		F		1002.62									
		T		957.17									
10	SD331 - 500 g/t	C1	2	8.88	128.29	8.88	128.29	5.73	40.07	4.98	17.16	14.20	53.66
	SIBX - 300 g/t	C2	6	5.94	152.63	14.82	280.92	4.27	49.80	4.47	25.71	10.93	68.93
	Sasfroth200 - 75 g/t	C3	12	9.06	282.13	23.88	563.05	2.90	54.49	3.22	29.81	7.69	78.15
		C4	20	9.84	359.86	33.72	922.91	2.17	57.56	2.50	32.67	5.72	82.08
		F		998.88									
		T		950.42									
11	SD331 - 100 g/t	C1	2	48.54	335.67	48.54	335.67	1.68	56.22	2.02	34.08	3.80	75.40
	SIBX - 300 g/t	C2	6	49.28	489.95	97.82	825.62	0.95	64.35	1.23	41.91	2.18	87.00
	Sasfroth200 - 75 g/t	C3	12	32.47	432.87	130.29	1258.49	0.76	68.35	1.02	46.20	1.71	91.05
		C4	20	24.04	375.72	154.33	1634.21	0.67	71.21	0.92	49.45	1.48	93.12
		F		1007.11									
		T		837.51									
12	SD331 - 100 g/t	C1	2	46.13	290.53	46.13	290.53	1.72	55.63	2.08	33.55	3.81	73.53
	SIBX - 300 g/t	C2	6	56.23	524.28	102.36	814.81	0.87	62.58	1.15	41.06	1.99	85.44
	Sasfroth200 - 75 g/t	C3	12	37.44	493.13	139.80	1307.94	0.69	67.16	0.94	46.06	1.54	89.79
		C4	20	20.63	348.46	160.43	1656.40	0.62	69.65	0.87	48.86	1.36	91.56
		F		1014.38									
		T		843.72									

Thank you